Sensing Intracellular Calcium: STIM1 and Orai1 Interactions at the Plasma Membrane

by Nathaniel Taylor Calloway

SENSING INTRACELLULAR CALCIUM: STIM1 AND ORAI1 INTERACTIONS AT THE PLASMA MEMBRANE

A Dissertation

Presented to the Faculty of the Graduate School

of Cornell University

In Partial Fulfillment of the Requirements for the Degree of

Doctor of Philosophy

by

Nathaniel Taylor Calloway

August 2010

SENSING INTRACELLULAR CALCIUM: STIM1 AND ORAI1 INTERACTIONS AT THE PLASMA MEMBRANE

Nathaniel Taylor Calloway, Ph. D.

Cornell University 2010

Store operated Ca^{2+} entry (SOCE) is a ubiquitous process in nonexcitable cells important for receptor signaling in hematopoietic and other cell types. The ER-transmembrane Ca^{2+} sensor STIM1 and the plasma membrane Ca^{2+} channel Orai1 are the two essential protein components of SOCE. To further understand the mechanism by which STIM1 and Orai1 facilitate SOCE, I have characterized bimolecular and supramolecular electrostatic interactions involving these proteins, using an imaging-based fluorescence resonance energy transfer (FRET) assay in RBL mast cells. Using this assay I initially identified positively-charged small molecule inhibitors of the STIM1-Orai1 interaction. Based on this information I hypothesized that these small molecules could be binding to and disrupting the C-terminal acidic coiled-coil of Orai1. Mutation of these acidic residues in Orai1 reduced its association with STIM1 and caused constitutive clustering of Orai1 at the plasma membrane. I then identified a short polybasic sequence in the Ca^{2+} activating domain (CAD) of STIM1 that binds to this acidic region of Orai1. Mutation of this three amino acid basic sequence prevented association with wild type Orai1, but not with the Orai1 coiled-coil mutant. Despite the residual association between the Orai1 and STIM1 mutants, they cannot initiate SOCE, suggesting that the polybasic sequence in STIM1 and the acidic coiled-coil of Orai1 are important for Ca^{2+} gating.

Using multiple isoforms of type I phosphoinositide-5-kinase (PI5KI) and lipid

domain targeted inositol-5-phosphatases, I found that the STIM1-Orai1 interaction has a dual dependence on two pools of of phosphoinositide-(4,5)-bisphosphate (PIP_2) in the plasma membrane that are distinguishable by their association with detergent resistant membranes and detergent solubilized membranes. These correspond to distinctive ordered lipid subregions and disordered lipid subregions in the membrane, respectively. Deletion of an N-terminal polyarginine sequence on Orai1 or a C-terminal polylysine sequence on STIM1 interferes with these selective interactions with PIP_2 pools localized to these subregions. Based on these findings, I propose a model in which Orai1 must translocate between functionally distinct membrane domains in a PIP_2 dependent fashion, to engage STIM1 associated with PIP_2 in ordered lipid subregions of the membrane.

BIOGRAPHICAL SKETCH

Nathaniel Calloway was born in Durham, NC, to James and Marion Calloway, who fostered his love of science from a very early age. Even as a child, one of his favorite activities included “running experiments” in his parent’s bathroom or kitchen, to their great dismay. He perused his scientific interests at UNC-Chapel Hill, where he majored in chemistry. At Columbia university, while studying fluorescent dyes with Virginia Cornish, he met his fiancée Jennifer, and they decided together to relocate to Ithaca. At Cornell, Nathaniel worked for Barbara Baird and David Holowka studying the store operated Ca^{2+} response. Jennifer and Nathaniel are moving back to New York where they met to continue their careers.

This dissertation is dedicated to Jennifer Rokhsar, whose steadfast love and support has made this work possible

ACKNOWLEDGMENTS

I would like to thank the National Institude of Health for funding this research. I would like to thank my various fellowship organizations for supporting me throughout my career at Cornell: the NIH chemistry-biology interface training grant program, the American Chemical Society Division of Medicinal Chemistry, and the American Heart Association Founder's Affiliate predoctoral fellowship program.

I would like to thank everyone in the Baird Lab, past and present, for creating a wonderful research environment. I would especially like to thank Norah Smith for her constant patience and willingness to help. I would like to thank Barbara Baird for being a great PI, and always supporting me, even if she wasn't so crazy about some of my ideas. But perhaps most of all, I would like to thank Dave Holowka for being a wonderful mentor. I would not be half the scientist I am today without his guidance.

TABLE OF CONTENTS

LIST OF FIGURES

LIST OF ABBREVIATIONS

AcGFP	*Aequorea coerulescens* Green Fluorescent Protein
Ag	Antigen
2-APB	2-aminoethoxydiphenylborane
BSA	Bovine Serum Albumin
BSS	Buffered Salt Solution
Ca^{2+}	Calcium
CAD	CRAC Activating Domain
CaM	Calmodulin
CRAC	Ca^{2+} Release Activated Ca^{2+}
CRACM1	Ca^{2+} Release Activated Ca^{2+} Mediator 1 (a.k.a. Orai1)
COS7	Green monkey kidney epithelial cell
CTB	Cholera Toxin subunit B
DAG	Diacyl Glycerol
DMEM	Dulbecco's Modified Eagle's Medium
DMS	Dimethylsphingosine
DNP-BSA	Dinitrophenyl conjugated Bovine Serum Albumin
DRM	Detergent-Resistant Membrane
DSM	Detergent-Solublized Membrane
eCFP	Enhanced Cyan fluorescent Protein
EGF	Epidermal Growth Factor
eGFP	Enhanced GFP
ENaC	Epithelial Sodium Channel
ER	Endoplasmic Reticulum
eYFP	Enhanced Yellow fluorescent Protein
FBS	Fetal Bovine Serum
FcεRI	High affinity receptor for immunoglobulin E
FRET	Fluorescence Resonance Energy Transfer
GAP-43	Growth Associated Protein 43
Gd^{3+}	Gadolinium
GFP	Green Fluorescent Protein
HEK	Human Embryonic Kidney cell
I_{CRAC}	Ca^{2+} Release Activated Ca^{2+} Current
IgE	Immunoglobulin E
Inp54p	Yeast phosphatidylinositiol-(4,5)-bisphosphate 5-phosphatase
IP_3	Inositol-(1,4,5)-trisphosphate
IP_3R	Inositol-(1,4,5)-trisphosphate Receptor
ITAM	immunotyrosine activation motif
L10	Lck membrane targeting sequence
LAT	Linker for Activation of T-cells
MARCKS	Myristoylated Alanine-Rich C-Kinase Substrate
MβCD	Methyl-β-cyclodextrin
MEM	Minimal Essential Medium
mRFP	Monomeric Red Fluorescent Protein
NFAT	Nuclear Factor of Activated T-cells

PDI	Protein Disulfide Isomerase
PI	Phosphatidylinositol
PI4P	Phosphatidylinositol-4-phosphate
PI5KI	Type I phosphotidylinositol-4-phosphate 5-kinase
PIP_2	Phosphatidylinositol-(4,5)-bisphosphate
PIPs	Phosphatidylinositol phosphates
PKC	Protein Kinase C
PLC	Phospholipase C
PM	Plasma Membrane
RBL	Rat Basophilic Leukemia cell
S15	c-Src membrane targeting sequence
SAM	Sterile α Motif
STIM1	Stromal Interaction Molecule 1
SERCA	Sarcoplasmic-Endoplasmic Reticulum Ca^{2+} ATPase
SOC	Store Operated Ca^{2+}
SOCE	Store Operated Ca^{2+} Entry
TCR	T-Cell Receptor
TIRF	Total Internal Reflection Fluorescence
TMS	Trimethylsphingosine
TRPC	Canonical Transient Receptor Potential Channel

CHAPTER 1

INTRODUCTION

1.1 Mast cells mediate allergic reactions through the IgE receptor signaling pathway

Allergic disorders cause a spectrum of pathologies from rhinitis, asthma, and eczema to acute anaphylaxis. Despite the diversity of symptoms and severity, all allergic disorders are characterized by a hypersensitivity of the body's immune system to an otherwise innocuous substance. This so called type I hypersensitivity is caused by generation of immunoglobulin IgE in response to exposure to an allergen, and the subsequent sensitization of the body's immune system to this allergen via the binding of IgE to the membrane of immune cells. The primary cells associated with IgE mediated sensitization are basophils, primarily found in the circulatory system, and mast cells, found in peripheral tissues such as skin and mucosa. Because mast cells reside in tissues that are the primary sites of contact with foreign substances and therefore allergen exposure, they are considered the primary mediators of IgE mediated hypersensitivity. Both mast cells and basophils are characterized by a dense accumulation of allergic mediators into granules in the cytoplasm. Sensitized mast cells respond to exposure to allergen by releasing these allergic mediators such as histamine into the surrounding tissue in a process called degranulation, resulting in the characteristic symptoms associated with a particular allergic disorder. Because of both the widespread prevalence of allergic disorders and the severity of some cases, understanding the mechanism of IgE mediated mast cell degranulation is of significant importance.

1.1.1 Mast cells express the high affinity IgE Receptor, FcεRI

Mast cells are derived from CD34+ progenitor cells. During an allergic response, mast cells become sensitized to a particular antigen via the binding of IgE to the high affinity IgE receptor, FcεRI. This receptor in mast cells is a heterotetramer consisting of an α, β, and two γ subunits (Figure 1.1A). The α subunit binds IgE (Hakimi 1990) and is responsible for the high affinity of this receptor (10^{-10} M^{-1}), as opposed to so-called low affinity IgE receptor found in other cell types (Gould 2008). The γ subunits form a disulfide linked dimer and are associated with initiation of downstream signal transduction. The pairing of an α and two γ subunits constitutes an active IgE receptor associated with antigen presentation in other hematopoietic cell types (Kinet 1999), but in mast cells, the presence of the β subunit to form a tetrameric complex is associated with increased surface expression and increased signal transduction (Hartman 2008, Lin 1996). Both the β and γ subunits contain tyrosine phosphorylation sites conserved across all immunoglobulin receptors termed immune tyrosine activation motifs (ITAMs). In the resting state, tyrosine phosphatases maintain the ITAMs in a dephosphorylated state.

1.1.2 Multivalent antigen crosslinks the FcεRI receptor and initiates a tyrosine phosphorylation cascade

The IgE receptor signaling cascade leading to degranulation occurs in sensitized mast cells after exposure to multivalent antigen. Antigens with multiple epitopes simultaneously bind multiple IgEs on the cell surface and aggregate the associated FcεRI receptors. This aggregation is associated with translocation of the complex into

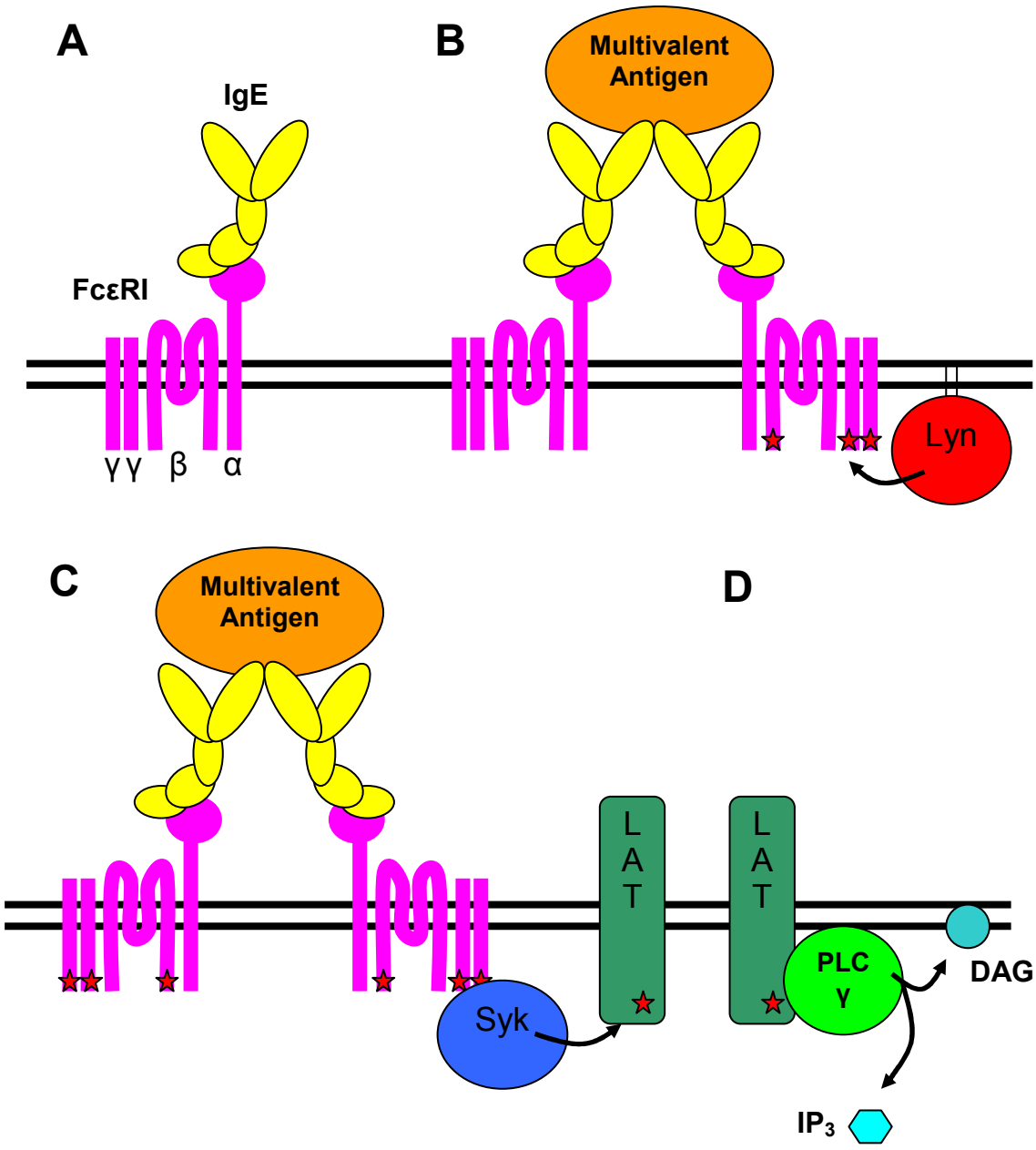

Figure 1.1: **Early IgE Receptor Signaling.** Schematic diagram depicting the first stages in IgE receptor signaling. A) The high affinity IgE receptor, FcεRI, consists of one IgE binding α subunit, a β subunit, and two γ subunits. B) After multiple receptors are crosslinked by multivalent antigen, the membrane-bound tyrosine kinase, Lyn, phosphorylates the β and γ subunits of FcεRI. C) The phosphorylated receptor recruits the cytoplasmic tyrosine kinase Syk, which phosphorylates LAT. D) Phosphorylated LAT recruits PLCγ to the plasma membrane, which cleaves PIP_2 to IP_3 and DAG.

detergent resistant membrane (DRM) domains in the plasma membrane (Sheets 1999). The DRM domains, also called lipid rafts, are distinguishable regions of the plasma membrane with increased concentrations of cholesterol, sphingolipids and saturated acyl chain phospholipids. DRM domains are associated with decreased mobility of transmembrane proteins, while letting proteins anchored to the membrane by lipids diffuse more readily. After translocation of the FcεRI receptor complex into the DRM domain, the accessibility of deactivating transmembrane phosphatases is significantly reduced, whereas the acylated tyrosine kinase Lyn is fully active and free to engage the FcεRI complex (Young 2005) (Figure 1.1B). The differential mobility of these proteins results in a 5x increase in the specific activity of Lyn (Young 2003), and the phosphorylation of ITAM sites on FcεRI (Lin 1996, Sil 2007). The phosphorylated γ subunit recruits the cytosolic tyrosine kinase Syk to the plasma membrane, where it phosphorylates the Linker for Activation of T-cells (LAT) (Saito 2000) (Figure 1.1C). LAT is a plasma membrane-associated adaptor protein that recruits phospholipase Cγ (PLCγ) to the plasma membrane, where it is phosphorylated and activated by Syk.

1.1.3 PLCγ mobilizes secondary messengers necessary for degranulation

Activated PLCγ cleaves the headgroup of the phospholipid phosphatidylinositol 4,5,-bisphosphate (PIP_2) to produce the secondary messengers inositol 1,4,5-trisphosphate (IP_3) and diacylglycerol (DAG) (Figure 1.1D). IP_3 binds to IP_3 receptor (IP_3R) on the ER membrane, activating Ca^{2+} efflux from ER stores. This Ca^{2+} store depletion results in the influx of extracellular Ca^{2+} via a mechanism termed Store Operated Calcium Entry (SOCE). The rise in intracellular Ca^{2+} is necessary for a wide range of effects including granule exocytosis (James 2008), and translocation of the Nuclear Factor of Activated T-cells (NFAT) to the nucleus, where it enhances transcription of

inflammatory cytokines (Yusang 2007). The other cleavage product of PLCγ, DAG, activated protein kinase C (PKC) at the plasma membrane. The combination of a rise in intracellular Ca^{2+} and PKC activation at the plasma membrane is necessary and sufficient to cause granule exocytosis (Sagi-Eisenberg 1984).

1.2 Store Operated Calcium Entry

Historically, SOCE was first proposed as a mechanism to explain why the release of Ca^{2+} associated with IP_3 generation was larger than the pool of Ca^{2+} in stores governed by IP_3R (Putney 1986). Depletion of stores using the sarcoplasmic/endoplasmic reticulum Ca^{2+} ATPase (SERCA) pump inhibitor, thapsigargin, similarly causes influx of extracellular Ca^{2+}, bolstering the hypothesis that influx was primarily controlled by the state of the internal Ca^{2+} stores (Putney 1993). The electrophysiological identification of Ca^{2+} Release Activated Ca^{2+} current (I_{CRAC}) was consistent with the presence of a store operated pool of Ca^{2+} (Hoth 1993). I_{CRAC} is an inwardly rectifying Ca^{2+} current triggered by release of Ca^{2+} from the lumen of the ER. I_{CRAC} is also characterized by its high sensitivity to inhibition by Gd^{3+} ions (Hoth 1993) and the pharmacological inhibitor 2-aminoethoxydiphenylborane (2-APB) (Ma 2000).

As described above, SOCE is an essential step in the mast cell mediated allergic response. However, SOCE is the primary mode of intracellular Ca^{2+} modulation in all non-excitable cells, and is utilized in a wide range of physiological processes. There are several varieties of Severe Combined Immunodeficiency Syndrome (SCIDS) associated with defects in SOCE (Feske 2010), due to its central role in the signaling of all hematopoietic cell types. Proliferation of T-cells is a SOCE dependent process (Lewis 2001). SOCE is essential in platelets for the formation of pathological thrombi, (Varga-Szabo 2008, Braun 2009). Migration of both metastatic

breast cancer cells (Yang 2009) and PDGF stimulated smooth muscle cells (Bisaillon 2010) is dependent on SOCE. Because of the wide range of clinical applications, the importance of understanding SOCE is not limited to the pursuit of understanding mast cell mediated signaling.

1.2.1 STIM1 and Orai1 are the essential protein components of SOCE

Two proteins are essential for SOCE: Stromal Interaction Molecule 1 (STIM1), an ER-transmembrane Ca^{2+} sensor (Liou 2005), and Orai1 (a.k.a. CRACM1), a tetraspan plasma membrane Ca^{2+} channel (Feske 2006) (Figure 1.2). The coexpression of STIM1 and Orai1 is sufficient to reconstitute SOCE in deficient cell types (Soboloff 2006). STIM1 contains a luminal EF-hand domain that senses depletion of Ca^{2+} from the ER (Zhang 2005). Mutation of the EF-hand domain in STIM1 to prevent Ca^{2+} binding results in constitutive influx of Ca^{2+} ions. Release of Ca^{2+} from the EF-hand domain following store depletion triggers oligomerization of STIM1 through its luminal, juxtamembrane sterile-α motif (SAM) domain (Stathopulos 2006), and this oligomerization triggers the translocation of STIM1 to regions of the ER that come into close proximity to the plasma membrane (Luik 2008) (Figure 1.3). Oligomerization of STIM1 triggers translocation to ER-plasma membrane junctions via the clustering of its C-terminal polylysine domain (Park 2009). Clustering of these basic motifs due to STIM1 oligomerization provides the energetic driving force for interaction with acidic phospholipids at the plasma membrane. Orai1 coaggregates with STIM1 at these ER-plasma membrane junctions, which opens its Ca^{2+} selective

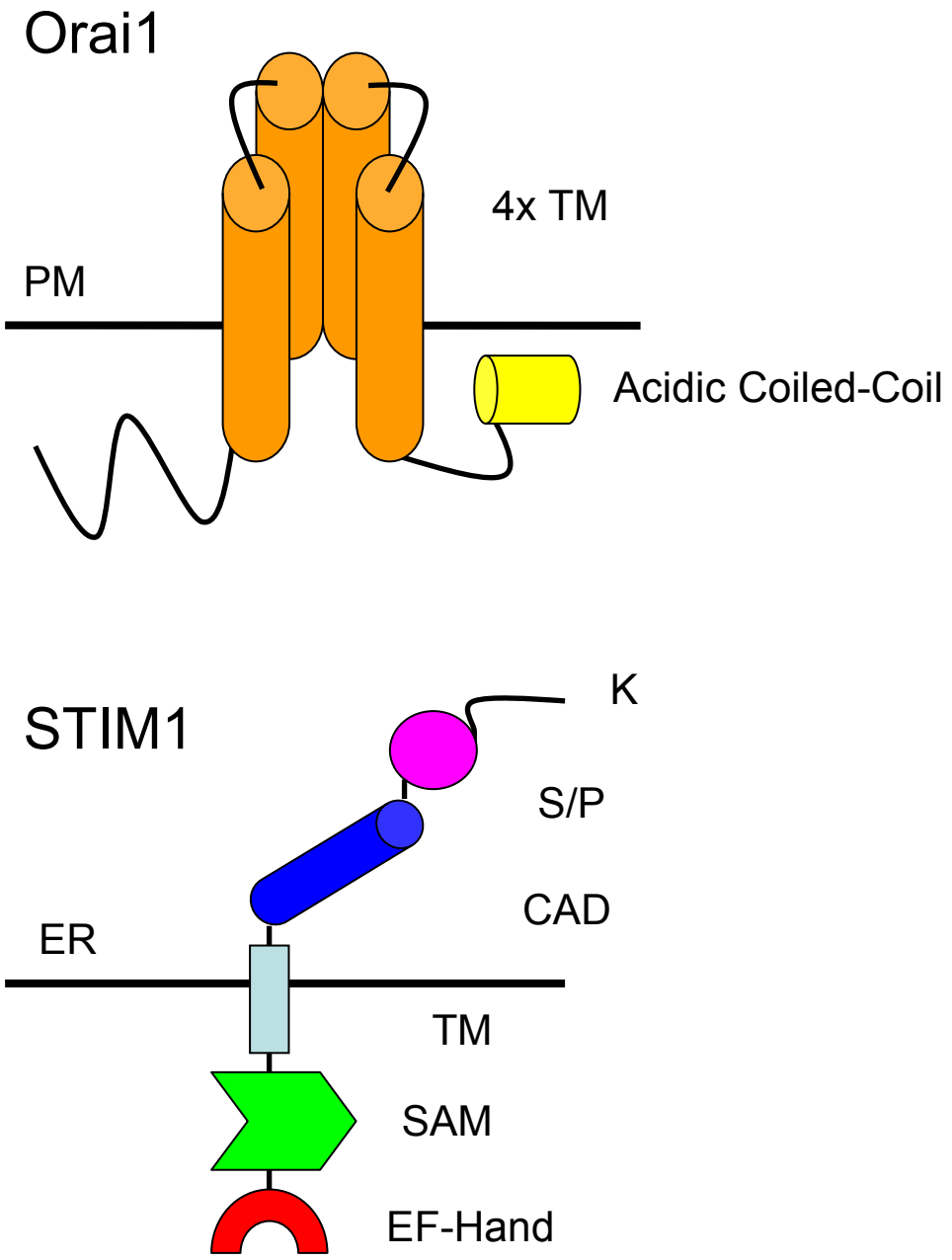

Figure 1.2: **Domain Strucure of Orai1 and STIM1.** Orai1 (top) is a plasma membrane (PM) localized Ca^{2+} channel, with the ion selective pore formed by four α-helical transmembrane domains (TM). Additionally, Orai1 contains a regulatory N-terminus and a C-terminus consisting of an acidic coiled-coil domain. STIM1 (bottom) is an ER transmembrane protein with a Ca^{2+} sensing luminal EF-hand domain. Additionally, STIM1 contains a sterile alpha motif (SAM), the CRAC activating domain (CAD), serine/proline rich domain (S/P), and a polylysine sequence (K).

pore, resulting in the characteristic inwardly rectifying Ca^{2+} current associated with SOCE. Orai1 interacts with the CRAC activating domain (CAD) on STIM1 to elicit influx (Park 2009). The CAD domain consists of a series of coil-coils, and also appears to be important for the oligomerization of STIM1 (Covington 2010). Soluble CAD spontaneously oligomerizes and initiates SOCE. However, the coupling of the CAD domain to either the polylysine motif or to the ER transmembrane domain of STIM1 prevents the activation of SOCE in the absence of stimulated oligomerization. The precise molecular nature of the interaction between the STIM1 CAD domain and Orai1 and the gating of Ca^{2+} influx is still poorly understood. STIM1 has one mammalian homologue, STIM2, that is associated with maintenance of the basal cytoplasmic Ca^{2+} levels and has a low level of constitutive translocation to the plasma membrane (Brandman 2007). STIM1 and STIM2 coaggregate after Ca^{2+} store depletion via their respective SAM domains. Orai1 has two homologues, Orai2 and Orai3. Heteropentameric complexes formed between Orai1 and Orai3 are arachidonate regulated Ca^{2+} channels instead of SOC channels (Mingnen 2009). Orai2 function is poorly understood. The interactions between all STIM and Orai isoforms are governed by the same CAD dependent mechanism.

1.2.2 Mutational analysis of STIM1 and Orai1

Numerous studies have been performed to elucidate the molecular mechanism of SOCE activation. The first studies to identify STIM1 as the ER Ca^{2+} sensor mutated residues in the Ca^{2+} binding EF-hand domain of STIM1 to produce a mutant that constitutively activates SOCE and punctae formation (Zhang 2005). Structural mutations in the EF-hand and SAM domains reveal that binding of Ca^{2+} into the EF-

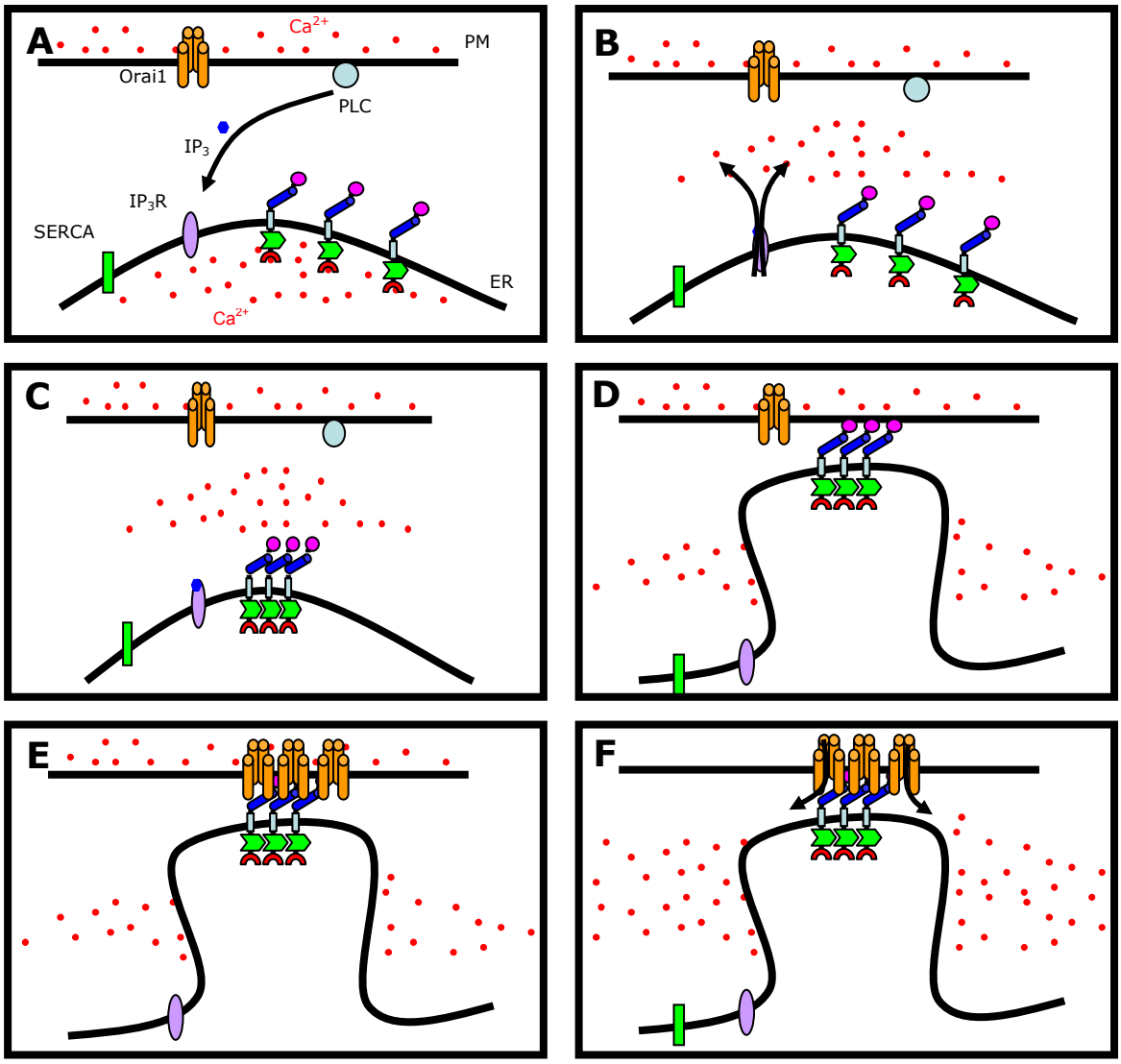

Figure 1.3: **Mechanism of STIM1 and Orai1-mediated SOCE.** A) Recruitment of PLCγ to the plasma membrane generates IP_3 by cleaving PIP_2. B) IP_3 binds to IP_3R in the ER membrane, releasing Ca^{2+} from the ER stores. C) Dissociation of Ca^{2+} from the EF-hand domain of STIM1 (red crecent) causes oligomerization mediated by the SAM domain of STIM1 (green). D) Oligomerization of STIM1 causes translocation to ER-plasma membrane junctions. E) Orai1 clusters with the STIM1 CAD domain at ER-plasma membrane junctions. F) Clustering of Orai1 initiates SOCE.

hand stabilizes the structure of both domains, and that in the Ca^{2+} unbound form, oligomerization is mediated by a poorly structured SAM domain (Staphopulos 2008). Mutations to remove the cytosolic coiled-coil domain of STIM1 impared its capacity to engage Orai1 and initiate SOCE (Baba 2006). However, the same study revealed that removal of the C-terminal polylysine motif of STIM1 did not impair its capacity to initiate Ca^{2+} influx. Mutations in this coiled-coil domain have been found to alter the selectivity of STIM1 for different Orai isoforms: STIM1 (L373S) cannot engage Orai1 or initiate SOCE without the simultaneous expression of Orai3 (Frischauf 2009).

Orai1 was initially identified as a dominant negative gene causing SCIDS. This gene encoded a mutant of Orai1 (R91W) that was dysfunctional in SOCE (Feske 2006). Later, it was determined that this mutation caused an increase in the hydrophobicity of the N-terminus of Orai1, leading to impaired Ca^{2+} influx (Derler 2009). Although Orai1 was known to be essential for SOCE, it was not definitively identified as the Ca^{2+} selective channel until mutations in the four transmembrane domains were demonstrated to alter the ion selectivity of the store operated response (Yeromin 2006). Muik, *et al*., demonstrated that the coiled-coil domain at the C-terminus of Orai1 is important for SOCE and the interaction with STIM1, because mutations to disrupt or delete this domain resulted in reduced Ca^{2+} influx and lack of punctae formation (Muik 2008). Additionally, they demonstrated that the N-terminus of Orai1 is important for SOCE, but mutations in this region did not reduce the capacity of STIM1 to bind Orai1.

1.3 PIP_2 as a signaling molecule

Phosphatidylinositol (PI) and its derivatives are phospholipid signaling molecules with

a diverse range of intracellular functions. The inositol head group can be multiply phosphorylated at the 3, 4, and 5 positions to yield different signaling molecules with different subcellular localizations. These phosphatidylinositol phosphates (PIPs) serve as biochemical markers for the recognition of different intracellular compartments. For instance, $PI(4,5)P_2$ is primarily localized at the plasma membrane, whereas PI4P and PI3P are localized at the Golgi and at endosomes, respectively (De Matteis 2004). Other PIPs serve to send broad spectrum signals about the state of the cell. For instance $PI(3,4,5)P_3$ is a signaling molecule associated with survival and differentiation (Cantley 2002)

$PI(4,5)P_2$ (or simply PIP_2) is one of the earliest identified and most widely studied PIPs, although it constitutes only ~1% of the total phospholipids content in the cell (McLaughlin 2002). PIP_2 is generated by the phosphorylation of PI(4)P at the plasma membrane by PI(4)P-5-kinase (PIP5K). PIP_2 is the primary mediator of the interaction between the cytoskeleton and the plasma membrane, and has therefore been implicated as essential for cell adhesion (Ling 2002), membrane ruffling (Honda 1999), and phagocytosis (Coppolino 2002). PIP_2 promotes membrane remodeling by recruiting the Wiscott-Aldrich syndrome protein (WASP) to the plasma membrane, where it initiates actin polymerization (Janmey 2004). PIP_2 also promotes integrin-mediated interaction with the extracellular matrix by activation of focal adhesion kinase (Ling 2002) and the formation of clathrin-coated pits by recruitment of AP-2 (Di Paolo 2006). The concentration of PIP_2 at the plasma membrane is tightly controlled by PIP5K and other enzymes, because in addition to its role in membrane remodeling, PIP_2 also serves as the substrate for phospholipase C (PLC) to generate IP_3 and DAG by cleavage of the inositol headgroup.

1.3.1 Interactions with PIP_2 at the plasma membrane are mediated by polybasic peptide sequences

PIP_2 contains a very high charge density with a net charge of -5 when fully deprotonated. This high negative charge density provides the driving force for the association PIP_2 with polybasic peptides carrying a high positive charge density (McLaughlin 2005). Polybasic motifs are very common throughout the proteome. For instance, of the approximately 60 known small GTPases, 37 are functionally recruited to the plasma membrane via polybasic motifs (Heo 2006). Moreover, PIP_2 is necessary for the function and trafficking of transmembrane proteins. T-cell receptor ζ (TCRζ), FcεRIγ, and epidermal growth factor (EGF) receptor all contain polybasic motifs important for their functionality (Sato 2006, Sigalov 2006). Based on their studies of the myristylated alanine-rich C-kinase substrate (MARCKS), McLaughlin and Aderem proposed that proteins use polybasic domains as a form of biochemical switch that senses a particular concentration of PIP_2 at the plasma membrane (McLaughlin 1995). Other studies have demonstrated that binding of Ca^{2+}-calmodulin (CaM) to the polybasic peptides in MARCKS and EGF receptor can reverse this association with PIP_2 (Arbuzova 1998, Sato 2006).

1.3.2 Pools of PIP_2

PIPs are the biochemical markers that delineate different membrane pools inside the cell. However, there are multiple lines of evidence suggesting that there are multiple distinctive pools of PIP_2 residing at the plasma membrane. Multiple functional pools of PIP_2 were identified in erythrocytes as early as 1987 (King 1987), but the nature of these pools has remained elusive. Vasudevan, *et al.*, found that PIP5Kβ and PIP5Kγ

generate two distinct functional pools of PIP_2 at the plasma membrane associated with SOCE and IP_3 production, respectively (Vasudevan 2009).

Because PIPs are normally the biological markers for membrane pools, there must be a different mechanism of differentiating multiple pools of PIP_2 in the plasma membrane. A distinct possibility is that PIP_2 pools are differentiated based on their localization to ordered lipid domains commonly called rafts and disordered membrane domains. Caveolin was originally implicated in the transport of PIP_2 into the raft fraction and the delineation of multiple PIP_2 pools (Pike 1996), but PIP_2 constitutively enters the raft membrane fraction as determined by sucrose gradient fractionation even in the absence of caveolin (Liu 1998). Besides simply concentrating at the plasma membrane, the polybasic effector domain of MARCKS and other polybasic small molecules have also been found to kinetically trap PIP_2 into lateral clusters (Denizov 1998, Wang 2002). The polybasic PIP_2 binding protein GAP-43 is known to recruit PIP_2 into the raft fraction (Tong 2007), and there are demonstrable differences in the biological function of PIP_2 in the raft and non-raft domains: non-raft localized PIP_2 appears to be more important for cytoskeletal remodeling and migration (Johnson 2008). There is also some evidence that signaling events leading to production of PIP_2 produce PIP_2 with more heavily saturated acyl chains than PIP_2 in the resting state in *Arabidopsis* (König 2007).

1.3.3 Role of PIP_2 in regulating ion channels.

Besides its role in regulating the cytoskeleton, PIP_2 is an important signaling molecule for the regulation of plasma membrane ion channels. PIP_2 has a clearly defined role in the regulation of TRP channels, voltage gated Ca^{2+} channels, IP_3R, ryanodine receptor (RyR), and Na^{+}-Ca^{2+} exchangers (Hilgemann 2001, Voets 2007). Moreover, the

signaling products of PIP_2, IP_3 and DAG, have been implicated in the regulation of intracellular ions as well: IP_3 is the master regulator of intracellular Ca^{2+} by releasing Ca^{2+} from intracellular stores via IP_3R, and DAG has been implicated in the gating of certain TRP channels (Hardie 2002). The same regulatory C-terminal coiled-coil on certain TRP channels that recognizes the presence of DAG also binds to and is activated by PIP_2 in other TRP channel isoforms. The TRP isoforms that bind PIP_2 contain a polybasic motif on this coiled-coil, whereas those that are gated by DAG contain a polyacidic motif. Mechanisms have been proposed whereby TRP channel regulation by DAG is mediated by the avoidance of unfavorable charge-charge interactions between the acid coiled-coil and PIP_2, whereas DAG can occupy the binding site without forcing these interactions. Similarly, the epithelial Na^+ channel (ENaC) is activated by PIP_2, and this activation is mediated by a juxtamembrane polybasic motif (Pochynyuk 2007a, Pochynyuk 2007b). Similar to other PIP_2 binding proteins, the polybasic PIP_2 binding motifs also serve as substrates for Ca^{2+}-calmodulin binding (Voets 2007), resulting in dual modulation by PIP_2 and Ca^{2+}.

1.4 Contributions from these studies

Despite the abundance of biochemical evidence indicating that the proteins STIM1 and Orai1 are necessary for SOCE and important for mast cell signaling, the precise molecular interactions between these proteins that facilitate SOCE are still poorly understood. In this dissertation, I present a series of studies to examine the molecular basis of the STIM1-Orai1 interaction. In Chapter 2, I describe a FRET-based assay for the interaction between fluorescently labeled STIM1 and Orai1. In this study, we find that following the antigen mediated stimulation of SOCE, there is remarkable little interaction between STIM1 and Orai1, suggesting that Ca^{2+} stores are quickly refilled

under these conditions. Also using this FRET assay, we determine that electrostatics at the plasma membrane play an important role in the clustering and activation of STIM1 and Orai1. We find that either the small molecule D-sphingosine or mutation of the C-terminal acidic coiled-coil of Orai1 induce punctae formation in the absence of colocalization of STIM1 and inhibites the STIM1-Orai1 association in response to thapsigargin.

In Chapter 3, we extend our initial identification of the C-terminal acidic coiled-coil of Orai1 as an important determinant of SOCE in order to identify its intermolecular binding partner on STIM1. We find that a short stretch of positively charged amino acids in the CAD domain of STIM1 is important for the interaction with Orai1. However, we find that when this STIM1 mutant was paired with the Orai1 coiled-coil mutant, a residual interaction between the two proteins was restored in the absence of Ca^{2+} influx. These results suggest that the interaction between the positively charged sequence in the STIM1-CAD and the acidic coiled-coil of Orai1 electrostatically gate Ca^{2+} influx.

In Chapter 4, I investigated the role of PIP_2 in the interaction between STIM1 and Orai1. Based on previous work (Vasudevan 2009), we understand that PI5KIβ and PI5KIγ have differential effects on SOCE, but the mechanism by which two functionally distinct pools of PIP_2 are maintained at the plasma membrane is poorly understood. We find that these two PI5KI isoforms differentially enrich PIP_2 in the DRM and DSM fractions. Using targeted PIP_2 phosphatases, we find that the STIM1-Orai1 interaction is differentially regulated by these two pools of PIP_2, and we identify polybasic sequences on both STIM1 and Orai1 that drive this selectivity.

REFERENCES

Arbuzova, A., Murray, D., and McLaughlin, S. (1998) MARCKS, membranes, and calmodulin: kinetics of their interaction. Biochim Biophys Acta. *1376*, 369-79.

Baba, Y., Hayashi, K., Fujii, Y., Mizushima, A., Watarai, H., Wakamori, M., Numaga, T., Mori, Y., Iino, M., Hikida, M., and Kurosaki, T. (2006) Coupling of STIM1 to store-operated Ca^{2+} entry through its constitutive and inducible movement in the endoplasmic reticulum. Proc Natl Acad Sci U S A. *103*, 16704-9.

Baba, Y., Nishida, K., Fujii, Y., Hirano, T., Hikida, M., and Kurosaki, T. (2008) Essential function for the calcium sensor STIM1 in mast cell activation and anaphylactic responses. Nat Immunol. *9*, 81-8.

Bisaillon, J.M., Motiani, R.K., Gonzalez-Cobos, J.C., Potier, M., Halligan, K.E., Alzawahra, W.F., Barroso, M., Singer, H.A., Jourd'heuil, D., and Trebak, M. (2010) Essential role for STIM1/Orai1-mediated calcium influx in PDGF-induced smooth muscle migration. Am J Physiol Cell Physiol. *298*, C993-1005.

Brandman, O., Liou, J., Park, W.S., and Meyer, T. (2007) STIM2 is a feedback regulator that stabilizes basal cytosolic and endoplasmic reticulum Ca^{2+} levels. Cell. *131*, 1327-39.

Braun, A., Varga-Szabo, D., Kleinschnitz, C., Pleines, I., Bender, M., Austinat, M., Bösl, M., Stoll, G., and Nieswandt, B. (2009) Orai1 (CRACM1) is the platelet SOC channel and essential for pathological thrombus formation. Blood. *113*, 2056-63.

Cantley, L.C. (2002) The phosphoinositide 3-kinase pathway. Science. *296*, 1655-7.

Coppolino, M.G., Dierckman, R., Loijens, J., Collins, R.F., Pouladi, M., Jongstra-Bilen, J., Schreiber, A.D., Trimble, W.S., Anderson, R., and Grinstein, S. (2002) Inhibition of phosphatidylinositol-4-phosphate 5-kinase Ialpha impairs localized actin remodeling and suppresses phagocytosis. J Biol Chem. *277*, 43849-57.

Covington, E.D., Wu, M.M., and Lewis, R.S. (2010) Essential Role for the CRAC Activation Domain in Store-dependent Oligomerization of STIM1. Mol Biol Cell. Apr 7. [Epub]

De Matteis, M.A., and Godi, A. (2004) PI-loting membrane traffic. Nat Cell Biol. *6*, 487-92.

Denisov, G., Wanaski, S., Luan, P., Glaser, M., and McLaughlin, S. (1998) Binding of basic peptides to membranes produces lateral domains enriched in the acidic

lipids phosphatidylserine and phosphatidylinositol 4,5-bisphosphate: an electrostatic model and experimental results. Biophys J. *74*, 731-44.

Derler, I., Fahrner, M., Carugo, O., Muik, M., Bergsmann, J., Schindl, R., Frischauf, I., Eshaghi, S., and Romanin, C. (2009) Increased hydrophobicity at the N terminus/membrane interface impairs gating of the severe combined immunodeficiency-related ORAI1 mutant. J Biol Chem. *284*, 15903-15.

Di Paolo, G., and De Camilli, P. (2006) Phosphoinositides in cell regulation and membrane dynamics. Nature. *443*, 651-657

Feske, S., Gwack, Y., Prakriya, M., Srikanth, S., Puppel, S. H., Tanasa, B., Hogan, P. G., Lewis, R. S., Daly, M. and Rao, A. (2006) A mutation in Orai1 causes immune deficiency by abrogating CRAC channel function. Nature *441*, 179–185.

Feske, S., Picard, C., and Fischer, A. (2010) Immunodeficiency due to mutations in ORAI1 and STIM1. Clin Immunol. *135*, 169-82.

Frischauf, I., Muik, M., Derler, I., Bergsmann, J., Fahrner, M., Schindl, R., Groschner, K., and Romanin, C. (2009) Molecular determinants of the coupling between STIM1 and Orai channels: differential activation of Orai1-3 channels by a STIM1 coiled-coil mutant. J Biol Chem. *284*, 21696-706.

Gould, H.J., and Sutton, B.J. (2008) IgE in allergy and asthma today. Nat Rev Immunol. *8*, 205-17.

Gwack, Y., Feske, S., Srikanth, S., Hogan, P.G., and Rao, A. (2007) Signalling to transcription: Store-operated Ca^{2+} entry and NFAT activation in lymphocytes. Cell Calcium. *42*, 145-156

Hakimi, J., Seal,s C., Kondas, J.A., Pettine, L., Danho, W., and Kochan, J. (1990) The α subunit of the human IgE receptor (FcεRI) is sufficient for high affinity IgE binding. J Biol Chem. *265*, 22079-81.

Hardie, R.C. (2002) Regulation of TRP channels via lipid second messengers. Annu Rev Physiol. *65*, 735-59.

Hartman, M.L., Lin, S.Y., Jouvin, M.H., and Kinet, J.P. (2008) Role of the extracellular domain of FcεRIα in intracellular processing and surface expression of the high affinity receptor for IgE FcεRI. Mol Immunol. *45*, 2307-11.

Heo, W.D., Inoue, T., Park, W.S., Kim, M.L., Park, B.O., Wandless, T.J., and Meyer, T. (2006) $PI(3,4,5)P_3$ and $PI(4,5)P_2$ lipids target proteins with polybasic clusters to the plasma membrane. Science. *314*, 1458-61.

Hilgemann, D.W., Feng, S., and Nasuhoglu, C. (2001) The complex and intriguing lives of PIP_2 with ion channels and transporters. Sci STKE. *2001*, re19.

Hoth, M., and Penner, R. (1993) Calcium release-activated calcium current in rat mast cells. J Physiol *465*, 359–386.

James, D.J., Khodthong, C., Kowalchyk, J.A., and Martin, T.F. (2008) Phosphatidylinositol 4,5-bisphosphate regulates SNARE-dependent membrane fusion. J Cell Biol. *182*, 355-66.

Johnson, C.M., Chichili, G.R., and Rodgers, W. (2008) Compartmentalization of phosphatidylinositol 4,5-bisphosphate signaling evidenced using targeted phosphatases. J Biol Chem. *283*, 29920-8.

Honda, A., Nogami, M., Yokozeki, T., Yamazaki, M., Nakamura, H., Watanabe, H., Kawamoto, K., Nakayama, K., Morris, A.J., Frohman, M.A., and Kanaho, Y. (1999) Phosphatidylinositol 4-phosphate 5-kinase α is a downstream effector of the small G protein ARF6 in membrane ruffle formation. Cell. *99*, 521-32.

Janmey, P.A., and Lindberg, U. (2004) Cytoskeletal regulation: rich in lipids. Nat Rev Mol Cell Biol. *5*, 658-66.

Kinet, J.P. (1999) The high-affinity IgE receptor (FcεRI): from physiology to pathology. Annu Rev Immunol. *17*, 931-72.

King, C. E., Stephens, L. R., Hawkins, P. T., Guy, G. R., Michell, R. H. (1987) Multiple metabolic pools of phosphoinositides and phosphatidate in human erythrocytes incubated in a medium that permits rapid transmembrane exchange of phosphate. Biochem. J. *244*, 209-217.

König, S., Mosblech, A., and Heilmann, I. (2007) Stress-inducible and constitutive phosphoinositide pools have distinctive fatty acid patterns in Arabidopsis thaliana. FASEB J. *21*, 1958-67.

Lewis, R.S. (2001) Calcium signaling mechanisms in T lymphocytes. Ann. Rev. Immunol. *19*, 497–521.

Lin, S., Cicala, C., Scharenberg, A.M., and Kinet, J.P. (1996) The FcεRIβ subunit functions as an amplifier of FcεRIγ-mediated cell activation signals. Cell. *85*, 985-95.

Ling, K., Doughman, R.L., Firestone, A.J., Bunce, M.W., and Anderson, R.A. (2002) Type Iγ phosphatidylinositol phosphate kinase targets and regulates focal adhesions. Nature. *420*, 89-93.

Liou, J., Kim, M. L., Heo, W. D., Jones, J. T., Myers, J. W., Ferrell, J. E., Jr. and Meyer, T. (2005) STIM is a Ca^{2+} sensor essential for Ca^{2+}-store-depletion-

triggered Ca^{2+} influx Curr. Biol. 15, 1235– 1241.

Liu, Y., Casey, L., and Pike, L.J. (1998) Compartmentalization of phosphatidylinositol 4,5-bisphosphate in low-density membrane domains in the absence of caveolin. Biochem Biophys Res Commun. *245*, 684-90.

Luik, R.M., Wang, B., Prakriya, M., Wu, M.M., and Lewis, R.S. (2008) Oligomerization of STIM1 couples ER calcium depletion to CRAC channel activation. Nature. *454*, 538-42.

Ma, H.T., Patterson, R.L., Van Rossum, D.B., Birnbaumer, L., Mikoshiba, K., and Gill, D.L. (2000) Requirement of the inositol trisphosphate receptor for activation of store-operated Ca^{2+} channels. Science *287*, 1647–1651.

McLaughlin, S., and Aderem, A. (1995) The myristoyl-electrostatic switch: a modulator of reversible protein-membrane interactions. Trends Biochem Sci. *20*, 272-6.

McLaughlin, S., and Murray, D. (2005) Plasma membrane phosphoinositide organization by protein electrostatics. Nature. *438*, 605-11.

McLaughlin, S., Wang, J., Gambhir, A., and Murray, D. (2002) PIP_2 and proteins: interactions, organization, and information flow. Annu Rev Biophys Biomol Struct. *31*, 151-75.

Mignen, O., Thompson, J.L., and Shuttleworth, T.J. (2009) The molecular architecture of the arachidonate-regulated Ca^{2+}-selective ARC channel is a pentameric assembly of Orai1 and Orai3 subunits. J Physiol. *587*, 4181-97.

Muik, M., Frischauf, I., Derler, I., Fahrner, M., Bergsmann, J., Eder, P., Schindl, R., Hesch, C., Polzinger, B., Fritsch, R., Kahr, H., Madl, J., Gruber, H., Groschner, K., and Romanin, C. (2008) Dynamic coupling of the putative coiled-coil domain of ORAI1 with STIM1 mediates ORAI1 channel activation. J Biol Chem. *283*, 8014-22.

Parekh, A.B., and Penner, R. (1997) Store-operated calcium influx. Physiol Rev *77*, 901–930.

Park, C.Y., Hoover, P.J., Mullins, F.M., Bachhawat, P., Covington, E.D., Raunser, S., Walz, T., Garcia, K.C., Dolmetsch, R.E., and Lewis R.S. (2009) STIM1 clusters and activates CRAC channels via direct binding of a cytosolic domain to Orai1. Cell. *136*, 876-90.

Pike, L.J., and Casey, L. (1996) Localization and turnover of phosphatidylinositol 4,5-bisphosphate in caveolin-enriched membrane domains. J Biol Chem. *271*, 26453-6.

Pochynyuk, O., Tong, Q., Staruschenko, A., and Stockand, J.D. (2007a) Binding and direct activation of the epithelial Na^+ channel (ENaC) by phosphatidylinositides. J Physiol. *580*, 365-72

Pochynyuk, O., Tong, Q., Medina, J., Vandewalle, A., Staruschenko, A., Bugaj, V., and Stockand, J.D. (2007b) Molecular determinants of PI(4,5)P_2 and PI(3,4,5)P_3 regulation of the epithelial Na^+ channel. J Gen Physiol. *130*, 399-413.

Putney, J.W. (1986) A model for receptor-regulated calcium entry. Cell Calcium. *7*, 1-12

Putney, J.W., and Bird, G.S. (1993) The inositol phosphate-calcium signaling system in nonexcitable cells. Endocr Rev. *14*, 610-31

Sagi-Eisenberg, R., and Pecht, I., (1984) Protein kinase C, a coupling element between stimulus and secretion of basophils. Immunol. Lett. *8*, 237–241.

Saitoh, S., Arudchandran, R., Manetz, T.S., Zhang, W., Sommers, C.L., Love, P.E., Rivera, J., and Samelson, L.E. (2000) LAT is essential for FcεRI-mediated mast cell activation. Immunity. *12*, 525-35.

Sato, T., Pallavi, P., Golebiewska, U., McLaughlin, S., and Smith, S.O. (2006) Structure of the membrane reconstituted transmembrane-juxtamembrane peptide EGFR(622-660) and its interaction with Ca^{2+}/calmodulin. Biochemistry. *45*, 12704-14.

Sheets, E.D., Holowka, D., and Baird, B. (1999) Critical role for cholesterol in Lyn-mediated tyrosine phosphorylation of FcεRI and their association with detergent-resistant membranes, J. Cell Biol. *145*, 877–887

Sigalov, A.B., Aivazian, D.A., Uversky, V.N., and Stern, L.J. (2006) Lipid-binding activity of intrinsically unstructured cytoplasmic domains of multichain immune recognition receptor signaling subunits. Biochemistry. *45*, 15731-9.

Sil, D., Lee, J.B., Luo, D., Holowka, D., and Baird, B. (2007) Trivalent ligands with rigid DNA spacers reveal structural requirements for IgE receptor signaling in RBL mast cells. ACS Chem Biol. *2*, 674-84.

Soboloff, J., Spassova, M.A., Tang, X.D., Hewavitharana, T., Xu, W., and Gill, D.L. (2006) Orai1 and STIM reconstitute store-operated calcium channel function. J Biol Chem. *281*, 20661-5.

Stathopulos, P.B., Li, G.Y., Plevin, M.J., Ames, J.B., and Ikura, M. (2006) Stored Ca^{2+} depletion-induced oligomerization of stromal interaction molecule 1 (STIM1) via the EF-SAM region: An initiation mechanism for capacitive Ca^{2+} entry. J Biol Chem. *281*, 35855-62.

Stathopulos, P.B., Zheng, L., Li, G.Y., Plevin, M.J., and Ikura, M. (2008) Structural and mechanistic insights into STIM1-mediated initiation of store-operated calcium entry. Cell. *135*, 110-22.

Tong, J., Nguyen, L., Vidal, A., Simon, S.A., Skene, J.H., and McIntosh T.J. (2008) Role of GAP-43 in sequestering phosphatidylinositol 4,5-bisphosphate to Raft bilayers. Biophys J. *94*, 125-33.

Varga-Szabo, D., Braun, A., Kleinschnitz, C., Bender, M., Pleines, I., Pham, M., Renné, T., Stoll, G., and Nieswandt, B. (2008) The calcium sensor STIM1 is an essential mediator of arterial thrombosis and ischemic brain infarction. J Exp Med. *205*, 1583-91.

Vasudevan, L., Jeromin, A., Volpicelli-Daley, L., De Camilli, P., Holowka, D., and Baird, B. (2009) The β- and γ-isoforms of type I PIP5K regulate distinct stages of Ca^{2+} signaling in mast cells. J Cell Sci. *122*, 2567-74.

Vig, M., Peinelt, C., Beck, A., Koomoa, D. L., Rabah, D., Koblan-Huberson, M., Kraft, S., Turner, H., Fleig, A., Penner, R. and Kinet, J. P. (2006) CRACM1 is a plasma membrane protein essential for store-operated Ca^{2+} entry. Science *312*, 1220– 1223.

Voets, T., and Nilius, B. (2007) Modulation of TRPs by PIPs. J Physiol. *582*, 939-44.

Wang, J., Gambhir, A., Hangyás-Mihályné, G., Murray, D., Golebiewska, U., and McLaughlin, S. (2002) Lateral sequestration of phosphatidylinositol 4,5-bisphosphate by the basic effector domain of myristoylated alanine-rich C kinase substrate is due to nonspecific electrostatic interactions. J Biol Chem. *277*, 34401-12.

Yang, S., Zhang, J.J., and Huang, X.Y. (2009) Orai1 and STIM1 are critical for breast tumor cell migration and metastasis. Cancer Cell. *15*, 124-34.

Yeromin, A.V., Zhang, S.L., Jiang, W., Yu, Y., Safrina, O., and Cahalan, M.D. (2006) Molecular identification of the CRAC channel by altered ion selectivity in a mutant of Orai. Nature. *443*, 226-9.

Young, R.M., Holowka, D., and Baird, B. (2003) A lipid raft environment enhances Lyn kinase activity by protecting the active site tyrosine from dephosphorylation. J Biol Chem. *278*, 20746-52.

Young, R.M., Zheng, X., Holowka, D., and Baird, B. (2005) Reconstitution of regulated phosphorylation of FcepsilonRI by a lipid raft-excluded protein-tyrosine phosphatase. J Biol Chem. *280*, 1230-5.

Zhang, S. L., Yu, Y., Roos, J., Kozak, J. A., Deerinck, T. J., Ellisman, M. H.,

Stauderman, K. A. and Cahalan, M. D. (2005) STIM1 is a Ca^{2+} sensor that activates CRAC channels and migrates from the Ca^{2+} store to the plasma membrane. Nature *437*, 902– 905.

CHAPTER 2

MOLECULAR CLUSTERING OF STIM1 WITH ORAI1/CRACM1 AT THE PLASMA MEMBRANE DEPENDS DYNAMICALLY ON DEPLETION OF CA^{2+} STORES AND ON ELECTROSTATIC INTERACTIONS[1]

2.1 Abstract

Activation of store operated Ca^{2+} entry involves stromal interaction molecule 1 (STIM1), localized to the endoplasmic reticulum (ER), and Ca^{2+} channel subunit (Orai1/CRACM1), localized to the plasma membrane. Confocal microscopy shows that thapsigargin-mediated depletion of ER Ca^{2+} stores in RBL mast cells causes a redistribution of STIM1, labeled with monomeric red fluorescent protein mRFP, to micron-scale ER-plasma membrane junctions that contain Orai1/CRACM1, labeled with monomeric green fluorescent protein AcGFP. Using fluorescence resonance energy transfer (FRET), we determine that this visualized co-redistribution is accompanied by nanoscale interaction of STIM1-mRFP and AcGFP-Orai1/CRACM1. We find that antigen stimulation of IgE receptors causes much less Orai1/CRACM1 and STIM1 association, but strong interaction is observed under conditions that prevent refilling of ER stores. Stimulated association monitored by FRET is inhibited by sphingosine derivatives in parallel with inhibition of Ca^{2+} influx. Similar structural and functional effects are caused by mutation of acidic residues in the cytoplasmic segment of Orai1/CRACM1, suggesting a role for electrostatic interactions via these residues in the coupling of Orai1/CRACM1 to STIM1. Our results reveal dynamic molecular interactions between STIM1 and Orai1/CRACM1 that depend

[1] Reproduced with permission from *Mol Biol Cell*. (2009) *20*, 389-99. Copyright 2009, American Society of Cell Biology

quantitatively on electrostatic interactions and on the extent of store depletion.

2.2 Introduction

Modulation of cytosolic Ca^{2+} levels is central to the regulation of a wide range of physiological processes. One of the key mechanisms of Ca^{2+} regulation in mammalian cells is Ca^{2+} release activated Ca^{2+} (CRAC) influx, in which the depletion of intracellular stores of Ca^{2+} triggers a sustained influx of Ca^{2+} from the extracellular medium. The CRAC current (I_{CRAC}) was characterized initially in hematopoietic cells in electrophysiological studies (Lewis 1989, Hoth 1992), but the proteins that mediate this process eluded investigators for nearly 20 years.

Recent advances are identification of two key proteins that regulate I_{CRAC}: STIM1 that localizes to the ER and Orai1/CRACM1 that is found in the plasma membrane. Expression of these two proteins is sufficient to reconstitute I_{CRAC} in deficient cells (Soboloff 2006). STIM1 has a Ca^{2+} binding, EF-hand domain positioned in the ER lumin (Roos 2005, Liou 2005). Orai1/CRACM1 has been identified as the CRAC channel in the plasma membrane (Feske 2006, Vig 2006a). Both STIM1 (Baba 2008) and Orai1/CRACM1 (Vig 2008) have recently been shown to be essential for stimulated mast cell degranulation. These discoveries have opened up a pathway to mechanistic understanding of I_{CRAC} and, in particular, the participation of these two proteins.

In initial studies, treatment of cells with the sarcoplasmic/endoplasmic reticulum Ca^{2+} ATPase (SERCA) inhibitor, thapsigargin, were shown to cause redistribution of STIM1 to form punctae at or near the plasma membrane, and these were identified as locations of CRAC activity (Liou 2005, Luik 2006). Mutations in the EF-hand domain of STIM1 resulted in constitutively active I_{CRAC} and translocation

of STIM1 to the plasma membrane, indicating that this protein is the Ca^{2+} sensor responsible for transmitting the signal for store-operated Ca^{2+} entry (SOCE) (Liou 2005). These results imply that these punctae are regions where ER and plasma membranes become closely associated, such that STIM1 can relay the signal that stores are empty to Orai1/CRACM1. This visualization by microscopy provides evidence that functionally relevant STIM1-Orai1/CRACM1 association occurs on the micron-scale, but it cannot specify whether direct interactions between these two proteins are involved in this activation mechanism. Two recent studies demonstrated nanoscale interactions between STIM1 and Orai1/CRACM1 as detected with fluorescence resonance energy transfer (FRET) in HEK cells (Muik 2008) and in T cells (Barr 2008).

The present study shows that interactions between STIM1 and Orai1/CRACM1 occur in a highly regulated manner when SOCE is activated by IgE receptor stimulation of RBL mast cells. To understand this regulation we compared, with confocal imaging and FRET, the antigen-stimulated association of STIM1 and Orai1/CRACM1 under conditions where the extent of store refilling is altered: by elimination of extracellular Ca^{2+} and by treatment with Gd^{3+}, which inhibits SOCE. Our results reveal that molecular interaction between STIM1 and Orai1/CRACM1 depends dynamically on the extent of store depletion. Furthermore, inhibition of this interaction by sphingosine derivatives and by point mutations of acidic residues in Orai1/CRACM1 suggest an electrostatic mechanism involving the C-terminal segment of Orai1/CRACM1, providing new insights into the mechanism of antigen-mediated activation and regulation of I_{CRAC}.

2.3 Experimental

2.3.1 Cloning and Constructs.

STIM1 cDNA encoded in a pcDNA4-myc-his vector was a genous gift from Monika Vig and Jean-Pierre Kinet (Vig 2006b). The fusion of monomeric red fluorescent protein (mRFP) to the 3' end of STIM1 was constructed by cloning mRFP cDNA from mRFP-pRSETb plasmid (Campbell 2002), a gift from Dr. E. Cox, Princeton University. This cDNA was inserted into the NotI and XhoI sites of the STIM1 vector. A Kozac consensus sequence was inserted at the start codon to enhance expression, and inclusion of a stop codon on the 3' tail of mRFP prevented expression of the myc and his epitope tags. Orai1/CRACM1 cDNA encoded as a C-terminally FLAG-tagged construct in a pcDNA4 vector was a generous gift of Monika Vig and Jean-Pierrre Kinet (Vig 2006b). The fusion of Orai1 to the 3' end of *Aequorea coerulescens* green fluorescent protein 1 (AcGFP) was constructed by cloning Orai1/CRACM1 from the pcDNA4 vector and inserting it into the BglII and KpnI sites of pAcGFP1-C1 (Clontech). Mutants of Orai1/CRACM1 were constructed by overlap-extension PCR and ligated into the BglII and KpnI sites of the pAcGFP1-C1 vector. A detailed description of the primers involved is included in Supplemental Methods. A plasmid containing cDNA for the PIP_2-specific PH domain from phospholipase C δ fused to the N-terminus of eGFP (PH-eGFP; Várnai 1998) was obtained from Dr. Andreas Jeromin, Allen Institute for Brain Science, Seattle WA. The construct ER-eGFP was constructed by ligation of the gene encoding the calreticulin ER localization sequence into the BglII and EcoRI sites and ligation of KDEL signal sequence into the BsrGI and NotI sites of pEGFP-N1 vector.

2.3.2 Cell culture.

RBL-2H3 mast cells were cultured as monolayers in minimal essential medium supplemented with 1 μg/ml gentamicin and 20% (v/v) fetal bovine serum. In preparation for imaging, cells were harvested with trypsin/EDTA and passed at 25% confluence into 35 mm Mat-Tek dishes. After approximately 20 h, cells were transfected with fluorescent or epitope-tagged versions of STIM1 and Orai1/CRACM1. These constructs were co-transfected using either Geneporter (Genlantis) or Fugene HD (Roche) per manufacturers' instructions, with modifications to enhance transfection efficiency in the RBL cells previously described (Gosse 2005). Cells were sensitized with IgE by incubation with 650 ng/mL monoclonal anti-DNP IgE overnight. Cells were imaged live or fixed 24 h after transfection.

COS7 cells were cultured as monolayers in Dulbecco's modified Eagle's medium supplemented with 1 μg/ml gentamicin and 10% (v/v) fetal bovine serum. In preparation for imaging, cells were harvested and trasfected with Fugene HD according to manufacturer's instructions.

2.3.3 Live cell imaging.

Immediately prior to imaging, RBL-2H3 cells were washed and incubated for 5 min at 37°C in 2.5 mL buffered salt solution (BSS: 135 mM NaCl, 5 mM KCl, 1 mM $MgCl_2$, 5.6 mM glucose, 1 mg/ml BSA, 20 mM HEPES, pH 7.4) in the absence or presence of 1.8 mM $CaCl_2$, or $CaCl_2$ with or without 6 μM $GdCl_3$. Cells imaged in the presence of D-sphingosine, N,N-dimethylsphingosine (DMS) , or N,N,N-trimethylsphingosine (TMS) (Avanti Polar Lipids, Inc.) were treated with 0.5 mL of BSS containing the compound (7.6 μM final concentration) immediately prior to imaging. Cells were then

imaged on a Leica TCS SP2 microscope with a Leica APO 63x dipping objective. Cells were excited at 488 nm and 543 nm, with laser intensity and phototube sensitivity adjusted to maximize signal/noise. Fluorescence emission was monitored at 495-540 nm and 555-675 nm. All live cell imaging was carried out at 37°C. After observing the resting state of the cells, they were stimulated by the addition of 0.5 mL of BSS containing thapsigargin (150 nM final concentration) or multivalent antigen DNP-BSA (final concentration 3 nM in BSA). Leica Confocal Software was used during the experiment to acquire images, and ImageJ was used post acquisition to prepare composite micrographs by uniform contrast adjustment.

2.3.4 Calcium measurements.

Immediately prior to imaging, COS7 cells were incubated with 0.9 μM fluo-4-AM (Molecular Probes) for 10 minutes in BSS containing 0.5 mM sulfinpyrizone. Cell were then washed and resuspended in BSS/sulfinpyrazone. Fields of cells were imaged during thapsigargin stimulation with an Olympus APO 40x dipping objective, under the same conditions and settings as described for multicolor imaging. The increase in green fluorescence in the cell body due to stimulation with thapsigargin was quantified using ImageJ software. For Ca^{2+} measurement in RBL-2H3 cells, indo-1 was loaded and monitored in a stirred cuvette by steady-state fluorimetry as previously described (Pierini 1997).

2.3.5 FRET imaging.

RBL-2H3 cells were imaged for FRET using the imaging system and cell preparation described above for multicolor live cell imaging. For cells stimulated with antigen,

cytochalasin D (2 μM) was added immediately prior to imaging to minimize stimulated cell ruffling. Under these conditions, antigen stimulated Ca^{2+} responses are slightly enhanced (Pierini 1997). Cytochalasin D did not alter the FRET response to thapsigargin (data not shown). The Förster distance corresponding to the distance for 50% efficiency of FRET between eGFP and DsRed is calculated to be between 47 and 58 Å (Erickson 2003), and this is expected to be similar for AcGFP and mRFP used in our measurements. Cross-sectional images of cells containing both protein constructs were monitored for fluorescence emission at 495-540 nm for AcGFP and 575-700 nm for mRFP (chosen to minimize bleedthrough), using an excitation wavelength of 476 nm. Irradiation at this wavelength provides adequate excitation of the AcGFP donor with negligible direct excitation of the mRFP acceptor. Laser intensity (set to minimize photobleaching of the donor), phototube sensitivity, and other settings remained constant for all FRET experiments. Throughout the time course of an individual experiment, images were taken simultaneously every 10 seconds for the red and green emission channels, and all FRET imaging was carried out at 37°C. Cells in 2.5 ml BSS were treated with thapsigargin, DNP-BSA, $CaCl_2$, or $GdCl_3$ by addition of 0.5 mL of BSS containing each, similarly to live cell imaging experiments. Cells were treated with D-sphingosine, N,N-dimethylsphingosine (DMS) , or N,N,N-trimethylsphingosine (TMS) similarly by addition of 0.5 mL BSS containing the sphingosine derivative immediately prior to the first image collected in each FRET sequence.

2.3.6 FRET calculations.

The collected series of fluorescence images were quantified using a script written in Matlab to determine the degree of FRET (see Supplemental Methods). The script,

based on previous analyses of FRET data (Guo 1994, van Rheenen 2004), begins by using the green channel image at each time point to make a mask of the pixels containing donor fluorescence (Das 2008). Next, the integrated intensity of the pixels under the mask for each time point is calculated. Because the acceptor does not detectably co-localize with the donor prior to stimulation, the red pixel values prior to stimulation were attributed to bleed-through of donor fluorescence into the red channel. These pre-stimulation red and green integrated intensities were used to calculate the coefficient of bleed-through (β) by least squares analysis, accordingly to correct all other red channel integrated intensities for bleed-through. β was found to be nearly constant at approximately 0.1 for all experiments. Lastly, the corrected ratio between the red and green integrated intensities at each time point was calculated as a relative measure of FRET according to Eq 1 (van Rheenen 2004):

$$FRET = \frac{M_A - \beta M_D}{M_D} \qquad (1)$$

where M_d is the measured donor fluorescence and M_A is the measured acceptor fluorescence as integrated from the equatorial image at each time point. Both M_d and M_A are corrected by subtracting background pixel gray values. Time course data from individual cells (between 6-20 cells analyzed for each condition) were averaged, and these average time courses are plotted in Figures 2.4 and 2.5. The variation in protein expression for FRET measurements was quantified as a function of AcGFP fluorescence for the set of data used to calculate FRET after thapsigargin stimulation (Figure 2.4A). The expression levels of AcGFP-Orai1/CRACM1 and STIM1-mRFP are highly correlated between different cells (data not shown), so the measured AcGFP fluorescence provides an indication of expression levels for both proteins. As seen in Supplemental Figure B.1, variation in the level of

protein expression is >3-fold for these cells, but no correlation between expression levels and the magnitude of stimulated FRET was observed.

2.3.7 Supplemental Material.

Supplemental Methods (see apendex B) include the primer sequences used in cloning, description of the results shown in figure B.5, supplemental figures B.1 – B.5, and the annotated Matlab script used to quantify image data for FRET measurement.

2.4 Results

2.4.1 STIM1 redistribution upon thapsigargin stimulation is accompanied by rearrangement of the ER in RBL mast cells.

Previous reports indicated that the subcellular localization of STIM1 in unstimulated cells depends on microtubules (Kurosaki 2006, Mercer 2006), and that STIM1 co-localizes with an ER marker (Liou 2005, Wu 2006). In unstimulated RBL cells, STIM1-mRFP substantially colocalizes with α-tubulin-eGFP (Supplemental Figure B.2). To evaluate spatial relationships to ER components in RBL cells, STIM1-mRFP and ER-eGFP, a luminally targeted protein, were transiently co-expressed. In unstimulated cells, STIM1-mRFP shows very limited co-localization with ER-eGFP largely because of its greater mictrotubule association than this luminal ER marker (Figure 2.1A). However, upon stimulation with thapsigargin, STIM1-mRFP and ER-eGFP become more extensively co-localized in reticulated, micron-sized sheets of ER membrane (Figure 2.1B). Under these conditions, microtubule association of STIM1 appears reduced (data not shown). Similar results are obtained when the subcellular

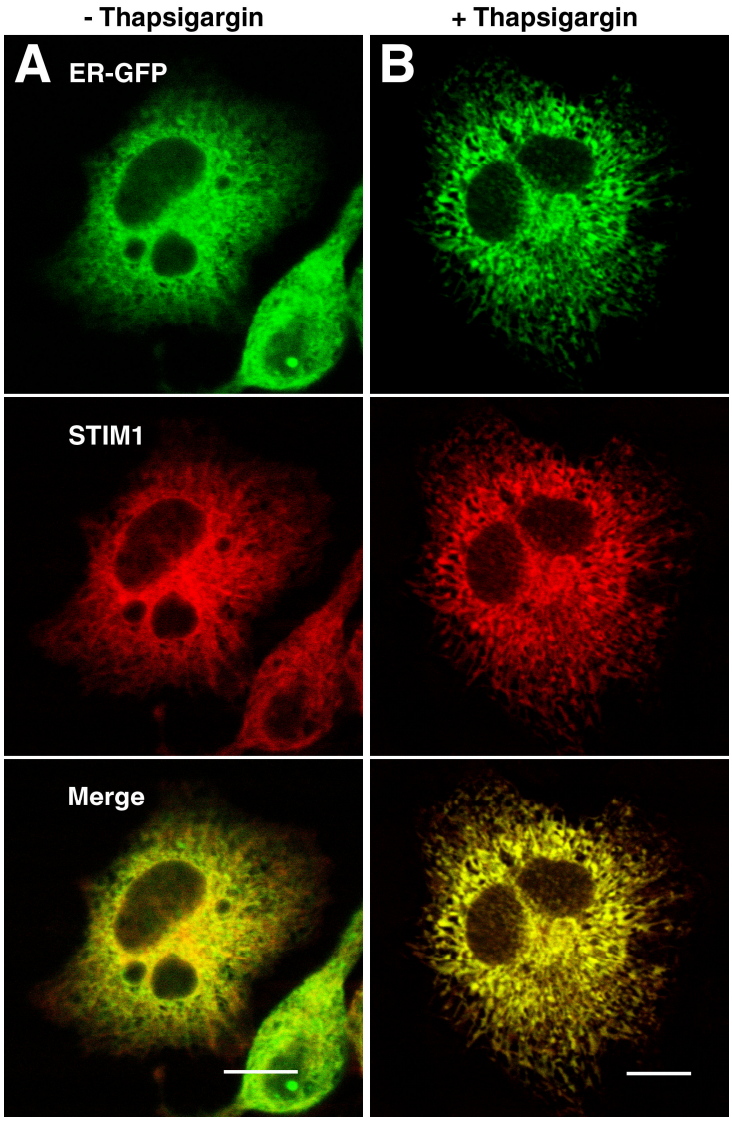

Figure 2.1: **RBL mast cell expressing STIM1-mRFP (red) and ER-eGFP (green) exhibits stimulation-dependent changes in localization of these proteins.** Representative cells are shown prior to (A) and after (B) stimulation with thapsigargin. Note the extention of the ER network throughout the cytoplasm after stimulation and the increased co-localization of STIM1 with the luminal ER marker. Scale bars indicate 10 μm.These results are consistent with ER localization of STIM1 and preferential association with microtubules prior to stimulation. They also show the capacity of thapsigargin to induce large-scale ER rearrangement.

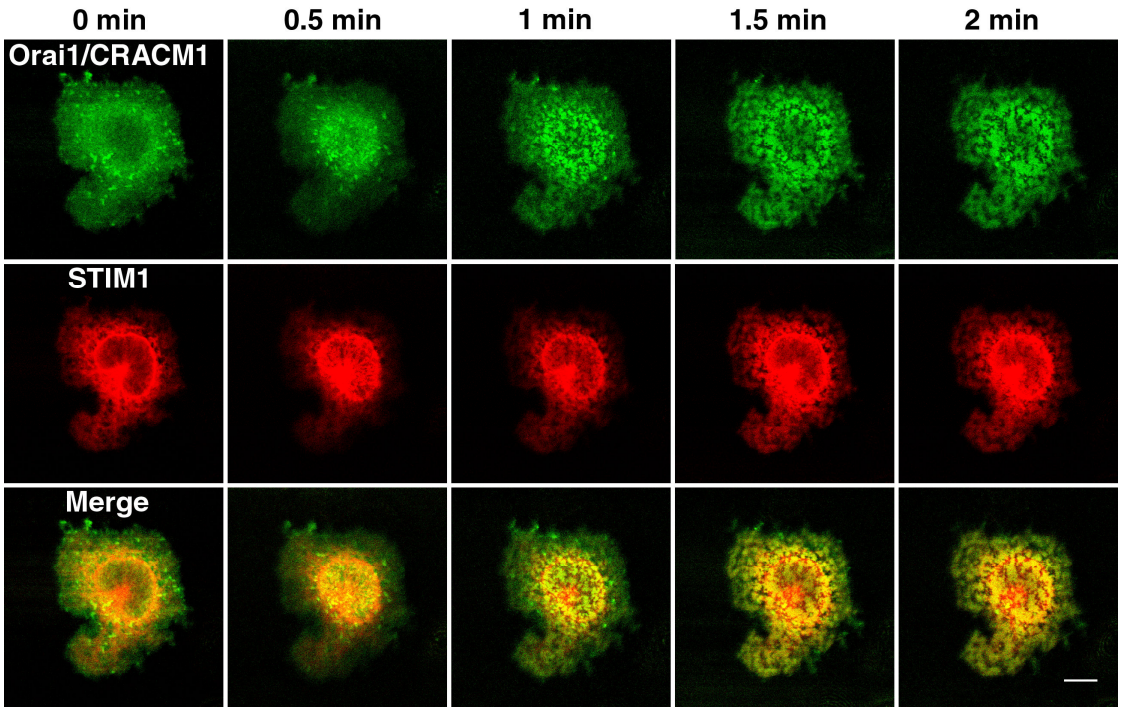

Figure 2.2: **Timecourse of AcGFP-Orai1/CRACM1 (green) and STIM1-mRFP (red) formation of co-labeled plasma membrane domains following thapsigargin stimulation**. The patches seen in the last image, formed after 2 min of stimulation, remained relatively unchanged for an additional 10 min (not shown). Dorsal cell surface images; scale bar indicates 10 μm.

distributions STIM1-mRFP are compared to the endogenous luminal ER marker, protein disulfide isomerase, before and after thapsigargin treatment (data not shown).

2.4.2 STIM1 and Orai1/CRACM1 co-redistribute to micron-sized dorsal membrane patches due to stimulation by thapsigargin.

Previous reports documented the localization of Orai1/CRACM1 at the plasma membrane (Vig 2006b) and its co-redistribution with STIM1 into plasma membrane-associated punctae in response to thapsigargin (Liu 2005, Luik 2006). We find in RBL cells that STIM1-mRFP and AcGFP-Orai1/CRACM1 co-redistribute into a mosaic pattern at the dorsal cell surface as early as 1 minute after addition of thapsigargin, and this pattern remains stable for more than several minutes (Figure 2.2). The time course we observe correlates with the time dependence of SOCE following thapsigargin-stimulated release from stores in these cells (Glitsch and Parekh, 2000). These micron-sized patches at the dorsal cell surface are larger than punctae initially reported for ventral surface confocal (Liou 2005) or TIRF images (Wu 2006), but these dorsal-localized patches are similar in size as other STIM1-Orai1/CRACM1 patches observed by confocal microscopy in several recent studies in other cell types (Varnai 2007, Smyth 2008). Moreover, using TIRF microscopy at the ventral cell surface of RBL cells, we observe the formation of smaller submicron scale STIM1-mRFP AcGFP-Orai1/CRACM1 punctae in response to thapsigargin, and these are similar to those observed in other studies (Liou 2005, Wu 2006) (Supplemental Figure B.3). Our results establish that, in response to thapsigargin, STIM1-mRFP and AcGFP-Orai1/CRACM1 expressed transiently in RBL cells undergo large-scale co-redistribution that is qualitatively similar to that observed for other fluorescent derivatives of these proteins in other cell types.

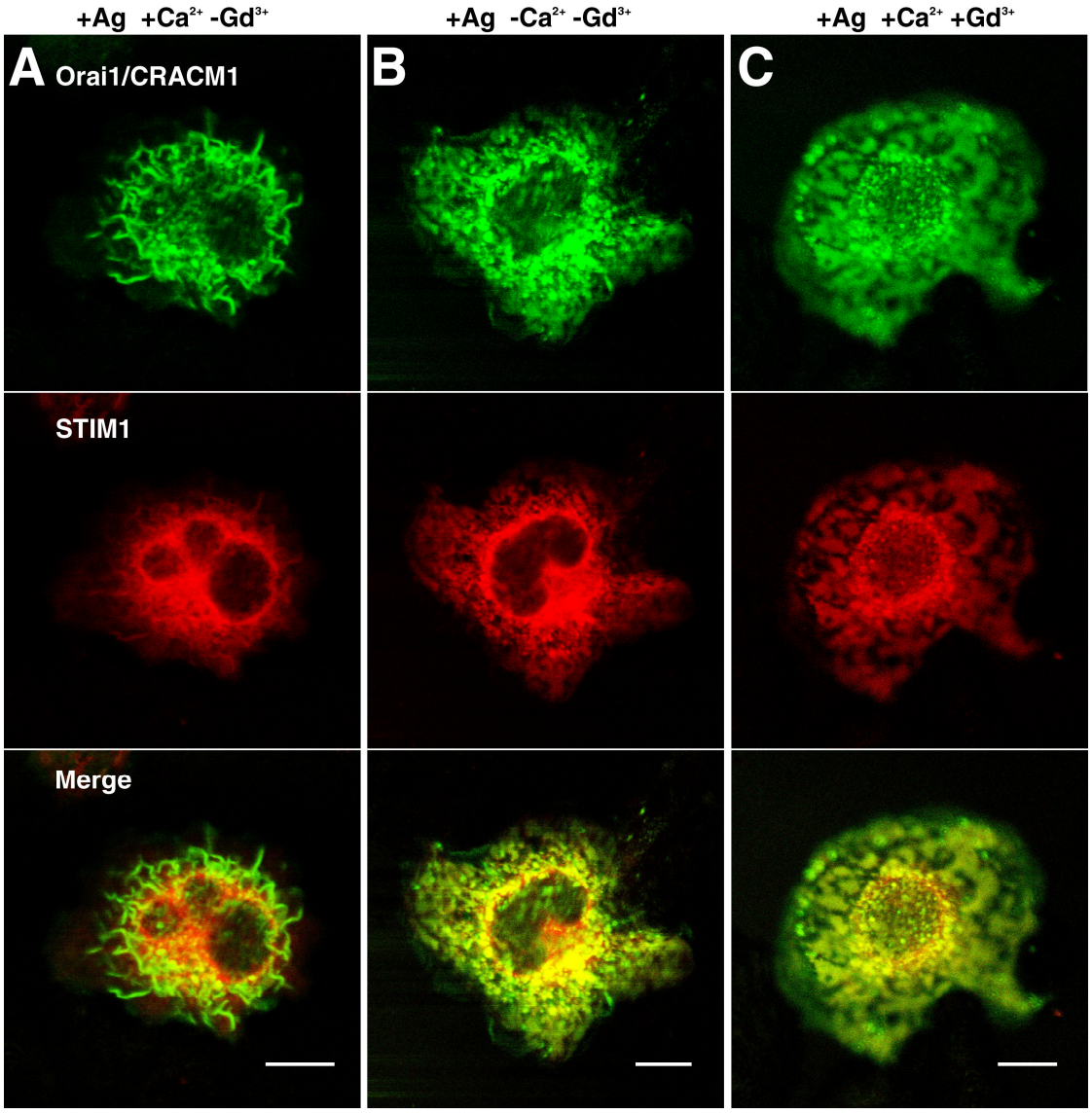

Figure 2.3: **Confocal images of AcGFP-Orai1/CRACM1 (green) and STIM1-mRFP (red) in dorsal slices of RBL mast cells stimulated with antigen under different conditions affecting Ca^{2+} influx**. Cell stimulated in BSS buffer with (A) and without (B) $CaCl_2$. C) Cell stimulated in BSS with Ca^{2+} and 6μM $GdCl_3$. Scale bars indicate 10 μm.

2.4.3 Antigen-stimulated co-redistribution of Orai1/CRACM1 and STIM1is highly restricted compared to that stimulated by thapsigargin.

We found only limited co-redistribution of STIM1-mRFP and AcGFP-Orai1/CRACM1 following stimulation mediated by IgE-receptors after crosslinking by multivalent antigen. Under these conditions, AcGFP-Orai1/CRACM1 remains at the plasma membrane and is evident in the stimulated membrane ruffles (Figure 2.3A). Furthermore, STIM1-mRFP shows only dim localization with AcGFP-Orai1/CRACM1 in these ruffles, and the degree of translocation to the plasma membrane is substantially less than that seen with thapsigargin stimulation (Figure 2.2; see also below). This was not expected, in part because of the well-documented activation of I_{CRAC} activation by antigen in RBL cells (Hoth 1992, Zhang 1995; McCloskey 2000). Furthermore, the Ca^{2+} response to antigen is 71 ± 14% of that caused by thapsigargin during 5 min of activation (Supplemental Figure B.4A and B.4B and data not shown).

This striking difference between stimulation of STIM1-Orai1/CRACM1 co-redistribution by thapsigargin and antigen points to differences in mechanism, and in particular, that thapsigargin operates by inhibiting SERCA, thereby preventing refilling of ER Ca^{2+} stores. In contrast, antigen stimulation does not impose this restriction. We could evaluate the significance of Ca^{2+} influx during antigen stimulation by using two different conditions to prevent it: elimination of Ca^{2+} in the extracellular buffer and addition of $GdCl_3$ to block I_{CRAC} (Dellis 2006). We found that RBL cells stimulated by antigen under either of these conditions show redistributions of STIM1 and CRACM1 similar to cells stimulated with thapsigargin. In the absence of extracellular Ca^{2+} (Figure 2.3B) or in the presence of 6 μM $GdCl_3$ (Figure 2.3C), antigen stimulation causes STIM1-mRFP to localize to domains that also contain

AcGFP-Orai1/CRACM1. We confirmed that under these conditions, Ca^{2+} mobilization is substantially reduced (Figure B.4 C and D). Thus, our imaging results indicate that persistent store depletion is necessary for stable, large-scale co-redistribution of STIM1 and Orai1/CRACM1. This occurs with SERCA2 inhibition by thapsigargin, but not with stimulation by antigen in the presence of extracellular Ca^{2+}, which causes more dynamic and/or less complete store depletion.

Equatorial confocal images clearly distinguish the distribution of these labeled proteins at the plasma membrane verses the cytoplasm, and similar conclusions are reached (Supplemental results and Figure B.5A). Furthermore, comparison of the distribution of AcGFP-Orai1/CRACM1 to the plasma membrane marker Alexa555-cholera toxin B in equatorial images shows that Orai1/CRACM1 associated with STIM1 is localized to the non-ruffled regions of the plasma membrane (Supplemental Figure B.5B). Overall, our microscopy results support previous conclusions that Ca^{2+} depletion from stores causes STIM1 and Orai1/CRACM1 to co-redistribute in large domains at the plasma membrane, and they also shed light on the reversal or restriction of this process that is related to store refilling by Ca^{2+} influx.

2.4.4 FRET measurements reveal close interactions between STIM1-mRFP and AcGFP-Orai1/CRACM1 that are sustained if stores are not refilled.

Visualized co-localization of STIM1 with Orai1/CRACM1 at the plasma membrane (Figures 2.2, 2.3, and B.5A) is limited by optical resolution (>200 nm). To assess whether these proteins become close enough for direct interaction, we monitored changes in FRET from the donor AcGFP-Orai1/CRACM1 to the acceptor STIM1-mRFP in response to stimulation. The distance sensitivity of these measurements is represented by the Förster distance, which for this donor-acceptor pair is estimated to

be ~5 nm (Erickson 2003). Equatorial images were evaluated, with an image mask to isolate the fluorescence associated with the plasma membrane for each cell and time point. The ratio of corrected red (acceptor) fluorescence to the green (donor) fluorescence provides a relative measure of FRET as described in Eq 1.

Thapsigargin added to cells expressing STIM1-mRFP and AcGFP-Orai1/CRACM1 causes a robust increase in FRET on the timescale of several minutes. Figure 2.4A shows this time course derived from image analyses of individual cells and averaged over 18 representative cells. Following a lag period of up to 100 sec, FRET increases to a relatively constant value with an average half time of approximately 180 sec. This lag most likely reflects the period during which Ca^{2+} in ER stores is reduced, and the time dependent increase in FRET intensity is consistent with the time course for activation of Ca^{2+} influx that may be limited by the rate of STIM1 redistribution. These FRET results are consistent with fluorescence micrographs showing STIM1 and Orai1/CRACM1 co-localization in response to thapsigargin stimulation (e.g., Figures 2.2 and B.5A), and they reveal further that these SOCE components from ER and plasma membrane, respectively, are interacting stably in close ($\leq$10 nm) proximity under conditions where store refilling is prevented.

An important control to distinguish measured FRET from increases in acceptor fluorescence due to recruitment of STIM1-mRFP to the plasma membrane is to substitute AcGFP-Orai1/CRACM1 with another plasma membrane-localized GFP-labeled protein that does not associate directly with STIM1-mRFP. For this purpose, we used eGFP linked to the PIP_2-binding pleckstrin homology (PH) domain of phospholipase C δ (PH-eGFP). PH-eGFP strongly localizes to the plasma membrane in these cells in the presence and absence of thapsigargin, similar to AcGFP-Orai1/CRACM1 (Wu 2004; our data not shown). STIM1-mRFP, co-transfected with PH-eGFP and non-fluorescent Orai1/CRACM1, exhibits thapsigargin-stimulated

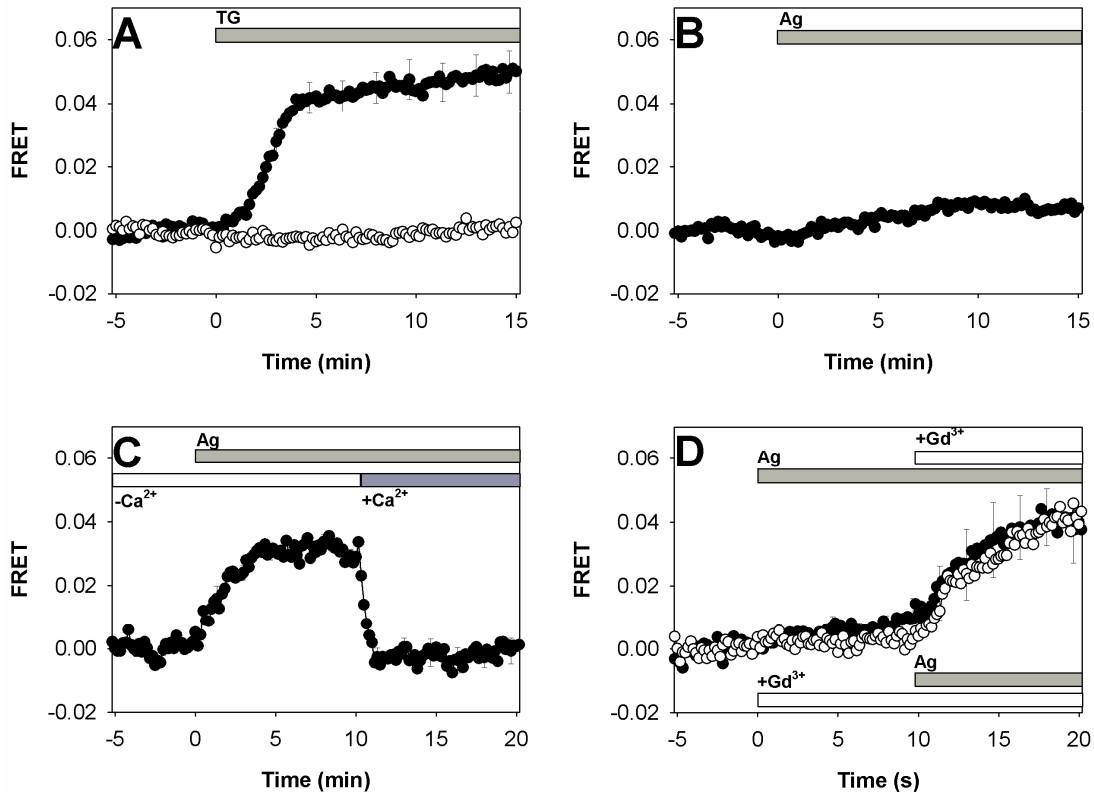

Figure 2.4: **FRET between AcGFP-Orai1/CRACM1 and STIM1-mRFP in plasma membrane of RBL mast cells** A) FRET following addition of 150 nM thapsigargin (indicated by bar) to labeled cells (solid circles; error bars show SEM) as compared to control cells expressing PH-eGFP and unlabeled Orai1/CRACM1 instead of AcGFP-Orai1/CRACM1 (open circles, SEM ~ 2.0 x 10^{-3}). B) FRET following antigen stimulation with 3 nM DNP-BSA in BSS (SEM ~ 1.0 x10^{-3}). C) FRET following same antigen stimulation but in the absence of extracellular Ca^{2+}. $CaCl_2$ (1.8 mM) was restored as indicated by bar (error bars show SEM). D) FRET after stimulation by antigen followed by addition of 6 μM $GdCl_3$ (solid circles; top bars; error bars show SEM; solid line) or after $GdCl_3$ addition followed by antigen stimulation (open circles; bottom bars; error bars omitted; dotted line).

translocation to patches at or near the plasma membrane, and this fluorescence is visualized by microscopy to be co-localized with uniformly-distributed PH-eGFP (data not shown). However, no change in FRET is detected between PH-eGFP and STIM1-mRFP in response to thapsigargin (Figure 2.4A).

In contrast to thapsigargin-stimulated FRET, only a small, time-dependent increase in FRET between AcGFP-Orai1/CRACM1 and STIM1-mRFP is caused by antigen (Figure 2.4B), consistent with the very limited redistribution of STIM1-mRFP to the plasma membrane visualized microscopically in response to antigen (Figures 2.3A and B.5A). Because robust SOCE is observed in RBL cells after antigen stimulation (Figure B.4), the results indicate that efficient SOCE can be achieved with more limited STIM1-Orai1/CRACM1 interactions than those observed with thapsigargin. We hypothesize that dynamic emptying and refilling of stores that occurs as part of this mechanism is manifest as more transient and/or local store depletion and consequently more limited STIM1 redistribution to the plasma membrane.

To test this hypothesis, we stimulated cells with antigen in the absence of extracellular Ca^{2+} to prevent refilling of stores. We observed a time-dependent increase to a large, sustained level of FRET between Orai1/CRACM1-AcGFP and STIM1-mRFP that is rapidly reversed ($t_{1/2}$ <30s) when millimolar Ca^{2+} is added back (Figure 2.4C). This FRET measurement is again consistent with visualization by microscopy (Figure 2.3B and B.5A), and it further demonstrates nanoscale proximity of STIM1 and Orai1/CRACM1 due to receptor-mediated cell activation. Under these conditions, we observe redistribution of STIM1 away from the plasma membrane that is slower than the reversal of FRET, taking 1-3 minutes to complete (data not shown). This difference suggests that the rate of redistribution of STIM1-mRFP uncoupled from its interaction with Orai1/CRACM1 is limited by its diffusion in the ER membranes, consistent with recent observations of Liou *et al.,* (2007).

To investigate whether the close interaction between Orai1/CRACM1 and STIM1 is sensitive to Ca^{2+} influx mediated by I_{CRAC} specifically, we examined the effect of $GdCl_3$ on the measured FRET. After 10 min of antigen stimulation that caused only a small increase in FRET, addition of 6 μM $GdCl_3$ resulted in a time-dependent increase in FRET that approached a steady state value after 10 min and was similar in magnitude to that for antigen stimulation in the absence of Ca^{2+} (Fig. 4D, closed circles). Similar results were obtained when cells were pretreated with $GdCl_3$ and subsequently stimulated with antigen (Fig. 4D, open circles). Evidently, $GdCl_3$-mediated inhibition of SOCE is sufficient to sustain Orai1/CRACM1-STIM1 interactions similarly to thapsigargin. These FRET results provide a nanoscale view of the interactions between Orai1/CRACM1 and STIM1 in antigen-stimulated cells that are dynamically regulated by ER luminal Ca^{2+} levels.

2.4.5 D-Sphingosine and N,N-Dimethylsphingosine inhibit the association between STIM1 and Orai1.

A previous study demonstrated the capacity of D-sphingosine and its derivative, N,N-dimethylsphingosine (DMS) to inhibit IP_3-elicited I_{CRAC} in RBL mast cells (Mathes 1998). To investigate whether sphingosine or DMS directly affects the interaction between STIM1 and Orai1/CRACM1 we measured FRET between AcGFP-Orai1 and STIM1-mRFP in the presence of 8 μM D-sphingosine or DMS after thapsigargin stimulation. These conditions are sufficient for inhibition of >60% of thapsigargin-stimulated Ca^{2+} influx by these amphiphiles (Figure 2.6A). As shown in Figure 2.5A, we find that both D-sphingosine and DMS strongly inhibit the interaction between STIM1 and Orai1/CRACM1. In contrast, N,N,N-trimethylsphingosine, the quarternary amine derivative of D-sphingosine, does not significantly reduce the FRET response

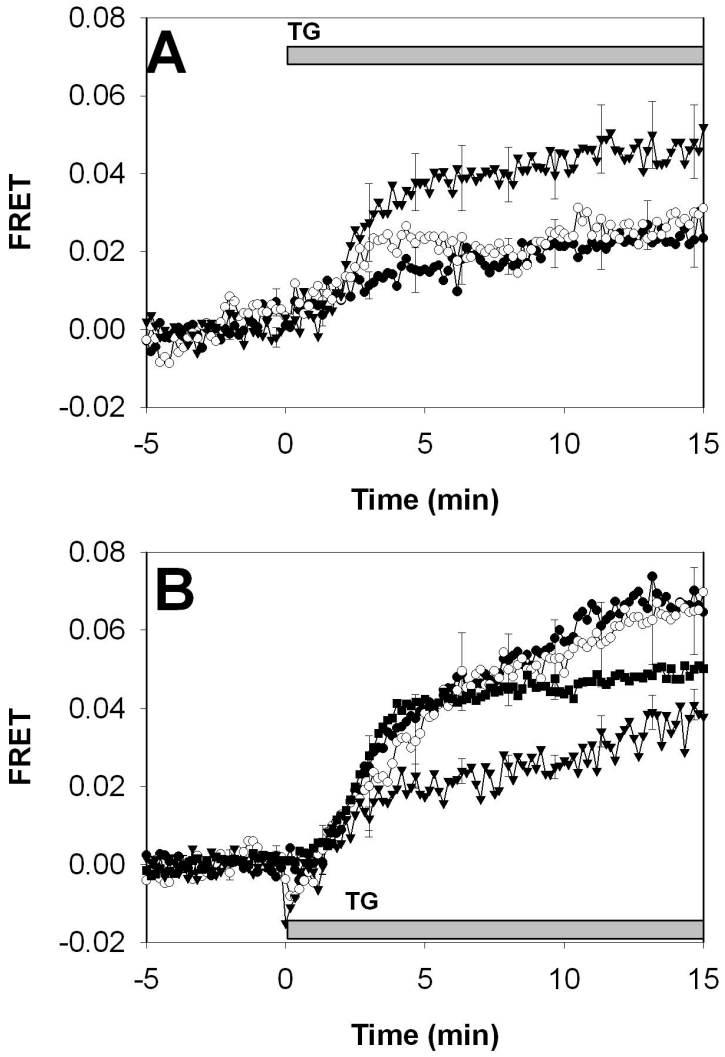

Figure 2.5: **Effects of sphingosine derivatives and mutation of the Orai1 C-terminal coiled-coil on the STIM1-Orai1 interaction.** A) Thapsigargin-stimulated FRET between AcGFP-Orai1/CRACM1 and STIM1-mRFP in the presence of D-sphingosine (7.6 μM, open circles), DMS (7.6 μM, closed circles; error bars omitted), and TMS (7.6 μM, triangles). B) Thapsigargin-stimulated FRET between STIM1-mRFP and AcGFP-Orai1/CRACM1 (squares, same as Figure 2.4A, shown for comparison; error bars omitted), AcGFP-Orai1/CRACM1ΔD (closed circles; error bars omitted), AcGFP-Orai1/CRACM1ΔE (open circles), and AcGFP-Orai1/CRACM1ΔDE (triangles). Error bars show SEM.

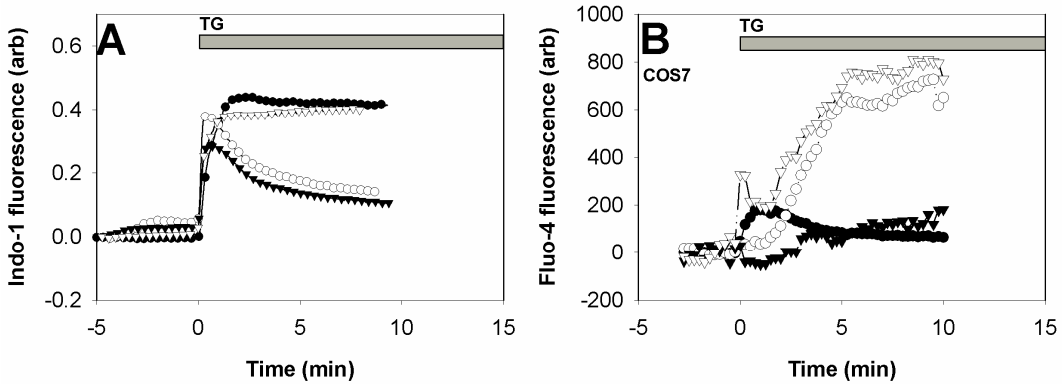

Figure 2.6: **Effects of sphingosine derivatives and mutation of the Orai1 C-terminal coiled-coil on SOCE.** A) Effects of sphingosine derivatives on thapsigargin induced Ca^{2+} mobilization, indo-1-monitored. Ca^{2+} response of suspended RBL cells for untreated cells (closed circles), cells in the presence of D-sphingosine (7.6 μM, open circles), DMS (7.6 μM, closed triangles), TMS (7.6 μM, open triangles). Every tenth data point is shown for clarity. B) Calcium measurements of COS7 cells monitored by fluo-4 imaging. Thapsigargin mediated Ca^{2+} mobilization is shown for untransfected cells (closed circles), cells expressing STIM1-mRFP with AcGFP-Orai1/CRACM1 (open circles), AcGFP-Orai1/CRACM1ΔE (open triangles), and AcGFP-Orai1/CRACM1ΔDE (closed triangles).

to thapsigargin compared with untreated cells (Figure 2.4) and does not inhibit SOCE (Figure 2.6A). In other studies, we find that all three of these amphiphiles efficiently insert into the outer leaflet of the plasma membrane, but only D-sphingosine and DMS can flip to the inner leaflet(N. Smith, B. Baird, and D. Holowka, unpublished results), where they can directly interfere with the STIM1-Orai1/CRACM1 interaction. These results suggest the possibility of direct, electrostatic interference by D-sphingosine and DMS of the interaction between STIM1 and Orai1/CRACM1. The capacity of these positively charged lipids with different headgroup structures to similarly inhibit this interaction is more consistent with an electrostatic mechanism than a specific binding interaction. Moreover, addition of both D-sphingosine and DMS induce the formation of large patches of Orai1/CRACM1 without co-localization of STIM1 (Figure 2.7A). Other plasma membrane proteins, such as FcεRI, do not detectably cluster under these conditions (data not shown). These results show that not only do these sphingosine derivatives disrupt the stimulated interaction between STIM1 and Orai1/CRACM1, but they also induce selective aggregation of Orai1/CRACM1.

2.4.6 Charged amino acid residues in the C-terminus of Orai1/CRACM1 are important for its interaction with STIM1.

A recent study provided evidence for the role of a coiled-coil domain at the C-terminus of Orai1/CRACM1 in the interaction between this protein and STIM1 (Muik, 2008). This domain contains a series of three aspartates (D284, D287, and D291) and a separate series of three glutamates (E272, E275, and E278) predicted to be on the hydrophilic face of the coiled-coil. We probed the importance of charge on these 6 amino acids by constructing three separate AcGFP-Orai1/CRACM1 mutants in which all three aspartates are converted to asparagine (AcGFP-Orai1/CRACM1ΔD), all three

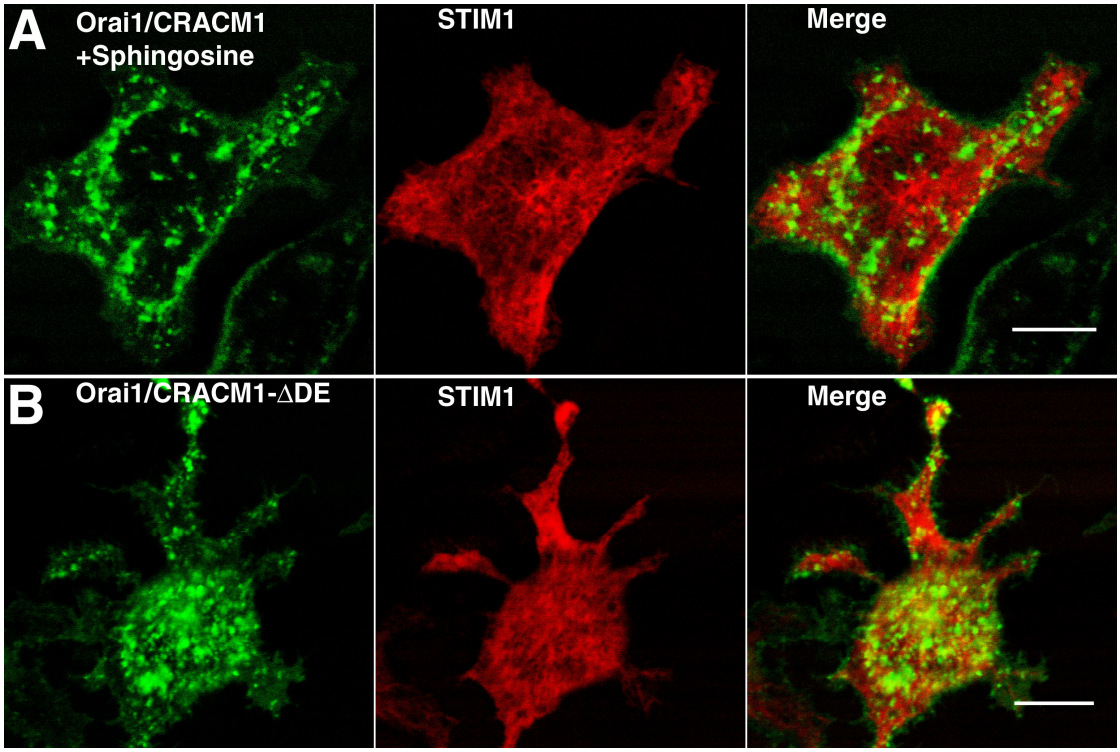

Figure 2.7: **Sphingosine and mutation of the Orai1 C-terminal coiled-coil induce punctae formation.** A) AcGFP-Orai1/CRACM1 in the presence of 7.6 μM D-sphingosine exhibits plasma membrane patches without STIM1-mRFP redistribution. B) AcGFP-Orai1/CRACM1ΔDE and STIM1-mRFP exhibits plasma membrane patches without STIM1-mRFP redistribution. Compare these dorsal surface images to Fig. 3, t=0. Scale bars indicate 10 μm.

glutamates are converted to glutamine (AcGFP-Orai1/CRACM1ΔE), or all six acidic amino acids are changed to their neutral analogues (AcGFP-Orai1/CRACM1ΔDE). We then monitored FRET between STIM1-mRFP and the AcGFP-Orai1/CRACM1 mutants and compared this to the FRET between STIM-mRFP and wild type AcGFP-Orai1/CRACM1 described above. As shown in Figure 2.5B, neutralization of three of the six acid residues resulted in an increase in thapsigargin-stimulated FRET at longer time points, whereas the neutralization of all six acidic residues resulted in a significant decrease in stimulated FRET. Moreover, cells expressing AcGFP-Orai1/CRACM1ΔDE exhibited large patches of this protein in the absence of stimulated clustering of STIM1, similar to cells treated with D-sphingosine or DMS (Figure 2.7B). These results suggest that D-sphingosine and DMS promote Orai1/CRACM1 clustering by neutralization of the negative charges in the putative coiled-coil at the C-terminus of this protein, and in so doing they prevent its interaction with the the C-terminus of STIM1 under cell activating conditions, possibly via its positively charged polybasic sequence (Li 2007).

2.4.7 Charged amino acid residues in the C-terminus of Orai1/CRACM1 are important for functional CRAC influx.

Because RBL cells have a large endogenous SOCE response, the functional consequences of mutations were examined in COS7 cells. The Ca^{2+} response to thapsigargin was monitored in COS7 cells transiently expressing STIM1-mRFP and AcGFP-Orai1/CRACM1 or one of the Orai1/CRACM1 mutants. COS7 cells exhibit relatively limited SOCE that is substantially enhanced by expression of STIM1-mRFP and AcGFP-Orai1/CRACM1 (Figure 2.6B, open circles). Potentiation of SOCE due to overexpression of STIM1 and Orai1/CRACM1 has been previously reported in COS7

cells (Varnai, 2007), and our results demonstrate the functional competence of STIM1-mRFP and AcGFP- Orai1/CRACM1 used in our FRET measurements. Cells expressing AcGFP-Orai1/CRACM1ΔE show a potentiation of Ca^{2+} influx similar to that observed with wild type Orai1/CRACM1. In contrast, cells expressing AcGFP-Orai1/CRACM1ΔDE and STIM1-mRFP show only a very slow, small increase in Ca^{2+} in response to thapsigargin (Figure 2.6B). Moreover, these cells show a substantially delayed or reduced Ca^{2+} release from stores when compared to untransfected COS7 cells. This observation indicates that these acidic residues on Orai1/CRACM1 can influence the sensitivity of these cells to thapsigargin mediated Ca^{2+} release from stores. These Ca^{2+} mobilization results correlate with the reduction in FRET observed with AcGFP-Orai1/CRACM1ΔDE (Figure 2.5B), indicating that the negatively charged residues in the C-terminus of Orai1/CRACM1 are important for functional SOCE.

2.5 Discussion

Our FRET measurements in conjunction with fluorescence confocal imaging reveal molecular interactions between Orai1/CRACM1 and STIM1 that are regulated by dynamic depletion and refilling of intracellular Ca^{2+} stores. Whereas thapsigargin inhibition of store refilling results in extensive association of Orai1/CRACM1 and STIM1, the SERCA-mediated store refilling that occurs normally during antigen stimulation substantially limits these molecular interactions. Additionally, our results show that store depletion results in the remodeling of the ER that accompanies redistribution of STIM1. STIM1 was previously identified as a transmembrane protein that co-localizes with the ER in unstimulated cells (Liou 2005, Wu 2006), while more recent studies have found STIM1 co-localization with microtubules (Kurosaki 2006,

Mercer 2006). Our results with RBL mast cells provide visual evidence that localization of STIM1 in unstimulated cells is templated to a large extent by microtubules, and this differs from luminal ER-localized fluorescent proteins, which show little or no microtubule association (Figures 2.1A and B.2).

It is not yet clear whether STIM1 associated with microtubules is preferentially recruited to the plasma membrane in stimulated cells, but we observe a reduction in microtubule-associated STIM1-mRFP upon thapsigarin treatment (Figure 2.1 and data not shown). Baba *et al.,* (2006) showed that GFP-STIM1-containing tubulovesicular structures rapidly move along microtubule tracks in DT40 B cells, and treatment of nocodazole to depolymerize microtubules halted this rapid movement but did not inhibit B cell receptor-stimulated SOCE. In another study, Smyth *et al.,* (2007) showed that eYFP-STIM1 associates with microtubules in HEK293 cells, and that nocodazol inhibition substantially inhibits thapsigargin-stimulated CRAC influx in these cells in the absence of eYFP-STIM1 expression.

Our observation that intracellular localization of STIM1 changes dramatically upon stimulation of RBL cells with thapsigargin is consistent with results reported for other cell types (Liou 2005, Wu 2006). We find that the distribution of both STIM1-mRFP and ER-eGFP appear to change, such that cytoplasmically localized STIM1-mRFP and ER-eGFP become more extensively colocalized in the variegated network of the ER (Figure 2.1B). The rearrangement of the ER network upon thapsigargin stimulation is consistent with the previously reported role of STIM1 in the microtubule assisted remodeling of the ER (Grigoriev 2008). In addition to this cytoplasmically localized STIM1-mRFP, a pool of STIM1-mRFP redistributes to the plasma membrane to form an extended network that colocalizes with AcGFP-Orai1/CRACM1 (Figure 2.2). Equatorial sections show that this network of plasma membrane-associated STIM1-mRFP localizes to the flat regions of the plasma

membrane between ruffles and other protrusions that are labeled by the plasma membrane marker A^{555}-CTB (Figure B.5B). This mosaic of plasma membrane-STIM1/ER junctions at the dorsal cell surface clearly represents a large percentage of the plasma membrane surface area under conditions of stimulation by thapsigargin in these cells. These results do not appear to be a consequence of overexpression of these proteins, as they are observed over a wide range of expression levels. Furthermore, expression of these proteins does not significantly alter Ca^{2+} responses to antigen or thapsigargin in these cells (data not shown). The size of the dorsal domains observed is consistent with Orai1/CRACM1-STIM1 patches reported in some other studies (Varnai 2007, Smyth 2008). More discrete punctae of STIM1 are observed at the ventral cell surface by TIRF microscopy (Supplemental Figure B.3) similar to those seen in other reports in these (Liou 2007) and other cells by both confocal (Liou 2005, 2007) and TIRF microscopy (Wu 2006, Liou 2007?).

To examine the molecular interactions of STIM1 and Orai1/CRACM1, we developed a microscopy-based FRET assay that is computationally similar to the membrane colocalization assay recently established in our laboratory (Das 2008). Our experimental system and membrane localized FRET analysis allowed the measurement of the interaction between STIM1-mRFP and AcGFP-Orai1/CRACM1 with high sensitivity, temporal resolution, and reproducibility. A distinct advantage of the AcGFP/mRFP donor/acceptor pair is that excitation of the green donor with the 476 nm laser line initiates energy transfer with negligible direct excitation of the red acceptor fluorophore, thus simplifying the FRET computation, which is targeted by automated masking of equatorial plasma membrane as the selected region of interest. Because selection of the measured regions of interest is automated on a frame-by-frame basis, the ratiometric analysis of energy transfer (Eq. 1) is insensitive to variations in the focal plane and laser intensity, as well as morphological differences

between cells. Individual cells are imaged over time (before and after stimulation), and the FRET time courses for multiple cells are averaged.

Previous TIRF imaging of thapsigargin-stimulated cells showed optical colocalization of labeled STIM1 and Orai1/CRACM1 in plasma membrane punctae (Liuk 2006), and further evidence for molecular level interactions comes from co-immunoprecipitation of STIM1 with Orai1/CRACM1 in complexes derived from lysates of thapsigargin-stimulated cells (Yeromin 2006). Our FRET measurements demonstrate that labeled STIM1 and Orai1/CRACM1 interact closely at the plasma membrane of live cells as a consequence of store depletion, and they are consistent with these two proteins associating directly to facilitate the CRAC response. These measurements detect proximity on the order of 5 nm, but do not rule out the participation of other molecular components in this interaction. A recent study in HEK-293 cells provided FRET evidence interactions between STIM1-eYFP and eCFP-Orai1/CRACM1 following store depletion by SERCA inhibitors (Muik 2008). Barr (2008) detected FRET between these proteins stimulated by surface-associated T cell receptor ligands, but they did not compare the magnitude of this FRET to that induced by SERCA inhibition. In contrast, Varnai *et al.,* (2007) showed that interactions between STIM1 and Orai1/CRACM1 detected by confocal microscopy were excluded from plasma membrane regions that were bridged to ER tethering proteins estimated to provide < 6 nm of inter-membrane spacing. These authors suggested that interactions between STIM1 and Orai1 involve additional proteins that extend spacing between the PM and ER to >8 nm, but alternative explanations for these observations, such as orientational or electrostatic interference by the bridging proteins, cannot be excluded.

Unexpectedly, antigen stimulation of RBL cells leads to STIM1 and Orai1/CRACM1 interactions at the plasma membrane that are highly restricted, as

observed with both confocal imaging (Figure 2.3A) and FRET (Figure 2.4B). The striking difference from thapsigargin stimulation can be explained by dynamic refilling of intracellular Ca^{2+} stores by influx that accompanies antigen stimulation and is prevented when the SERCA pumps are blocked by thapsigargin. Thus, dynamic refilling of Ca^{2+} stores apparently re-sets the baseline and reverses the interaction between STIM1 and Orai1/CRACM1. Consistent with this hypothesis, stimulation with antigen under conditions that prevent refilling of stores, either the absence of extracellular Ca^{2+} or the presence of Gd^{3+} to block CRAC-mediated Ca^{2+} entry, results in strongly enhanced interactions very similar to those observed with thapsigargin. Specifically, extensive co-localization of labeled STIM1 and Orai1/CRACM1 occurs at the plasma membrane as visualized with confocal microscopy (Figures 2.3B, C; B.5A) and substantially increased molecular interactions are detected with FRET (Figure 2.4C, D). Other recent reports are consistent with these observations. Muik *et al.,* (2008) showed that FRET between STIM1-CFP and Orai1-YFP stimulated by agonist together with a weak SERCA inhibitor in the absence of Ca^{2+} was reversed by Ca^{2+} addition in HEK293 cells; Varnai *et al.,* (2007) showed that ATP-stimulated STIM1 recruitment to the PM in COS7 cells was reversed by extracellular Ca^{2+}; and Smyth *et al.,* (2008) showed that carbacol-induced STIM1/Orai1 punctae formation detected by TIRF in HEK293 cells was reversed by Ca^{2+} addition. Our results highlight the physiological regulation of this interaction when stimulated by an immunoreceptor, FcεRI, during mast cell activation.

It is notable that the kinetics of the molecular association between STIM1 and Orai1/CRACM1, which increases to a steady-state with a half time of several minutes, are similar whether Gd^{3+} is added before or after antigen to initiate the response (Figure 2.4D). Thus it appears that the rate-limiting step in this process is the redistribution of STIM1 to the plasma membrane, rather than preceding steps of

antigen-stimulated signaling. In contrast, addition of extracellular Ca^{2+} to antigen-stimulated cells causes a rapid reduction in FRET, occurring with a half time of approximately 20 sec (Figure 2.5C), suggesting that stores are refilled very rapidly under these conditions. These results support the view that molecular interactions between STIM1 and Orai1/CRACM1 that are stimulated by antigen are highly dynamic and readily reversed by store refilling. Our FRET results provide a somewhat different picture than those of Liou *et al.,* (2007), who monitored FRET between CFP-STIM1 and YFP-STIM1 in RBL mast cells and observed increases that were similar for antigen and thapsigargin stimulation. They monitored STIM1/STIM1 interactions throughout the ER, and their data show that these interactions are initiated prior to localization of STIM1 in plasma membrane punctae. These STIM1-STIM1 interactions possibly depend differently on store depletion/refilling than do STIM1-Orai1/CRACM1 interactions. Direct measurement of intra-luminal free Ca^{2+} in the ER under different conditions of stimulation may help to address this question.

Inhibition of thapsigargin-stimulated FRET between Ac-GFP-Orai1/CRACM1 and STIM1-mRFP by D-sphingosine and DMS is consistent with the inhibitory effects of these amphiphiles on IP_3 mediated SOC influx in RBL cells (Mathes 1998). We confirmed that these molecules show a similar inhibitory effect on thapsigargin mediated SOCE in these cells (Figure 2.6). TMS does not significantly inhibit the interaction between Ac-GFP-Orai1/CRACM1 and STIM1-mRFP, and it seems likely that D-sphingosine and DMS are effective because of the net increase in positively charged lipids that they provide upon flipping to the inner leaflet of the plasma membrane (N. Smith, unpublished results; Sato 2006). Although DMS is a well-known inhibitor of sphingosine kinases (Yatomi 1996), it is unlikely that its effect on FRET depends on inhibition of this enzyme family, because the substrate for these enzymes, D-sphingosine, is equally effective in inhibiting FRET (Figure 2.5A) and

Ca^{2+} influx (Figure 2.6A). We hypothesize that D-sphingosine and DMS at the inner leaflet electrostatically interact with six acidic residues at the C-terminus of Orai1/CRACM1 to prevent the interaction of these residues with STIM1 under conditions of CRAC activation. This model is in contrast to those published in recent reports by Peinelt and Smyth in which pharmacological agents disrupt the interaction of STIM1 with Orai1/CRACM1 by reversing the store-dependent multimerization and translocation of STIM1 (Peinelt 2008, Smyth 2008). It is possible that the effects of these positively charged amphiphiles directly prevent the association with STIM1, or that this effect is mediated by alteration of the lipid environment, thereby preventing the association of Orai1/CRACM1 with STIM1. In this regard, electrostatic neutralization of negatively charged phospholipids, such as phosphoinositides, by these positively charged amphiphiles could play a role in their mechanism of inhibition. The hypothesis that this effect is mediated to a large extent by electrostatic neutralization is bolstered by the fact that the endogenous polyamine spermine dose dependently inhibits FRET between the two proteins and prevents SOC influx (N. Calloway, unpublished results).

Complementary to these results, we observe formation of Orai1/CRACM1 patches at the plasma membrane following addition of D-sphingosine or DMS (Figure 2.7). STIM1 does not co-patch under these conditions, suggesting that neutralization of the acidic residues by the sphingosine derivatives causes homo-oligomerization of Orai1/CRACM1, which could prevent its interaction with STIM1 by an effect on Orai1/CRACM1 structure. Importantly, SOC influx is not activated under these conditions (Figure 2.6A and data not shown).

Based on the primary structure of the recently identified interacting domains of STIM1 and Orai1/CRACM1 (Li 2007, Muik 2008), we hypothesized that association of the C-terminal polybasic region of STIM1 with the acidic C-terminal coiled-coil of

Orai1/CRACM1 is important for the initiation of I_{CRAC}. Thus, Orai1/CRACM1 could be regulated in a manner similar to some TRP channels in which a C-terminal polybasic region regulates the activation of channel opening by electrostatic interaction with the plasma membrane (for review, see Rohacs 2006). As described above, this model also provides an explanation for inhibition of the interaction between STIM1 and Orai1/CRACM1 by D-sphingosine and DMS. To test whether the negatively charged residues on the putative C-terminal coiled-coil of Orai1/CRACM1 are involved in the interaction with STIM1, we mutated these residues to their neutral amide analogues. The results of our FRET measurements between STIM1-mRFP and AcGFP constructs of these Orai1/CRACM1 mutants provide clear evidence that these residues participate in the interaction between the two proteins (Figure 2.5B). The increase in FRET at long time points when only three residues are mutated could be the result of an altered stoichiometry between STIM1 molecules and Orai1/CRACM1 molecules in the interacting complex. This level of reduction in charge may require more Orai1/CRACM1 molecules to neutralize the charge on the polybasic region of STIM1. However, when all six acidic residues are mutated, the stimulated FRET is substantially decreased, potentially because the electrostatic driving force is largely eliminated. Residual FRET between STIM1-mRFP and AcGFP-Orai1/CRACM1ΔDE could be due to the presence of unmutated endogenous Orai1/CRACM1 in the clustered complex that interacts with clustered STIM1. Indeed, imaging of cells transfected with AcGFP-Orai1/CRACM1ΔDE reveals the formation of patches of this charge-neutralized protein in the absence of stimulation. The residual interaction between STIM1-mRFP and AcGFP-Orai1/CRACM1ΔDE detected by FRET could also involve other structural features of Orai1/CRACM1. Additionally, these mutations may affect other molecular interactions by Orai1/CRACM1, either with lipids or other proteins containing polybasic sequences.

As described above, the minimal effects of STIM1-mRFP and AcGFP-Orai1/CRACM1 expression on the strong SOCE response of endogenous STIM1and Orai1/CRACM1 provide evidence that our expression system does not significantly alter the homeostasis of RBL cells, but it limits our capability to observe changes in Ca^{2+} influx caused by mutant Orai1/CRACM1 constructs. We therefore carried out these measurements in COS7 cells, which display very low levels of SOCE in untransfected cells (Figure 2.6B, solid circles). Consistent with previous results in these (Varnai 2007) and other cell types (Soboloff 2006), transient expression of STIM1-mRFP with AcGFP-Orai1/CRACM1 reconstituted robust SOCE (Figure 2.6B, open circles). However, when cells are transfected with STIM1-mRFP and AcGFP-Orai1/CRACM1ΔDE, this enhancement is dramatically reduced. These results confirm the functionality of the C-terminal acidic coiled-coil domain of Orai1/CRACM1, showing that these residues are necessary for both the interaction with STIM1 and the activation of Ca^{2+} influx. Furthermore, these results show that the micron-scale clustering of AcGFP-Orai1/CRACM1ΔDE observed in the absence of STIM1-mRFP co-clustering (Figure 2.7B) does not represent functional activation of CRAC.

The similarity of our findings with AcGFP-Orai1/CRACM1ΔDE and with D-sphingosine and DMS suggest a common mechanism for their effects and for the response to thapsigargin stimulation: Electrostatic neutralization of the C-terminal acidic residues of Orai1/CRACM1 by mutation, by interaction with positively charged D-sphingosine and DMS, and possibly by interaction with the polybasic region of STIM1 all induce the formation of micron-scale Orai1/CRACM1 clusters. Interestingly, only clustering induced by STIM1 activates I_{CRAC}, for reasons that are not yet clear.

In summary, our FRET measurements are consistent with our confocal

imaging and provide a direct, quantitative measure of STIM1-Orai1/CRACM1 interactions that occur in molecular proximity in the plasma membrane of live cells. We observe time-dependent formation of STIM1-Orai1/CRACM1 complexes due to stimulation by thapsigargin or by antigen when Ca^{2+} influx is prevented. However, under normal conditions of antigen stimulation, when refilling of Ca^{2+} in ER stores is not prevented, STIM1-Orai1/CRACM1 interactions are highly regulated by store refilling. Furthermore, pharmacologic and mutational analyses provide evidence for an electrostatic mechanism for STIM1-Orai1/CRACM1 interactions and for the regulation of Orai1/CRACM1 oligomerization. These critical molecular interactions are dynamically regulated under physiological conditions of receptor-mediated Ca^{2+} mobilization.

REFERENCES

Baba, Y., Hayashi, K., Fujii, Y., Mizushima, A., Watarai, H., Wakamori, M., Numaga, T., Mori, Y., Iino, M., Hikida, M., and Kurosaki, T. (2006). Coupling of STIM1 to store-operated Ca^{2+} entry through its constitutive and inducible movement in the endoplasmic reticulum. Proc. Natl. Acad. Sci. USA. *103*, 16704-9.

Baba, Y., Nishida, K., Fujii, Y., Hirano, T., Hikida, M. and Kurosaki, T. (2008). Essential function for the calcium sensor STIM1 in mast cell activation and anaphylactic responses. Nature Immunology 9: 81-8.

Bakowski, D., Glitsch, M.D., and Parekh, A.B. (2006). An examination of the secretion-like coupling model for the activation of the Ca^{2+} release-activated Ca^{2+} current I (CRAC) in RBL-1 cells. J. Physiol. *532,* 55-71.

Barr, V.A., Bernot, K.M., Srikanth, S., Gwack, Y., Balagopalan, L., Regan, C.K., Helman, D.J., Sommers, C.L., Oh-Hora, M., Rao, A., and Samelson, L.E. (2008) Dynamic Movement of the Calcium Sensor STIM1 and the Calcium Channel Orai1 in Activated T-Cells: Puncta and Distal Caps.Mol Biol Cell.*19*, 2802-17.

Campbell, R.E., Tour, O., Palmer, A.E., Steinbach, P.A., Baird, G.S., Zacharias, G.S., and Tsien, R.Y. (2002). A monomeric red fluorescent protein. Proc. Natl. Acad. Sci. USA. *99,* 7877-82.

Das, R., Hammond, S., Holowka, D. and Baird, B. (2008) Real-time cross-correlation image analysis of early events in IgE receptor signaling. Biophys. J., in press.

Dellis, O., Dedos, S.G., Tovey, S.C., Taufiq-Ur-Rahman , Dubel, S.J., and Taylor, C.W. (2006). Ca^{2+} entry through plasma membrane IP_3 receptors. Science. *313*, 229-33.

Erickson, M.G., Moon, D.L., and Yue, D.T. (2003). DsRed as a potential FRET partner with CFP and GFP. Biophys. J. *85,* 599-611

Feske, S., Gwack, Y., Prakriya, M., Srikanth, S., Puppel, S.H., Tanasa, B., Hogan, P.G., Lewis, R.S., Daly, M., and Rao, A. (2006). A mutation in Orai1 causes immune deficiency by abrogating CRAC channel function. Nature. *441*, 179-85.

Glitsch, M.D., and Parekh, A.B. (2000). Ca^{2+} store dynamics determines the pattern of activation of the store-operated Ca^{2+} current I(CRAC) in response to InsP3 in rat basophilic leukaemia cells. J. Physiol. *523*, 283-90.

Gosse, J.A., Wagenknecht-Wiesner, A., Holowka, D., and Baird, B. (2005).

Transmembrane sequences are determinants of immunoreceptor signaling. J. Immunol. *175*, 2123-31

Grigoriev, I., Gouveia, S.M., van der Vaart, B., Demmers, J., Smyth, J.T., Honnappa, S., Splinter, D., Steinmetz, M.O., Putney, J.W. Jr, Hoogenraad, C.C., and Akhmanova, A. (2008) STIM1 is a MT-plus-end-tracking protein involved in remodeling of the ER. Curr Biol. *18*, 177-82.

Guo, C., Holowka, D., and Baird, B. (1994). Fluorescence Resonance Energy Transfer Reveals Interleukin (IL)-1-dependent Aggregation of IL-1 Type I Receptors That Correlates with Receptor Activation. J. Biol. Chem. *207*, 27562-68.

Hoth, M. and Penner, R. (1992) Depletion of intracellular calcium stores activates a calcium current in mast cells. Nature. *335,* 353-6.

Kaetzel, C.S., Rao, C.K., and Lamm, M.E. (1987). Protein disulphide-isomerase from human placenta and rat liver. Purification and immunological characterization with monoclonal antibodies. Biochem. J. *241*, 39-47

Lewis, R.S, and Cahalan, M.D. (1989). Mitogen-induced oscillations of cytosolic Ca^{2+} and transmembrane Ca^{2+} current in human leukemic T cells. Cell Regul. *1*, 99-112.

Li, Z., Lu, J., Xu, P., Xie, X., Chen, L., and Xu, T. (2007) Mapping the interacting domains of STIM1 and Orai1 in Ca^{2+} release-activated Ca^{2+} channel activation. J Biol Chem. *282*, 29448-56.

Liou, J., Kim, M.L., Heo, W.D., Jones, J.T., Myers, J.W., Ferrell, J.E. Jr, and Meyer, T. (2005). STIM is a Ca^{2+} sensor essential for Ca^{2+}-store-depletion-triggered Ca^{2+} influx. Curr. Biol. *15*, 1235-41.

Liou, J., Fivaz, M., Inoue, T., and Meyer, T. (2007). Live-cell imaging reveals sequential oligomerization and local plasma membrane targeting of stromal interaction molecule 1 after Ca^{2+} store depletion. Proc. Natl. Acad. Sci. USA. *104*, 9301-6.

Luik, R.M., Wu, M.M., Buchanan, J., and Lewis, R.S. (2006). The elementary unit of store-operated Ca^{2+} entry: local activation of CRAC channels by STIM1 at ER-plasma membrane junctions. J. Cell Biol. *174*, 815-25.

Mathes, C., Fleig, A., and Penner, R. (1998) Calcium release-activated calcium current (I_{CRAC}) is a direct target for sphingosine. J. Biol. Chem. *273,* 25020-30.

Matthews, G., Neher, E., and Penner, R. (1989). Second messenger-activated calcium influx in rat peritoneal mast cells. J. Physiol. *418*, 105-30.

McCloskey, M.A., and Zhang, L. (2000). Potentiation of Fcε receptor I-activated Ca^{2+}

current (I_{CRAC}) by cholera toxin: possible mediation by ADP ribosylation factor. J. Cell Biol. *148*, 137-46.

Mercer, J.C., Dehaven, W.I., Smyth, J.T., Wedel, B., Boyles, R.R., Bird, G.S., and Putney, J.W. (2006). Large store-operated calcium selective currents due to co-expression of Orai1 or Orai2 with the intracellular calcium sensor, Stim1. J Biol. Chem. *281*, 24979-90.

Muik, M., Frischauf, I., Derler, I., Fahrner, M., Bergsmann, J., Eder, P., Schindl, R., Hesch, C., Polzinger, B., Fritsch, R., Kahr, H., Madl, J., Gruber, H., Groschner, K., and Romanin, C. (2008) Dynamic coupling of the putative coiled-coil domain of ORAI1 with STIM1 mediates ORAI1 channel activation. J Biol Chem. *283*, 8014-22

Pierini, L.M., Harris, N.T., Holowka, D., and Baird, B. (1997). Evidence supporting a role for microfilaments in regulating the coupling between poorly dissociable IgE-FcεRI aggregates downstream signaling pathways. Biochemistry. *36*, 7447-56.

Penner, R., Matthews, G., and Neher, E. (1988). Regulation of calcium influx by second messengers in rat mast cells. Nature. *334*, 499-504.

Peinelt, C., Lis, A., Beck, A., Fleig, A., and Penner R. (2008) 2-Aminoethoxydiphenyl borate directly facilitates and indirectly inhibits STIM1-dependent gating of CRAC channels. J Physiol. *586*, 3061-73.

Rohacs, T. (2006) Regulation of TRP channels by PIP_2. Eur. J. Physiol. *453,* 753-62.

Roos, J., DiGregorio, P.J., Yeromin, A.V., Ohlsen, K., Lioudyno, M., Zhang, S., Safrina, O., Kozak, J.A., Wagner, S.L., Cahalan, M.D., Veliçelebi, G., and Stauderman, K.A.. (2005). STIM1, an essential and conserved component of store-operated Ca^{2+} channel function. J. Cell Biol. *169*, 435-45.

Sato, T., Pallavi, P., Goebiewska, U., McLaughlin, S., and Smith, S.O. (2006). Structure of the membrane reconstituted transmembrane-juxtamembrane peptide EGFP (622-660) and its interaction with Ca^{2+}/calmodulin. Biochem. 45:12704-14.

Smyth, J.T., DeHaven, W.I., Bird, G.S., and Putney, J.W. (2007) Role of the microtubule cytoskeleton in the function of the store-operated Ca^{2+} channel activator STIM1. J Cell Sci. 2007 *120,* 3762-71.

Smyth, J.T., DeHaven, W.I., Bird, G.S., and Putney, J.W. (2008) Ca^{2+}-store-dependent and –independent reversal of Stim1 localization and function. J Cell Sci. *121*, 762-7.

Soboloff, J., Spassova, M.A., Tang, X.D., Hewavitharana, T., Xu, W., and Gill, D.L.

(2006). Orai1 and STIM reconstitute store-operated calcium channel function. J. Biol. Chem. *281*, 20661-5.

Van Rheenen, J., Langeslag, M., and Jalink, K. (2004). Correcting Confocal Acquisition to Optimize Imaging of Fluorescence Resonance Energy Transfer by Sensitized Emission. Biophys. J. *86*, 2517–29.

Várnai, P., and Balla, T. (1998). Visualization of phosphoinositides that bind pleckstrin homology domains: calcium- and agonist-induced dynamic changes and relationship to myo-[3H]inositol-labeled phosphoinositide pools. J. Cell Biol. *19*, 501-10.

Varnai, P., Toth, B., Toth, D.J., Hunyady, L., and Balla, T. (2007) Visualization and manipulation of plasma membrane-endoplasmic reticulum contact sites indicates the presence of additional molecular components within the STIM1-Orai1 complex. J. Biol. Chem. 282, 29678-90.

Vig, .M, Beck, A., Billingsley, J.M., Lis, A., Parvez, S., Peinelt, C., Koomoa, D.L., Soboloff, J., Gill, D.L., Fleig, A., Kinet, J.P., and Penner, R. (2006a). CRACM1 multimers form the ion-selective pore of the CRAC channel. Curr. Biol. *16*, 2073-9.

Vig, M., C. Peinelt, A. Beck, Koomoa, D.L., Rabah, D., Koblan-Huberson, M., Kraft, S., Turner, H., Fleig, A., Penner, R., and Kinet, J.P. (2006b). CRACM1 is a plasma membrane protein essential for store-operated Ca^{2+} entry. Science. *312*, 1220-3.

Vig, M., DeHaven, W., Bird, G.S. Billingsley, J.M., Wang, H., Rao, R.E., Hutchings, A. B., Jouvin, M-H., Putney, J.W., and Kinet, J-P. (2008). Defective mast cell effector functions in mice lacking the CRACM1 pore subunit of store-operated calcium release-activated calcium channels. Nature Immunology 9: 89-96.

Wu, M.M., Buchanan, J., Luik, R.M., and Lewis, R.S. (2006). Ca^{2+} store depletion causes STIM1 to accumulate in ER regions closely associated with the plasma membrane. J. Cell Biol. *174*, 803-13.

Wu M., Holowka, D., Craighead, H.G., and Baird, B. (2004). Visualization of plasma membrane compartmentalization with patterned lipid bilayers. Proc. Natl. Acad. Sci. USA. *101*, 13798-803.

Yatomi, Y., Ruan, F., Megidish, T., Toyokuni, T., Hakomori, S., and Igarashi, Y. (1996). N,N-Dimethylsphingosine inhibition of sphingosine kinase and sphingosine 1-phosphate production in human platelets. Biochemistry 35: 623-33.

Yeromin A.V., Zhang, S.L., Jiang, W., Yu, Y., Safrina, O., and Cahalan, M.D. (2006). Molecular identification of the CRAC channel by altered ion selectivity in a

mutant of Orai. Nature. *443*, 226-9.

Zhang, L., and McCloskey, M.A. (1995). Immunoglobulin E receptor-activated calcium conductance in rat mast cells. J. Physiol. *483*, 59-66.

CHAPTER 3

A BASIC SEQUENCE IN STIM1 PROMOTES CA^{2+} INFLUX BY INTERACTING WITH THE C-TERMINAL ACIDIC COILED-COIL OF ORAI1[1]

3.1 Abstract

Store-operated Ca^{2+} entry (SOCE) is a ubiquitous signaling process in eukaryotic cells in which the endoplasmic reticulum (ER)-localized Ca^{2+} sensor, STIM1, activates the plasma membrane-localized Ca^{2+} release-activated Ca^{2+} (CRAC) channel, Orai1, in response to emptying of ER Ca^{2+} stores. In efforts to understand this activation mechanism, we recently identified an acidic coiled-coil region in the C-terminus of Orai1 that contributes to physical association between these two proteins, as measured by fluorescence resonance energy transfer, and is necessary for Ca^{2+} influx, as measured by an intracellular Ca^{2+} indicator. Here, we present evidence that a positively charged sequence of STIM1 in its CRAC channel activating domain, human residues 384-386, is necessary for activation of SOCE, most likely because this sequence interacts directly with the acidic coiled-coil of Orai1 to gate Ca^{2+} influx. We find that mutation to remove positive charges in these residues in STIM1 prevents its stimulated association with wild type Orai1. However, association does occur between this mutant STIM1 and Orai1 that is mutated to remove negative charges in its C-terminal coiled-coil, indicating that other structural features are sufficient for this interaction. Despite this physical association, we find that thapsigargin fails to activate SOCE following co-expression of mutant STIM1 with either wt or the mutant Orai1, implicating STIM1 384-386 in transmission of the Ca^{2+} gating signal to Orai1 following store depletion.

[1] Reproduced with permission from *Biochemistry* (2010) *49*, 1067-71. Copyright 2010, American Chemical Society

3.2 Introduction

Ca^{2+} release-activated Ca^{2+} (CRAC) channels play a key role in Ca^{2+} influx and mobilization in numerous cellular responses. These channels are activated by coupling of the ER-store Ca^{2+} sensor STIM1 (Liou 2005, Zhang 2005) to the plasma membrane channel protein Orai1, also known as CRACM1 (Feske 2005, Vig 2006). Recently we showed that six acidic residues in a putative coiled-coil at the C-terminus of Orai1 contribute to STIM1-Orai1 interactions in response to Ca^{2+} store depletion (Calloway 2009). The mutant lacking these acidic residues, Orai1ΔDE, exhibits a clustered distribution at the plasma membrane in the absence of and following stimulation with thapsigargin. Similar clustering of wtOrai1 in unstimulated cells is caused by sphingosine derivatives that flip to the inner leaflet of the plasma membrane (Calloway 2009), suggesting that electrostatic repulsion prevents homo-oligomerization of unliganded Orai1. Stimulated oligomerization of Orai1 that is induced by clustered STIM1 is known to play a role in channel activation (Liou 2007, Penna 2008).

Based on these results, we hypothesized that electrostatic attraction and resulting neutralization of the acidic coiled-coil in Orai1 by basic residues in STIM1 facilitates oligomerization of Orai1 necessary for activation of the complex in response to store depletion. We therefore sought to identify a sequence on STIM1 that could mediate this charge neutralization. We first considered that the C-terminal polybasic sequence of STIM1 could be responsible for this coupling. However, our findings and those of others (Kawasaki 2009, Park 2009, Yuan 2009) demonstrated that this region is not necessary for robust SOCE or for formation of the STIM1-Orai1 complex. Furthermore, STIM1 residues 342-448 (human numbering), named the

CRAC activating domain (CAD), was recently identified as a minimal region of STIM1 sufficient to activate Ca^{2+} mobilization (Park 2009, see also Kawasaki 2009, Yuan 2009). Motivated by this information, we identified a short, highly conserved, basic sequence within CAD, STIM1 (382-387), as a potential region for interaction with the Orai1 acidic coiled-coil. We used fluorescence resonance energy transfer (FRET) and Ca^{2+} mobilization measurements of mutants to show that these residues are key for functional coupling of STIM1 and Orai1.

3.3 Experimental

3.3.1 Constructs and cloning

STIM1 K(384-6)Q-mRFP cDNA was generated using the Stratagene Quickchange site-directed mutagenesis kit on our previously constructed STIM1-mRFP vector (Calloway 2009). The primers used are: 5'-GCCAAGGAGGGGGCTGAGAAGATACAACAGCAGAGAAACACACTCTTTG GCACCTTCCAC-3' and its reverse complement. Preparation of the constructs AcGFP-Orai1 and AcGFP-Orai1ΔDE was previously described (Calloway 2009).

3.3.2 Cell culture

RBL-2H3 mast cells were cultured in minimal essential medium supplemented with 1 μg/ml gentamicin and 20% (v/v) fetal bovine serum. In preparation for transfection and imaging, cells were plated at 25% confluence into 35 mm MatTek wells. After approximately 20 h, cells were transfected with either mutant or wild-type versions of STIM1-mRFP and AcGFP-Orai1. These constructs were transfected using either

Geneporter (Genlantis) or Fugene HD (Roche) per manufacturers' instructions, with modifications to enhance transfection efficiency in the RBL cells previously described (Gosse 2005). Cells were imaged 24 h after transfection.

COS7 cells were cultured as monolayers in Dulbecco's modified Eagle's medium supplemented with 1 μg/ml gentamicin and 10% (v/v) fetal bovine serum. In preparation for imaging, cells were harvested and transfected with wt or mutant mRFP-STIM1 and Orai1 using Fugene HD according to manufacturer's instructions. Cells were transfected with non-fluorescent derivatives of Orai1 and mRFP-labeled derivatives of STIM1 as a marker for positive transfectants. Cells were imaged 24 h after transfection.

3.3.3 Confocal Microscopy

Immediately prior to imaging, RBL-2H3 cells were washed and incubated for 5 min at 37°C in 2.5 mL buffered salt solution (BSS: 135 mM NaCl, 5 mM KCl, 1 mM $MgCl_2$, 1.8 mM $CaCl_2$, 5.6 mM glucose, 1 mg/ml BSA, 20 mM HEPES, pH 7.4). Cells were then imaged on a Leica TCS SP2 confocal microscope with a Leica APO 63x dipping objective. Cells were excited at 488 nm and 543 nm, with laser intensity and phototube sensitivity adjusted to maximize signal/noise. Fluorescence emission was monitored at 495-540 nm and 555-675 nm. All live cell imaging was carried out at 37°C. After observing the resting state of the cells, they were stimulated for the time specified by the addition of 0.5 mL of BSS containing thapsigargin (150 nM final concentration). Leica Confocal Software was used during the experiment to acquire images, and ImageJ was used post acquisition to prepare composite micrographs by uniform contrast adjustment.

3.3.4 Ca^{2+} Measurements

Immediately prior to imaging, COS7 cells were incubated with 0.9 μM fluo-4-AM (Molecular Probes) for 10 minutes in BSS containing 0.5 mM sulfinpyrazone. Cells were then washed and resuspended in BSS/sulfinpyrazone. Fields of cells were imaged before and during thapsigargin stimulation under the same conditions and settings as described for multicolor imaging. For single-cell time courses, images were collected every 15 seconds for 2.5 min prior to stimulation and for 10 min after thapsigargin stimulation. For quantitation of pre- and post-stimulation Ca^{2+} levels, several fields of cells were imaged before stimulation and 10 minutes after thapsigargin stimulation. Cytoplasmic Fluo-4 fluorescence was quantified using ImageJ software. For each dish of cells, the average prestimulation fluorescence in untransfected cells was normalized to 1.0 to account for small differences in dye loading between multiple samples.

3.3.5 FRET Measurement

RBL-2H3 cells were imaged for FRET as previously described (Calloway 2009). Briefly, cells expressing a combination of mutant or wild-type STIM1-mRFP and AcGFP-Orai1 were imaged at 10 second intervals with excitation at 476 nm to minimize spectral bleedthrough. An automated mask-drawing algorithm in Matlab was used to select the pixels of interest at the plasma membrane for every time point using fluorescence from AcGFP as the template. The integrated red and green intensities under the mask were adjusted by background subtraction and correction for spectral bleedthrough. We report the ratio of the corrected red fluorescence to corrected green fluorescence as FRET (Calloway 2009).

3.4 Results and Discussion

The majority of the STIM1 CAD sequence shows homology to coiled-coil regions from a wide array of proteins (based on homology search using the Position-Specific Iterated Basic Local Alignment Search Tool, PSI-BLAST, provided by the NIH, http://blast.ncbi.nlm.nih.gov/Blast.cgi), but residues 382-395 have lower sequence homology to other proteins, suggesting a specialized function of this segment. We therefore mutated the three central lysines in this sequence (384-386) to glutamines to eliminate their positive charge while maintaining the hydrophilic and steric character of the endogenous sequence (STIM1 K(384-6)Q). Our modeling predicts that the flanking basic residues (K382 and R387) in this sequence are involved in intramolecular salt bridges with neighboring acidic amino acids and therefore might be of structural importance. The sequence we selected is similar to a slightly longer sequence of homologous, positively charged amino acids in the CAD region of the *Bombyx mori* (silkmoth) homologue of STIM1 that was recently shown to be important for translocation of STIM1 to plasma membrane punctae (Hull 2009). It is very close to residue L373 that was identified by Fischauf *et al*. as being critical both for the interaction of STIM1 and Orai1 and for Ca^{2+} mobilization (Frischauf 2009). We speculate that the mutation STIM1 L373S may disrupt the coiled-coil structure in the segment of STIM1 containing the basic residues we identified, thereby preventing proper engagement with Orai1.

We previously developed a microscopy-based FRET assay to monitor the physical association of wtSTIM1-mRFP with AcGFP-wtOrai1 and AcGFP-Orai1ΔDE

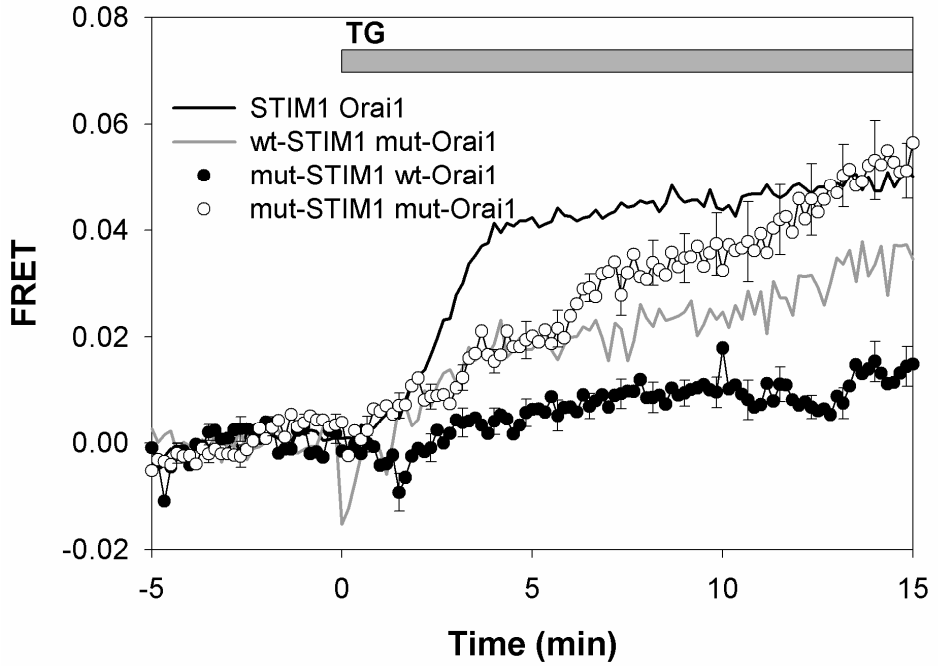

Figure 3.1: **Thapsigargin-mediated FRET. Thapsigargin (150 nM)-stimulated FRET between STIM1-mRFP and AcGFP-Orai1 constructs in RBL mast cells**. wtSTIM1-mRFP and AcGFP-wtOrai1 (black line), wtSTIM1-mRFP and AcGFP-Orai1ΔDE (mut-Orai1; grey line), STIM1 K(384-6)Q-mRFP (mut-STIM1) and AcGFP-Orai1ΔDE (○), and STIM1 K(384-6)Q-mRFP and AcGFP-wtOrai1 (●). Error bars show SEM for 12 to 18 cells from 4-5 different experiments, and every fifth error bar is shown for clarity.

(Calloway 2009). Using this method, we measured FRET between STIM1 K(384-6)Q-mRFP and AcGFP-wtOrai1 transfected into RBL mast cells. We found that these mutations in STIM1 almost completely prevent its association with wtOrai1 that is normally observed following stimulation by thapsigargin (Figure 3.1). In unstimulated cells, STIM1 K(384-6)Q-mRFP is expressed similarly to wtSTIM1-mRFP throughout the ER (Figure 3.2A,C) (Calloway 2009). However, unlike wt-STIM1-mRFP, this mutant fails to undergo thapsigargin-stimulated co-clustering with AcGFP-wtOrai1 in plasma membrane punctae (Figure 3.2D), consistent with the FRET results. Also shown in Figure 3.2A is the punctate distribution of AcGFP-Orai1ΔDE at the plasma membrane of this unstimulated RBL cell as previously described (Calloway 2009). To evaluate the functional capacity of this STIM1 mutant, we monitored Ca^{2+} mobilization in COS7 cells using Fluo-4 as previously described (Calloway 2009). COS7 cells exhibit little or no endogenous SOCE, but they exhibit a robust response to thapsigargin when wtSTIM1-mRFP and wtOrai1 are co-expressed (Figure 3.3A, blue circles). In contrast, when STIM1 K(384-6)Q-mRFP is co-expressed with wtOrai1 at similar levels, no thapsigargin-stimulated SOCE is observed (Figure 3.3A, green triangles). Results in Figures 3.1 and 3.3 indicate that STIM1 lysine residues 384-386 are necessary for coupling to Orai1 and consequent activation of SOCE.

These observations, together with our previous results, led us to hypothesize that basic residues 384-386 of STIM1 directly engage the acidic coiled-coil at the C-terminus of Orai1, involving electrostatic attraction between the oppositely charged residues. If this is the case, wtOrai1 might not couple with STIM1 K(384-6)Q without this electrostatic attraction. Alternatively, electrostatics may contribute but may not be the dominant energetic contribution to the interaction between STIM1 and Orai1. In this latter case, the stimulated association of the wild type proteins might be restored if the charged sequences on both of these proteins are mutated to neutral amino acids. To

distinguish these possibilities, we measured FRET between STIM1 K(384-6)Q-mRFP and AcGFP-Orai1ΔDE, and we found that thapsigargin stimulates their physical association to a similar extent as for the wild type proteins, but with substantially slower kinetics (Figure 3.1). This finding is similar to the slow FRET-detected association between wtSTIM1-mRFP and AcGFP-Orai1ΔDE that we previously reported (Calloway 2009; Figure 3.1). Consistent with the FRET observed, STIM1 K(384-6)Q-mRFP co-patches with AcGFP-Orai1ΔDE in plasma membrane punctae in response to thapsigargin, similar to that seen with wtSTIM1-mRFP and AcGFP-Orai1ΔDE (Figure 3.2B,F). As with FRET-detected association, this visible co-patching of STIM1 K(384-6)Q-mRFP with AcGFP-Orai1ΔDE requires longer stimulation times with thapsigarin than for the corresponding wt constructs.

This finding that STIM1 K(384-6)Q undergoes stimulated association with Orai1ΔDE, but does not associate with its wild-type partner, suggests a model for the interaction between these two proteins and the role of the charged sequences in this interaction (Figure 3.4). Although the charged sequence on STIM1 and its resulting electrostatic attraction to the acidic sequence on Orai1 appears to contribute little to the overall binding energy of the active complex, mutation to eliminate the charged residues on STIM1 clearly reduces the interaction energy with its wild type partner. Thus, the simplest model to account for these observations is one in which this acidic sequence on Orai1 normally interacts with the basic sequence on STIM1 in an attractive electrostatic interaction.

To determine whether stimulated association between STIM1 K(384-6)Q and Orai1ΔDE results in SOCE, we monitored Ca^{2+} mobilization in COS7 cells expressing these mutants. As shown in Figure 3.3A, we did not detect a significant Ca^{2+} response to thapsigargin (red squares), compared to untransfected COS7 cells (pink circles).

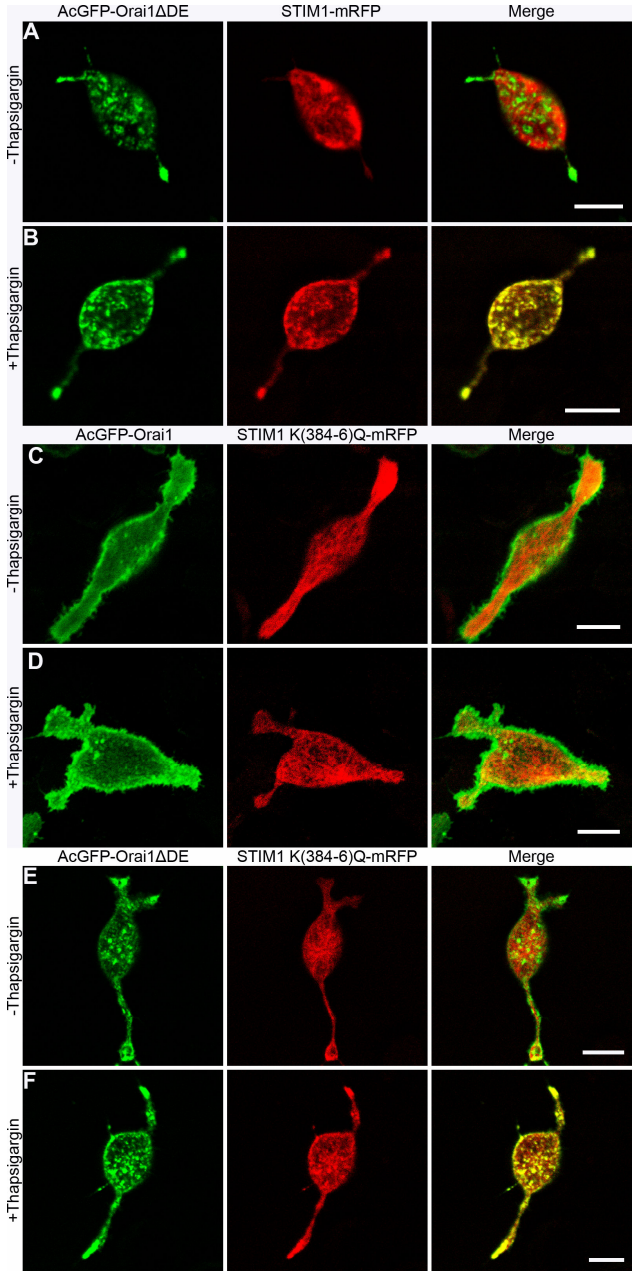

Figure 3.2**: Cellular distributions of Orai1 and STIM1**. Ventral surface confocal microscopy images of transfected RBL cells showing distributions of (A-B) AcGFP-Orai1ΔDE (green) and wtSTIM1-mRFP (red), (C-D) AcGFP-wtOrai1 (green) and STIM1 K(384-6)Q-mRFP (red), or (E-F) AcGFP-Orai1ΔDE and STIM1 K(384-6)Q-mRFP in the absence (A,C,E) or presence (B,D,F) of 150 nM thapsigargin for 30 min at 37^{o}C. Scale bars represent 10 μm.

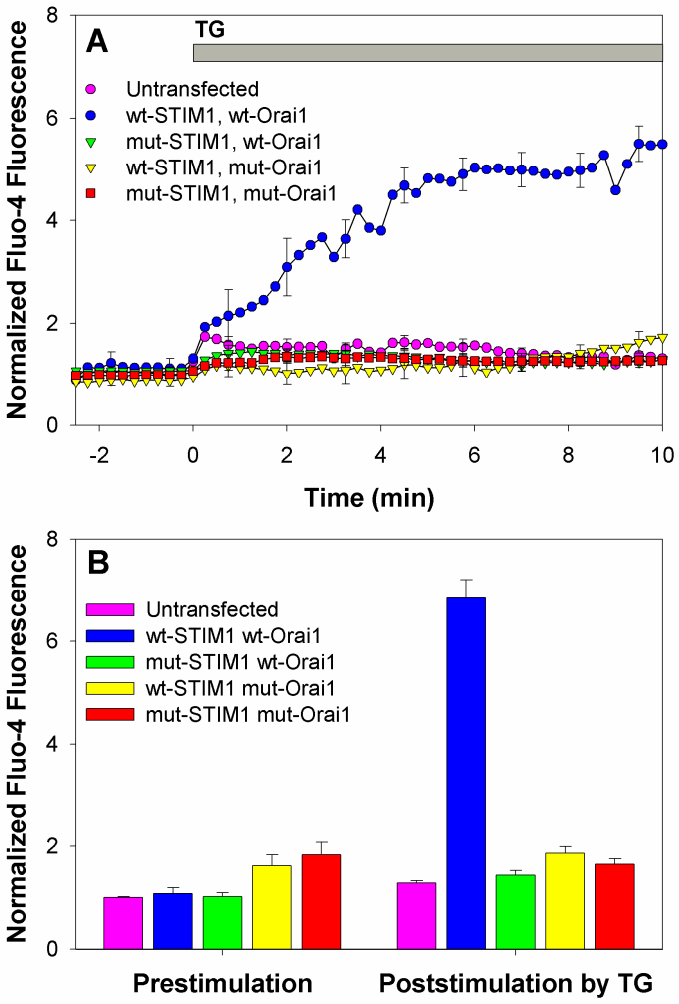

Figure 3.3: **Stimulated Ca^{2+} responses**. A) Ca^{2+} responses to 150 nM thapsigargin in COS7 cells expressing wtSTIM1-mRFP and wtOrai1 (●), STIM1 K(384-6)Q-mRFP and wtOrai1 (▼), wtSTIM1-mRFP and Orai1ΔDE (▼), STIM1 K(384-6)Q-mRFP and Orai1ΔDE (■), and untransfected cells (●). Fluo-4 fluorescence was normalized relative to the average prestimulation basal Ca^{2+} level in untransfected cells in the same field. Each time course represents the average of 10-18 cells, and error bars show SEM. Cells with basal Ca^{2+} levels >3x larger than the average for untransfected cells were excluded. B) Mean Ca^{2+} levels before and 10 min after addition of 150 nM thapsigargin for averaged individual COS7 cells expressing a combination of wtSTIM1-mRFP or mutant STIM1 K(384-6)Q-mRFP with wtOrai1 or mutant Orai1ΔDE. Each bar represents the mean for 20-60 cells from 3 or more different experiments, and error bars show SEM.

The absence of SOCE with these constructs, which clearly undergo thapsigargin-stimulated association detected by FRET (Figure 3.1) and co-patching (Figure 3.2F), implicates these sequences in the gating of Ca^{2+} influx. Our proposed model accounts for these results: Ca^{2+} gating is controlled by the C-terminal acidic coiled-coil of Orai1, and engagement of this sequence with basic residues 383-387 in the CAD region of STIM1 induces the formation of the active CRAC channel (Figure 3.4A).

Our previous results provided evidence that the acidic coiled-coil of Orai1 controls its oligomerization state, possibly based on mutual electrostatic repulsion (*5*). In our current model, STIM1 facilitates Ca^{2+} mobilization in part by inducing the oligomerization of Orai1. Modulation of electrostatics at the faces of coiled-coils has been implicated previously in the control of the oligomerization state of different proteins (Woolfson 2005, Fairman 1996), consistent with our view that, by neutralizing the acidic coiled-coil on Orai1, STIM1 383-387 reduces the charge-charge repulsion between individual Orai1 monomers and allows them to oligomerize into an active state. Our model is also consistent with our observations that neutralization of the acidic residues on the C-terminal coiled-coil of Orai1 induces plasma membrane patching of this protein in the absence of store depletion or STIM1 translocation (Figure 3.2A) (Calloway 2009).

We investigated possible Ca^{2+} influx through spontaneous oligomerization of Orai1ΔDE. Figure 3.3B summarizes average Ca^{2+} levels before and 10 min after addition of 150 nM thapsigargin for a large number of individual cells. For unstimulated cells, there is a small but significant increase in the average Ca^{2+} levels of cells expressing Orai1ΔDE compared to untransfected cells or cells transfected with wtOrai1. We find that a small fraction (~10-20%) of these cells have a basal state of cytoplasmic Ca^{2+} that is >3-fold above that of untransfected cells, suggesting they have spontaneously activated CRAC channels (supplemental Figure C.1A). However,

cells expressing Orai1ΔDE with both high and low resting Ca^{2+} levels are similarly unresponsive to thapsigargin, consistent with the incapacity of Orai1ΔDE to be activated by STIM1 (Figure C.1B). This variation in resting Ca^{2+} levels we observe for cells expressing clustered Orai1ΔDE indicates that there must be additional factor(s) controlling the gating of Ca^{2+} entry through Orai1 that varies among cells; one possibility is population differences in polyphosphoinositide levels (Vasudevan 2009).

To account for the activation of SOCE, we propose that, in addition to inducing Orai1 oligomerization, binding of the STIM1 K(384-386) sequence to the acidic residues in the coiled-coil of Orai1 causes an allosteric change that directly opens the Ca^{2+} selective pore in the STIM1-Orai1 complex. Park *et al*. showed that STIM1 CAD interacts with both the N and C termini of Orai1 (Park 2009). A possible scenario is that the C-terminal acidic coiled-coil of Orai1 interacts with its own N-terminus in the resting state, and STIM1 (346-348) disengages this interaction in activated cells, thereby opening the channel in an allosteric manner (Figure 3.4A). The N-terminus of Orai1 contains a poly-arginine sequence (Orai1 28-33) that could serve as a potential binding partner for its acidic coiled-coil in unstimulated cells. Yuan, *et al*. found that the N-terminus of Orai1 is important for activation of CRAC channels with full length STIM1, but not with a minimal interaction domain that is similar to CAD (Yuan 2009), suggesting additional changes in Orai1 structure may be involved in this activation process.

In summary, we find that the basic sequence in the C-terminus of STIM1, K384-386, is important for functional coupling of STIM1 with Orai1 that is driven by thapsigargin-mediated Ca^{2+} store depletion (Figure 3.4A,B). Futhermore, we demonstrate that mutation to neutralize acidic residues in the C-terminal coiled-coil of Orai1 restores its stimulated association with STIM1 K(384-6)Q, but does not restore SOCE (Figure 3.4C). Our results support a model in which both oligomerization of

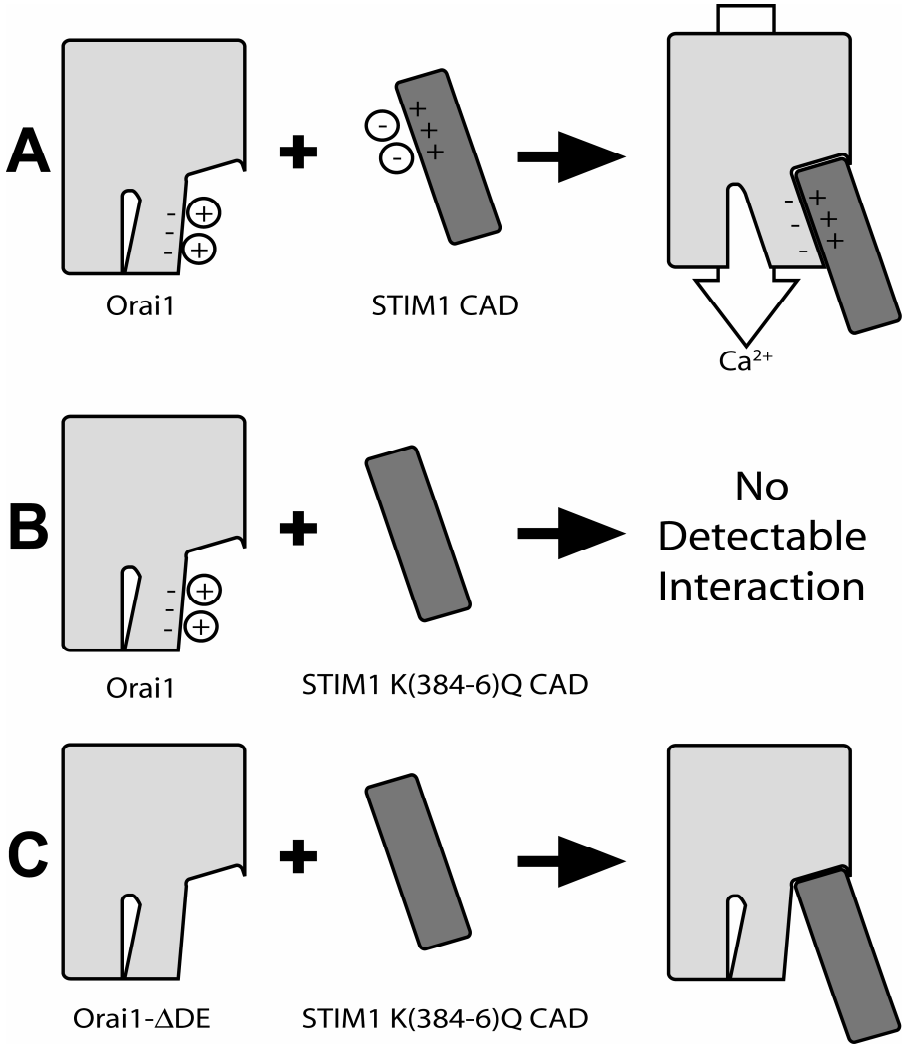

Figure 3.4: **Cartoon depicting basic features of proposed model for wild type and mutant STIM1 and Orai1 interactions**. A) In unstimulated cells, the negatively charged acidic amino acids on wtOrai1 and the positively charged lysine sequence (K384-386) in the STIM1 CAD domain (dark grey) defined by our mutations are shown associated with solvated counter ions. Upon stimulation, these ions are displaced from the binding cleft between the two proteins, allowing these charged regions to interact with each other and causing the Ca^{2+}-selective channel to open in an allosteric manner. B) When K384-386 in STIM1 is mutated to glutamines, STIM1 no longer binds and activates wtOrai1 due to the loss of electrostatic attraction and resulting repulsion at this interaction subsite. C) When these charged sequences on Orai1 and STIM1 are both mutated, STIM1 CAD regains the capacity to bind Orai1 via interactions at other sites because the electrostatic repulsion has been eliminated. However, this association does not cause allosteric activation of the Ca^{2+} gate. The oligomerization state of these proteins is omitted for clarity: Orai1 is oligomerized in the active wtSTIM-wtOrai1 complex and in all cases involving Orai1ΔDE.

Orai1 and Ca^{2+} gating are dependent on electrostatic interaction between these sequences in Orai1 and STIM1. In addition, our results reveal that these two processes can be uncoupled from each other in this exquisitely regulated mechanism of SOCE activation.

3.5 Supporting Information Available:

Figure C.1. Population distribution of Ca^{2+} levels in cells expressing mutant and wild type STIM1 and Orai1. This material is included in appendix C.

REFERENCES

Calloway, N., Vig, M., Kinet, J.P., Holowka, D., and Baird B. (2009). Molecular clustering of STIM1 with Orai1/CRACM1 at the plasma membrane depends dynamically on depletion of Ca^{2+} stores and on electrostatic interactions, *Mol. Biol. Cell 20*, 389-399.

Fairman, R., Chao, H. G., Lavoie, T. B., Villafranca, J. J., Matsueda, G. R., and Novotny, J. (1996). Design of heterotetrameric coiled coils: evidence for increased stabilization by Glu(-)-Lys(+) ion pair interactions, *Biochemistry 35*, 2824-2829.

Feske, S., Gwack, Y., Prakriya, M., Srikanth, S., Puppel, S.H., Tanasa, B., Hogan, P.G., Lewis, R.S., Daly, M., and Rao, A. (2006). A mutation in Orai1 causes immune deficiency by abrogating CRAC channel function, *Nature 441*, 179-185.

Frischauf, I., Muik, M., Derler, I., Bergsmann, J., Fahrner, M., Schindl, R., Groschner, K., and Romanin, C. (2009). Molecular determinants of the coupling between STIM1 and Orai channels: Differential activation of Orai1,2,3 channels by a STIM1 coiled-coil mutant, *J. Biol. Chem*. *284*, 21696-21706.

Gosse, J.A., Wagenknecht-Wiesner, A., Holowka, D., and Baird, B. (2005). Transmembrane sequences are determinants of immunoreceptor signaling, *J. Immunol*. *175*, 2123-2131.

Hull, J.J., Lee, J.M., Kajigaya, R., and Matsumoto, S. (2009) Bombyx mori homologs of STIM1 and Orai1 are essential components of the signal transduction cascade that regulates sex pheromone production. *J. Biol. Chem. 284,* 31200-31213.

Kawasaki, T., Lange, I., and Feske, S. (2009). A minimal regulatory domain in the C terminus of STIM1 binds to and activates ORAI1 CRAC channels, *Biochem. Biophys. Res. Commun*. *385*, 49-54.

Liou, J., Kim, M.L., Heo, W.D., Jones, J.T., Myers, J.W., Ferrell, J.E. Jr, and Meyer, T. (2005). STIM is a Ca^{2+} sensor essential for Ca^{2+}-store-depletion-triggered Ca^{2+} influx. *Curr. Biol. 15*, 1235-41.

Liou, J, Fivaz, M., Inoue, T., and Meyer, T. (2007) Live-cell imaging reveals sequential oligomerization and local plasma membrane targeting of stromal interaction molecule 1 after Ca^{2+} store depletion, *Proc. Nat. Acad. Sci. 104*, 9301-06.

Park, C.Y., Hoover, P.J., Mullins, F.M., Bachhawat, P., Covington, E.D., Raunser, S., Walz, T., Garcia, K.C., Dolmetsch, R.E., and Lewis R.S. (2009). STIM1 clusters and activates CRAC channels via direct binding of a cytosolic domain to Orai1, *Cell 136*, 814-816.

Penna, A., Demuro, A., Yeromin, A.V., Zhang, S.L., Safrina, O., Parker, I., and Cahalan M.D. (2008). The CRAC channel consists of a tetramer formed by Stim-induced dimerization of Orai dimers, *Nature 456*, 116-120.

Vasudevan, L., Jeromin, A., Volpicelli-Daley, L., De Camilli, P., Holowka, D., and Baird, B. (2009). The beta- and gamma-isoforms of type I PIP5K regulate distinct stages of Ca^{2+} signaling in mast cells, *J. Cell Sci*. *122*, 2567-2574.

Vig, M., Peinelt, C., Beck, A., Koomoa, D.L., Rabah, D., Koblan-Huberson, M., Kraft, S., Turner, H., Fleig, A., Penner, R., and Kinet, J.P. (2006). CRACM1 is a plasma membrane protein essential for store-operated Ca^{2+} entry, *Science 312*, 1220-1223.

Woolfson, D. N. (2005). The design of coiled-coil structures and assemblies, *Adv. Protein Chem. 70*, 79-112

Yuan, J.P., Zeng, W., Dorwart, M.R., Choi, Y.J., Worley, P.F., and Muallem, S. (2009). SOAR and the polybasic STIM1 domains gate and regulate Orai channels, *Nat Cell Biol*. *11*, 337-343.

Zhang, S.L., Yu, Y., Roos, J., Kozak, J.A., Deerinck, T.J., Ellisman, M.H., Stauderman, K.A., and Cahalan M.D. (2005) STIM1 is a Ca^{2+} sensor that activates CRAC channels and migrates from the Ca^{2+} store to the plasma membrane. *Nature 437,* 902-905.

CHAPTER 4

STIMULATED ASSOCIATION OF STIM1 AND ORAI1 IS REGULATED BY THE BALANCE BETWEEN DETERGENT RESISTANT AND DETERGENT SOLUBILIZED POOLS OF PIP_2

4.1 Abstract

We previously showed that PI5KIβ and PI5KIγ generate functionally distinct pools of phosphotidylinositol-(4,5)-bisphosphate (PIP_2) important for inositol trisphosphate (IP_3) production and Ca^{2+} mobilization, respectively (Vasudevan, L., Jeromin, A., Volpicelli-Daley, L., De Camilli, P., Holowka, D., and Baird, B., 2009, J Cell Sci. 122, 2567-74). In the present study, we demonstrate that the FRET detected interaction between the ER Ca^{2+} sensor, STIM1, and the store operated Ca^{2+} (SOC) channel, Orai1, following store depletion with thapsigargin is enhanced by overexpression of PI5KIβ and inhibited by overexpression of PI5KIγ. We also show that overexpression of these different isoforms results in the differential enhancement of PIP_2 in detergent-resistent membrane (DRM) and detergent-solubilized membrane (DSM) fractions. These biochemically extracted DRM and DSM fractions correspond roughly to membrane domains characterized by ordered lipids and disordered lipids, respectively. Over-expression of inositol 5-phosphatase L10-Inp54p that targets to ordered lipids causes depletion of PIP_2 from the DRM fraction, and also inhibits thapsigargin-mediated STIM1-Orai1 association. On the other hand, Over-expression of inositol 5-phosphatase S15-Inp54p that targets to disordered lipids causes depletion of PIP_2 from the DSM fraction, and this treatmentenhances STIM1-Orai1 association. Removal of either the STIM1 C-terminal polylysine sequence (a.a. 677-685) or a N-terminal polyarginine sequence in Orai1 (a.a. 28-33) interferes with the differential

sensitivity of the STIM1-Orai1 association to the concentrations of PIP_2 that isolate with DRM and DSM fractions. These results are consistent with a model in which, following Ca^{2+} store depletion, Orai1 translocates between structurally and functionally distinct membrane domains in a PIP_2-dependent fashion to engage STIM1 associated with the ordered lipid pool of PIP_2.

4.2 Introduction

Store-operated Ca^{2+} entry (SOCE) is a ubiquitous process that regulates intracellular Ca^{2+} as a secondary messenger in nonexcitable cells. The two proteins that are necessary for this process are the ER transmembrane Ca^{2+} sensor STIM1 (Liou 2005, Zhang 2005) and the plasma membrane tetraspan Ca^{2+} channel Orai1, also known as CRACM1 (Feske 2006, Vig 2006). Oligomerized Orai1 forms the Ca^{2+} release-activated Ca^{2+} (CRAC) channel that is activated by association with STIM1 at ER-plasma membrane (ER-PM) junctions following depletion of Ca^{2+} from the ER, resulting in Orai1-mediated influx of Ca^{2+} from the extracellular medium. We identified an acidic coiled-coil on the C-terminus of Orai1 as important for the functional interaction between STIM1 and Orai1 (Calloway 2009), and in a subsequent study we showed that a short sequence of lysine residues within the CRAC activating domain (CAD; Park 2009) of STIM1 must interact with the acidic coiled-coil of Orai1 for functional coupling (Calloway 2010).

In addition to these sequences, the lysine rich C-terminus of STIM1 (hu a.a. 677-685) has been a region of much interest for its hypothesized capacity to bind phosphatidylinositol phosphates (PIPs) at the plasma membrane in a STIM1 oligomerization-enhanced mechanism (Liou PNAS 2007). Korzeniowski, *et al*. (2009) demonstrated that activation of the CRAC current (I_{CRAC}) is sensitive to inhibition of

phosphatidylinositol 4-kinase, but is not prevented by depletion of PIP_2 at the plasma membrane. Walsh *et al*. (2010) showed that inhibition of multiple pathways of PIP_2 generation is necessary to prevent thapsigargin-mediated translocation of STIM1 to the plasma membrane, but that expression of Orai1 permits STIM1 to concentrate at ER-PM junctions even in the absence of PIP_2. Furthermore, they showed that PIP_2 can play an inhibitory role in the interaction of Orai1 with STIM1 (Walsh 2010). Additionally, several studies have provided evidence for roles for the C-terminal polylysine sequence of STIM1 in other interactions. This polylysine sequence has been identified as a direct binding partner for canonical transient receptor potential (TRP) channels (Zeng 2008), as a structural determinant of the inwardly rectifying character of I_{CRAC} (Yuan 2009), and as a binding site for calmodulin (Bauer 2008).

We previously demonstrated that different isoforms of type I phosphatidylinositol-4-phosphate 5-kinase (PI5KI), namely PI5KIβ and PI5KIγ, synthesize functionally distinguishable pools of phosphatidylinositol-4,5-bisphosphate (PIP_2) that have distinct roles in SOCE and inositol trisphosphate (IP_3) generation, respectively (Vasudevan 2009). In the current study we have characterized the membrane structure basis for these multiple pools of PIP_2, and we have illuminated their roles in the regulation of SOCE. Previous studies provided evidence for a role for ordered lipid membrane domains, known as “lipid rafts”, in the interaction between STIM1 and TRPC1 (Pani 2008, Alicia 2008) In the present study, we find evidence that the C-terminal polylysine sequence of STIM1, as well as a previously uncharacterized poylarginine sequence in Orai1 (hu a.a. 28-33) modulate STIM1-Orai1 association during SOCE by their differential association with PIP_2 pools in ordered and disordered membrane domains.

4.3 Experimental

4.3.1 Constructs and cloning

STIM1ΔK-mRFP was constructed from our previously described STIM1-mRFP vector (Calloway 2009) using the Stratagene Quickchange site directed mutagenesis kit. The primers used are 5'-GGAAACAGACTCCAGCCCAGGCC GGGCGGCCGCATCAGGCATGGCCTC-3' and its reverse complement. AcGFP-Orai1ΔR was constructed using site-directed mutagenesis on our previously described AcGFP-Orai1 vector (Calloway 2009). The mutagenic primers used are 5'-GCAGCACCACCAGCGGCAGCAGCGGGGACGGGGAGCCC-3' and its reverse complement. Additionally, flanking primers up and downstream of the multiple cloning site on AcGFP-Orai1 were used.

L10-Inp54p and S15-Inp54p were derived from the L10-GFP-Inp54p and S15-GFP-Inp54p vectors from Dr. William Rodgers (Johnson 2008). GFP was removed from each vector by recloning and ligating the targeting sequence (L10 or S15) with that for Inp54p. PI5KIβ, PI5KIγ87, STIM1-mRFP, and AcGFP-Orai1 vectors were previously described (Vasudevan 2009, Calloway 2009).

4.3.2 Cell Culture

RBL-2H3 mast cells were cultured in minimal essential medium supplemented with 1 μg/ml gentamicin and 20% (v/v) fetal bovine serum. In preparation for transfection and imaging, cells were plated at 25% confluence into 35 mm MatTek wells. After approximately 20 h, cells were transfected with either mutant or wild-type versions of STIM1-mRFP and AcGFP-Orai1. These constructs were transfected using either

Geneporter (Genlantis) or Fugene HD (Roche) per manufacturers' instructions, with modifications to enhance transfection efficiency in the RBL cells previously described (Gosse 2005). Additionally, modifications were made to the transfection protocol to achieve higher degrees of expression for both the L10-Inp54p and S15-Inp54p constructs: cells were transfected with 8 μg DNA (7 μg Inp54p construct, 0.5 μg each of STIM1 and Orai1 constructs) and 20 μL Geneporter in 100 μL OptiMem (Invitrogen) added to each MatTek well. Cells were imaged 24 h after transfection. For Ca^{2+} measurements in RBL-2H3 cells, indo-1 was loaded and monitored in a stirred cuvette using steady-state fluorimetry as previously described (Pierini 1997).

4.3.3 Confocal Microscopy and FRET

RBL-2H3 cells were imaged for FRET as previously described (Calloway 2009). Prior to imaging, RBL-2H3 cells were washed and incubated for 5 min at 37°C in 2.5 mL buffered salt solution (BSS: 135 mM NaCl, 5 mM KCl, 1 mM MgCl2, 1.8 mM CaCl2, 5.6 mM glucose, 1 mg/ml BSA, 20 mM HEPES, pH 7.4). Images of cells were collected on a Leica TCS SP2 confocal microscope with a Leica APO 63x dipping objective. Cells were excited at 488 nm and 543 nm, with laser intensity and phototube sensitivity adjusted to maximize signal/noise. For FRET measurements, cells were imaged at 10 second intervals with excitation at 476 nm to minimize spectral bleedthrough. All FRET measurements were carried out at 37°C. After observing the resting state of the cells, they were stimulated for the time specified by the addition of 0.5 mL of BSS containing thapsigargin (150 nM final concentration). An automated mask-drawing algorithm in Matlab was used to select the pixels of interest at the plasma membrane for every time point using fluorescence from AcGFP as the template (Calloway 2009). The integrated red and green fluorescence intensities

under the mask were adjusted by background subtraction and correction for spectral bleedthrough. We report the ratio of the corrected red fluorescence to corrected green fluorescence as FRET.

4.3.4 Membrane Fractionation and Dot-Blots

24 h prior to fractionation, cells were electroporated with the indicated construct at a concentration of 32 μg DNA/mL at 280 V and 950 μF using Gene Pulser X (Bio-Rad). Sucrose gradient fractionation was performed as previously described (Field 1999), with small modifications. Briefly, cells were harvested, resuspended in BSS, and solublized with Triton X-100 (Pierce) at a ratio of 0.013 % (v/v) Triton X-100 per 1 x 10^6 cells. Gradients were constructed by pipetting in order: 250 μL 80% sucrose, 500 μL 50% sucrose, 1.5 mL 40% sucrose containing cell lysate, 750 μL 30% sucrose, 500 μL 20% sucrose and 1 mL 10% sucrose (all concentrations are w/v). After 16-18 h of centrifugation at 49,000 rpm, each gradient was divided into two fractions at the top interface of the 40% sucrose band. Each of these fractions was subsequently extracted for lipids via the method described by Johnson, *et al*. (2008). After extraction, the dried lipid film was resuspended in water at a concentration normalized to 800 cell equivalents/μL. Dot-blotting was performed by first sealing the ventral holes in the dot-blot apparatus (BD Biosciences) with aluminum foil. Then 10 μL of resuspended extract was added to the nitrocellulose membrane in each well and allowed to air dry in the apparatus for 30 min, followed by removal of the membrane from the aparatus and further drying 1.5 h at ambient temperature. Blots were blocked in either 3% BSA (w/v) or 20% FBS (v/v), developed with anti-PIP_2 mAb (Assay Designs) and anti-mouse IgG conjugated to horseradish peroxidase (GE Healthcare). Blots were visualized using Supersignal West Pico chemiluminescent dye (Thermo Scientific).

Quantification was performed with ImageJ.

4.4 Results

4.4.1 Cholesterol and phosphoinositides contribute to stimulated association of STIM1 and Orai1.

Previous studies provided evidence for a role for cholesterol-dependent membrane heterogeneity in the activation of SOCE involving TRP channels (Pani 2008, Jardin 2008). As shown in Figure 4.1A, we find that relatively mild cholesterol depletion from RBL mast cells by 4 mM methyl β-cyclodextrin (MβCD) for 20 min at 37°C results in substantial inhibition of thapsigargin-stimulated SOCE. Under these conditions, cholesterol is reduced by approximately 30% in these cells (Surviladze 2001), and in multiple experiments, we find that SOCE measured 5 min after addition of thapsigargin is inhibited by 69 ± 6 % (SD, n=3). Sensitivity of this Ca^{2+} influx to 1 μM Gd^{3+} indicates that this is largely due to I_{CRAC} (Broad 1999). We previously established a method to monitor the stimulated association of STIM1 and Orai1 by fluorescence resonance energy transfer (FRET). Using this method in RBL cells transiently transfected with donor AcGFP-Orai1 and acceptor STIM1-mRFP, we find that similar mild cholesterol depletion by MβCD inhibits thapsigargin-stimulated association of STIM1 with Orai1 by 73 ± 8% after 10 minutes (Figure 4.1B), consistent with a role for cholesterol-dependent plasma membrane structure in this process. A previous study indicated that inhibition of SOCE by cholesterol depletion is due to depolarization of the plasma membrane (DeHaven 2009). To address this possibility, we evaluated the effect of high K^+-mediated depolarization on the Ca^{2+} response to thapsigargin in cells treated with MβCD and in control cells. We found

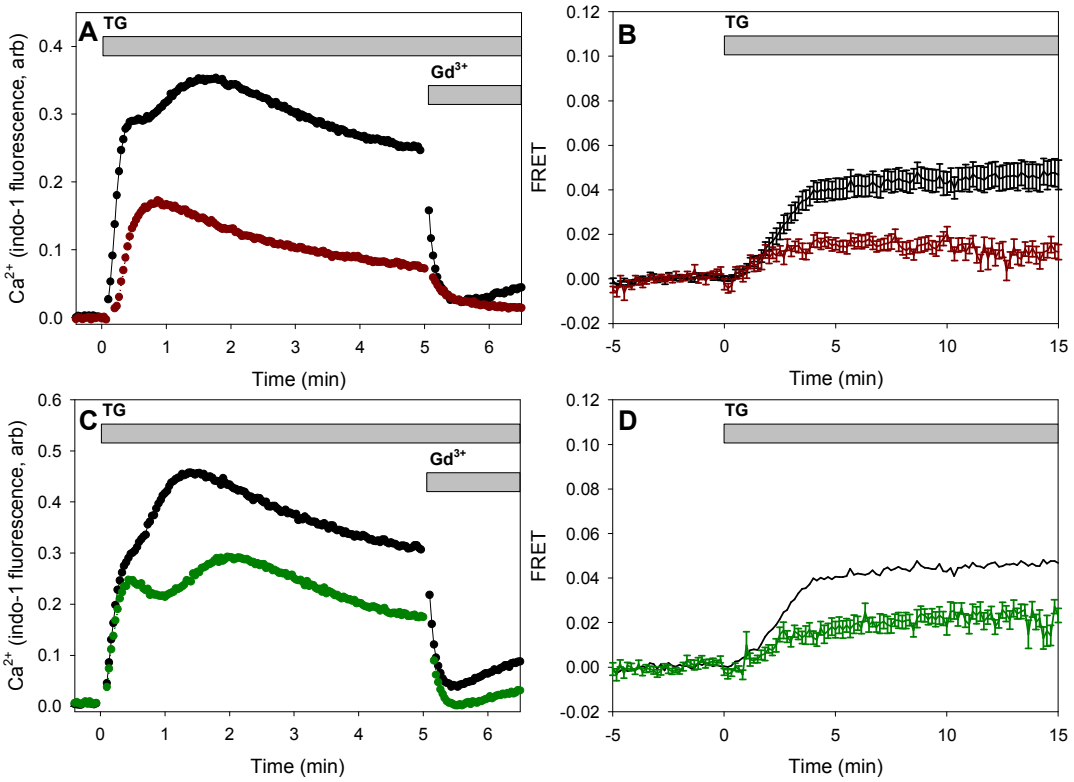

Figure 4.1**: Thapsigargin-stimulated SOCE and STIM1-Orai1 FRET following cholesterol depletion and PI4K inhibition**. A) Representative Ca^{2+} responses as measured by indo-1 fluorescence in control RBL-2H3 cells (black circles), and cells treated with 4 mM MβCD for 20 min (red circles). Sensitivity to 1 μM Gd^{3+} is shown by addition at the indicated time points. B) Effect of cholesterol depletion on thapsigargin-stimulated FRET between AcGFP-Orai1 and STIM1-mRFP. Cells were untreated (black) or incubated with 5 mM MβCD for 10 min (red) prior to stimulation by thapsigargin. Error bars show SEM. C) Representative Ca^{2+} responses in control RBL-2H3 cells (black), and cells treated with 10 μM wortmannin for 10 min (green) prior to stimulation by thapsigargin. D) Thapsigargin-stimulated FRET between AcGFP-Orai1 and STIM1-mRFP in unperturbed cells (black) and cells treated with 10 μM wortmannin (green). Error bars show SEM.

that the MβCD-inhibited Ca^{2+} response remains sensitive to depolarization to a similar extent as the untreated control cells (Figure D.1).

Broad *et al*. (2001) reported that inhibition of PI4P synthesis by 10-20 μM wortmannin causes substantial inhibition of I_{CRAC} in RBL mast cells, providing evidence for a role for phosphoinositides in SOCE. Consistent with these results, we find that treatment of RBL cells with 10 μM wortmannin for 10 min at 37°C inhibits thapsigargin-stimulated Ca^{2+} entry by ~40% when assessed 5 min after addition of thapsigargin (Fig. 1C). To investigate the mechanism of this inhibition, we examined the effect of wortmannin on stimulated FRET under similar conditions. As shown in Figure 4.1D, we find that thapsigargin-stimulated FRET between AcGFP-Orai1 and STIM1-mRFP is inhibited 52 ± 8% by 10 μM wortmannin after 10 min of stimulation. This is consistent with reports that wortmannin and other PI4K inhibitors prevent colocalization of STIM1 and Orai1 in ER-plasma membrane puncta (Korzeniowski 2009, Walsh 2010). Our results provide evidence that stimulated coupling between STIM1 and Orai1 depends on PI4P, either directly or because of it role as a precursor for other phosphoinositide species.

4.4.2 PI5KIβ and PI5KIγ differentially modulate stimulated association of STIM1 with Orai1.

In a recent study, our laboratory found that two related phosphatidylinositol 5' kinases, PI5KIβ and PI5KIγ, synthesize functionally distinguishable pools of PIP_2 that differentially affect antigen-stimulated SOCE (Vasudevan 2009). To investigate roles for PIP_2 synthesis by these PIP5K isoforms in STIM1-Orai1 interactions, we monitored stimulated FRET between AcGFP-Orai1 and STIM1-mRFP in cells overexpressing either PI5KIβ or PI5KIγ. As shown in Figure 4.2A, we found that

overexpression of the Iβ isoform consistently enhances thapsigargin-stimulated association between STIM1-mRFP and AcGFP-Orai1, whereas overexpression of the PI5KIγ isoform consistently inhibits this interaction (Figure 4.2A).

This differential modulation of STIM1-Orai1 association by two isoforms of PI5-kinase that both produce PI-4,5-bisphosphate implies that each isoform must produce a distinguishable pool of PIP_2. Previous studies utilized sucrose gradients to separate detergent-resistant membranes (DRM) from membrane proteins and lipids that are solubilized (DSM). This biochemical separation has proven useful for characterizing subregions of the plasma membrane that are distinguished by their composition of lipids with ordered (DRM) vs disordered (DSM) acyl chains (Brown 1992, Sheets 1999, Simons 2000, Brown recent review). In other studies, this approach provided evidence for two distinguishable pools of PIP_2 that are differentially altered by EGF-stimulated phospholipase C activation (Casey 1998). To test the possibility that PIP5KIβ and Iγ synthesize pools of PIP_2 that preferentially associate with either ordered or disordered lipid pools, we compared the relative concentrations of PIP_2 that fractionated with DRM and DSM from cells with and without overexpression of PI5KIβ and PI5KIγ. As summarized in Figure 4.2B, overexpression of both enzymes enhances total PIP_2 in RBL cells, but PI5KIγ selectively enhances PIP_2 in the DSM fraction, whereas PI5KIβ enhances PIP_2 in both DRM and DSM pools. These results suggest that the enhancing effect of PIP5KIβ overexpression on stimulated STIM1/Orai1 association correlates most strongly with an increase in PIP_2 in ordered lipid subregions, whereas the negative effect of PIP5KIγ on stimulated STIM1-Orai1 interactions correlates with a selective increase in PIP_2 in disordered lipid subregions.

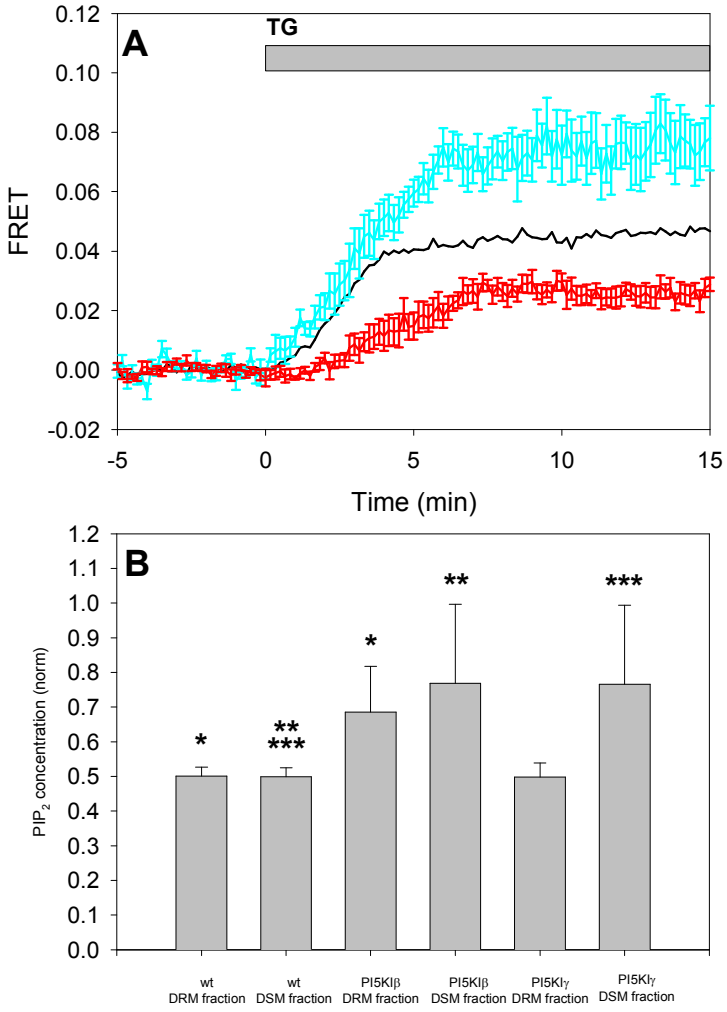

Figure 4.2: **Differential effects of PI5KI isoform overexpression on thapsigargin-stimulated association between AcGFP-Orai1 and STIM1-mRFP and PIP_2 concentrations.** A) Stimulated FRET between STIM1 and Orai1 in control cells (black), cells co-expressing PI5KIβ (cyan), and cells co-expressing PI5KIγ (red).. Error bars show SEM. B) PI5KI isoforms differentially enhance PIP_2 levels in DRMs and DSMs. Values are normalized to total PIP_2 levels in control cells from each experiment. Error bars show SD. Unpaired, one-tailed Student's t-test between indicated populations: * p = 0.03, ** p= 0.05, *** p = 0.05, n=3.

4.4.3 Depletion of PIP_2 from the DRM membrane pool inhibits the thapsigargin-stimulated association of STIM1 and Orai1.

To further evalutate different roles of PIP_2 in DRM and DSM pools on STIM1-Orai1 association, we measured the thapsigargin mediated FRET between STIM1 and Orai1 in RBL cells expressing PIP_2 phosphatases that are selectively targeted to membrane subregions. Phosphatase, L10-Inp54p targets ordered lipid regions (DRM), and Phosphatase, S15-Inp54p targets disordered regions (DSM), as characterized previously by Johnson *et al*., (2008). As shown in Figure 4.3A, co-expression of L10-Inp54p with AcGFP-Orai1 and STIM1-mRFP results in substantial inhibiton of thapsigargin-stimulated association of these proteins detected by FRET. In contrast, co-expression of S15-Inp54p with these reporter constructs results in a small increase in thapsigargin-stimulated FRET. As expected from previous results (Johnson 2008), we found that L10-Inp54p significantly depleted the levels of PIP_2 in DRMs, but it did not significantly reduce the pool of DSM-associated PIP_2 (Figure 4.3B). Also consistent with expectations, S15-Inp54p caused some reduction in the pool of DSM-associated PIP_2, but did not significantly reduce the pool of DRM-associated PIP_2. These results are consistent with the trends observed for overexpression of PIP5KIβ and Iγ, and they indicate that PIP_2 in ordered lipid regions promotes stimulated Orai1-STIM1 association, whereas PIP_2 in disordered lipid regions inhibits this association.

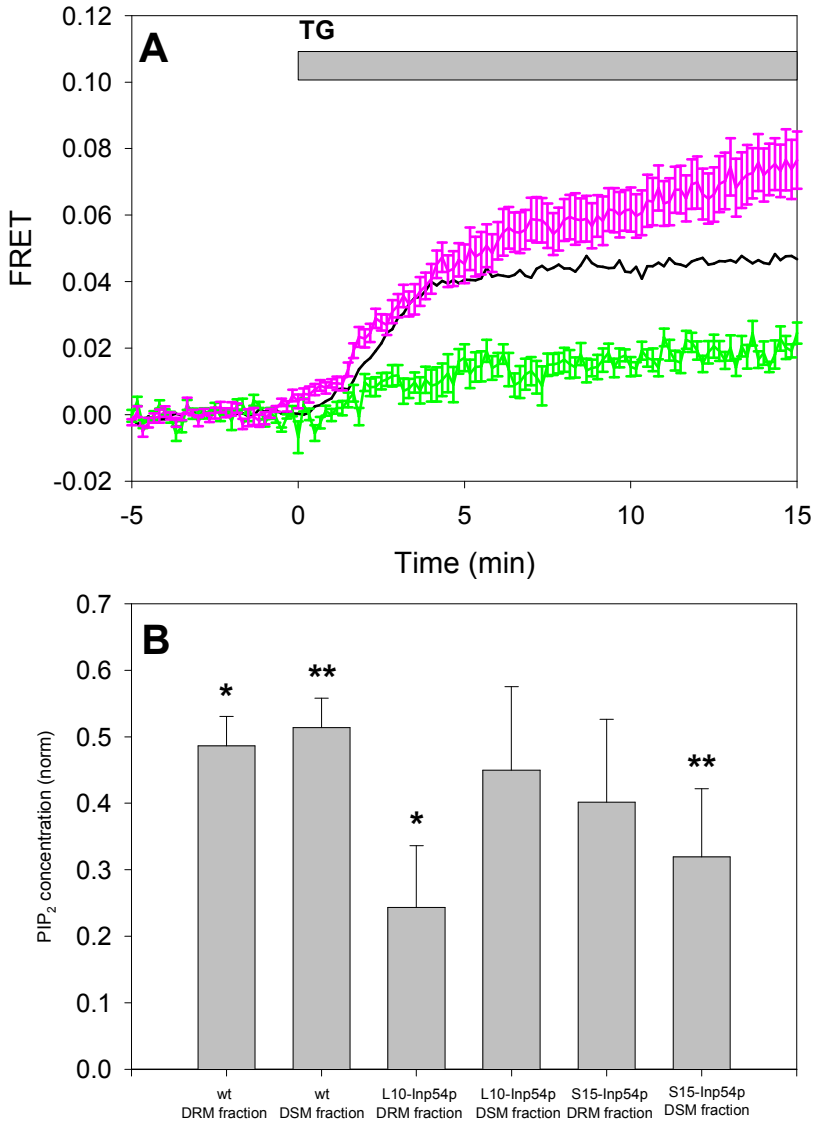

Figure 4.3: **Differential effects of targeted PIP_2 phosphatase expression on thapsigargin-stimulated association between AcGFP-Orai1 and STIM1-mRFP and PIP_2 concentrations.** A) Stimulated FRET between STIM1 and Orai1 in unperturbed cells (black), cells coexpressing the DRM-targeted PIP_2 phosphatase L10-Inp54p (green), and cells coexpressing the DSM-targeted PIP_2 phosphatase S15-Inp54p (pink). Error bars show SEM. B) Targeted PIP_2 phosphases selectively hydrolyze PIP_2. Values are normalized to the total PIP_2 from control cells for each experiment. Error bars show SD. Unpaired, one-tailed Student's t-test between indicated populations: * $p = 0.001$, ** $p = 0.007$; $n = 6$.

4.4.4 Polybasic sequences in STIM1 and Orai1 are determinants of the dependence of the STIM1-Orai1 interaction on PIP_2 in membrane subregions.

The polylysine sequence at the C-terminus STIM1 (a.a. 677-685) has been shown to mediate puncta formation by STIM1 in the plasma membrane puncta in the absence of Orai1 overexpression, but it is not necessary for this puncta formation in the presence of co-expressed Orai1 (Park 2009; Walsh 2009). When we deleted this basic sequence from STIM1-mRFP (STIM1ΔK-mRFP), we observed a modest enhancement in the kinetics of thapsigargin-stimulated FRET between this mutant protein and AcGFP-Orai1 compared with that for wtSTIM1-mRFP. However, the extent of this interaction was similar at longer time points to that seen between wild type STIM1-mRFP and AcGFP-Orai1 in the absence of PIP_2 perturbation (Figure 4.4A, black curve). Co-expression of S15-Inp54p with STIM1ΔK-mRFP and AcGFP-Orai1 did not significantly alter the magnitude or the kinetics of the stimulated interaction (Figure 4.4A, pink curve). In contrast, although the interaction between wild type STIM1-mRFP and AcGFP-Orai1 is substantially inhibited by co-expression of L10-Inp54p (Figure 4.4A, dark green curve), the interaction between STIM1ΔK-mRFP and AcGFP-Orai1 is slightly enhanced under these conditions (Figure 4.4A, green curve). These results suggest that the C-terminal polybasic sequence of STIM1 contributes a positive role in STIM1/Orai1 association by interacting with the ordered lipid pool of PIP_2. In the absence of this basic sequence, this pool of PIP_2 is not necessary for stimulated STIM1-Orai1 association.

When we examined the effect of PIP5KIβ overexpression on the stimulated association of STIM1ΔK-mRFP and AcGFP-Orai1, we found this to be similar but slightly slower than the same interaction in control cells (Figure 4.4B, cyan curve).

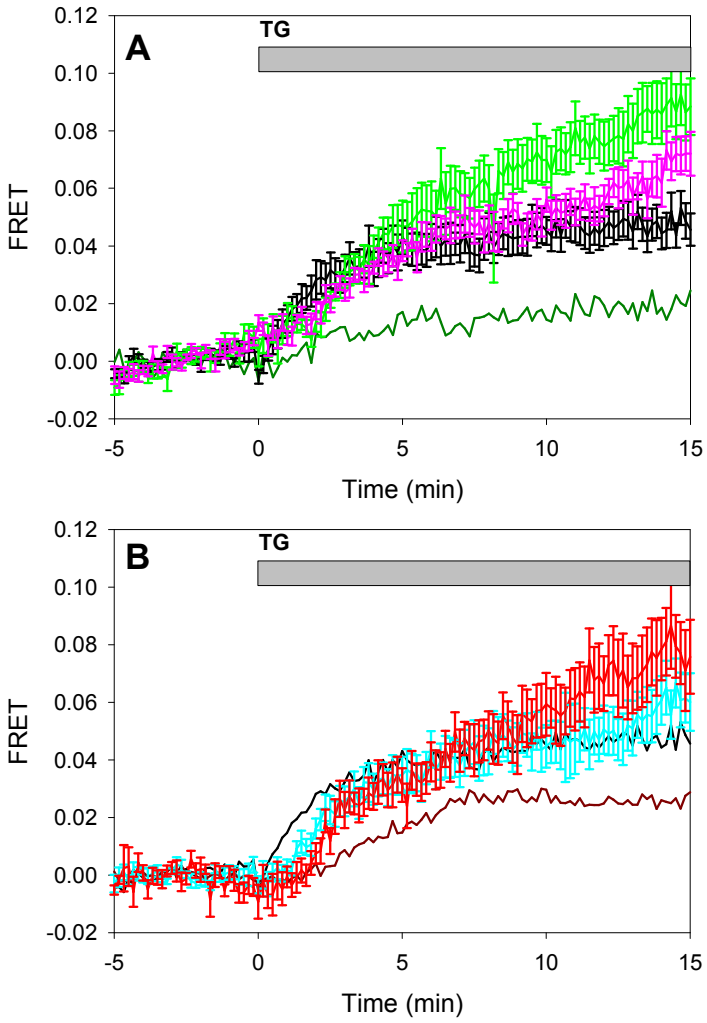

Figure 4.4: **The stimulated association between STIM1ΔK and Orai1 does not exhibit PIP_2 pool selectivity.** A) The thapsigargin-stimulated FRET between AcGFP-Orai1 and STIM1ΔK-mRFP in control cells (black), cells expressing L10-Inp54p (light green), and cells expressing S15-Inp54p (pink). Note that the inhibition of the interaction between wild type STIM1 and Orai1 in the presence of L10-Inp54p (dark green, from Fig. 4.3A) is lost with the STIM1ΔK mutant. B) The thapsigargin stimulated FRET between AcGFP-Orai1 and STIM1ΔK-mRFP in control cells (black), cells expressing PI5KIβ (cyan) and cells expressing PI5KIγ (light red). Note that the inhibition of the interaction between wild type STIM1 and Orai1 in the presence of PI5KIγ (dark red, from Fig. 4.2A) and the enhancement of the interaction in the presence of PI5KIβ (not reproduced) are lost with the STIM1ΔK mutant. Error bars show SEM.

Thus, the enhancing effect of PIP5KIβ on the association of wildtype proteins is not observed with STIM1ΔK-mRFP. As above, this is consistent with a positive role for an interaction between the STIM1 C-terminal polybasic sequence and PIP_2 in ordered lipid subregions of the membranein promoting STIM1-Orai1 association. In contrast, overexpression of PI5KIγ, which inhibits wildtype STIM1-Orai1 interactions, does not inhibit the association between STIM1ΔK-mRFP and AcGFP-Orai1 (Figure 4.4B, compare dark red curve to red curve). This result is consistent with a negative regulatory interaction between the disordered lipid pool of PIP_2 and the C-terminal polybasic sequence of STIM1. Note that although PIP5KIβ overexpression also increases the disordered lipid pool of PIP_2, this effect is compensated by the increase in PIP_2 in ordered lipid regions that it causes.

Orai1 has a polybasic sequence composed primarily of arginine residues near its N-terminus, (a.a 28-33). When this sequence is removed (AcGFP-Orai1ΔR), this mutant Orai1 localizes normally to the plasma membrane (Figure D.2), and stimulated FRET between AcGFP-Orai1ΔR and STIM1-mRFP is similar to that for the wildtype proteins (Figure 4.5A, black curve). Also similar to the wildtype proteins, stimulated FRET between AcGFP-Orai1ΔR and STIM1-mRFP is significantly reduced in cells expressing L10-Inp54p (Figure 4.5A, green curve). This indicates that the polyarginine sequence in Orai1 is not involved in the sensitivity of STIM1/Orai1 association to depletion of the ordered lipid pool of PIP_2. In contrast, stimulated association of STIM1-mRFP and AcGFP-Orai1ΔR is significantly inhibited after depletion of the disordered lipid pool of PIP_2 by S15-Inp54p, even though it is enhanced for wildtype STIM1 and Orai1 under these conditions (Figure 4.5A, compare purple curve to pink curve). These results indicate that this basic sequence in Orai1 contributes to positive regulation of STIM1-Orai1 association that involves the disordered lipid pool of PIP_2.

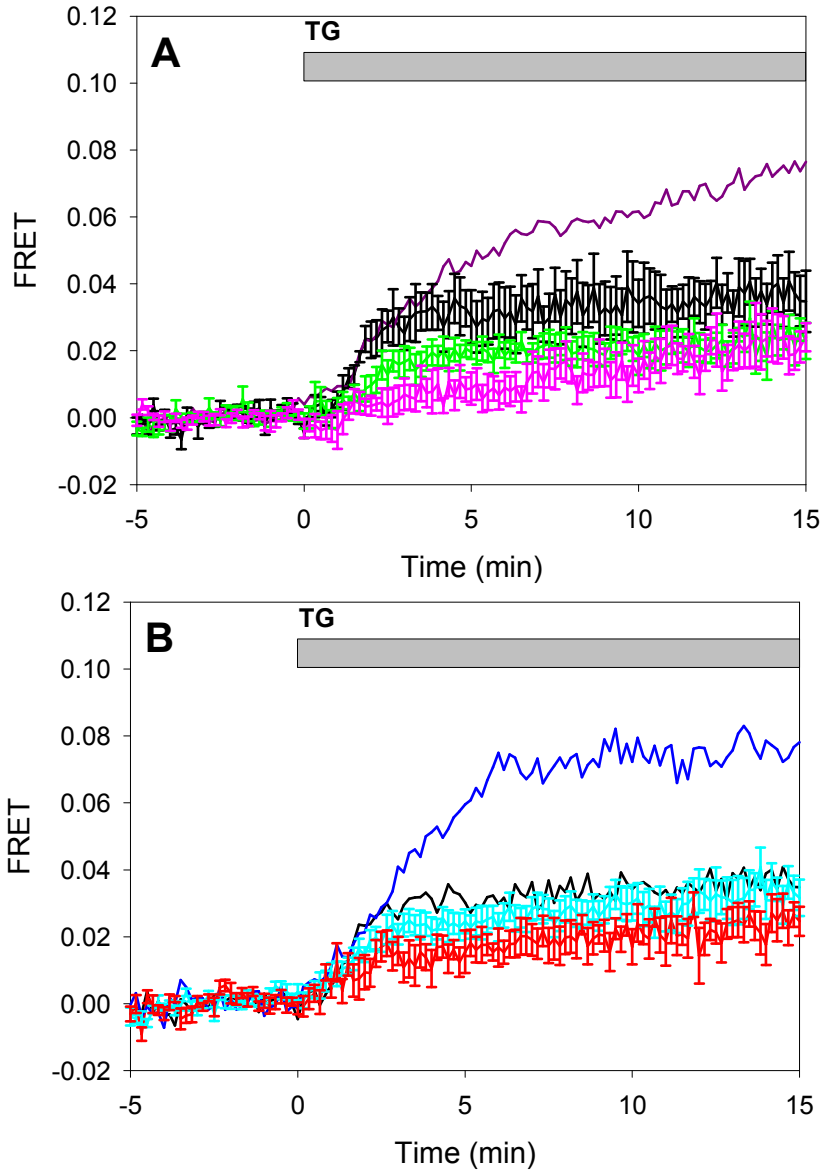

Figure 4.5: **The interaction between STIM1 and Orai1ΔR has altered PIP_2 pool selectivity.** A) Thapsigargin-stimulated FRET between AcGFP-Orai1ΔR and STIM1-mRFP in control cells (black), cells expressing L10-Inp54p (light green), and cells expressing S15-Inp54p (pink). Note that the enhancement of the interaction between STIM1 and wild type Orai1 in the presence of S15-Inp54p (purple, from Fig. 4.3A) is replaced by inhibition with the Orai1ΔR mutant. B) Thapsigargin-stimulated FRET between AcGFP-Orai1ΔR and STIM1-mRFP in control cells (black), cells expressing PI5KIβ (cyan) and cells expressing PI5KIγ (red). Note that the enhancement of the interaction between STIM1 and wild type Orai1 in the presence of PI5KIβ (blue, from Fig. 4.2A) is lost with the Orai1ΔR mutant. Error bars show SEM.

Deletion of the polyarginine sequence near the N-terminus of Orai1 also alters the effect of overexpressing PI5KIβ on the STIM1-Orai1 association. For the wild-type proteins, this stimulated association is enhanced by overexpression of PI5KIβ, but for STIM1-mRFP and AcGFP-Orai1ΔR this association is reduced (Figure 4.5B, compare dark blue curve to cyan curve). In contrast, overexpression of PI5KIγ similarly affects stimulated FRET between STIM1-mRFP and either AcGFP-Orai1ΔR or wildtype AcGFP-Orai1, causing modest inhibition in both cases (Figure 4.5B, red curve). These results indicate that the basic polyarginine sequence at the N-terminus of Orai1 is important for the enhancing effect of PI5KIβ, but not for the inhibitory effect of PIP5KIγ. They can be accounted by a mechanism in which this basic sequence promotes the association of STIM1 with Orai1 by interacting with the ordered lipid pool of PIP_2.

4.4.5 Segregation of Orai1 into ordered lipid and disordered lipid subregions of the plasma membrane is dynamically controlled by the distribution of PIP_2 between these subregions.

When unstimulated cells overexpressing STIM1-mRFP and AcGFP-Orai1 are solublized with TX-100 and separated by sucrose gradient fractionation, most AcGFP-Orai1 fractionates with DSM (disordered lipids) when detected with anti-GFP mAb (Figure 4.6). However, when PIP_2 from the DSM fraction is depleted by coexpression of S15-Inp54p, a larger percentage of Orai1 is found in the DRM (ordered lipids) fraction. Conversely, the percentage of Orai1 that fractionates with DRMs decreases when PIP_2 in this fraction is preferentially depleted by L10-Inp54p. These results provide evidence that although Orai1 primarily resides in disordered lipid subregions in unstimulated cells, its relative concentration in the ordered vs disorded lipid

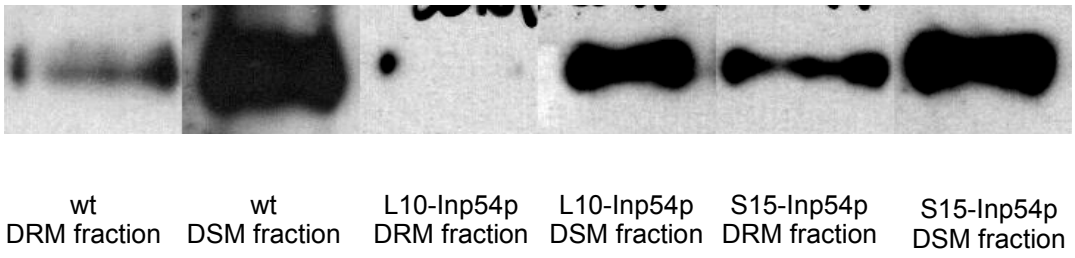

Figure 4.6: **Localization of Orai1 to DRM or DSM fractions depends on the presence of PIP_2.** Comparative distribution of AcGFP-Orai1 in DRM and DSM fractions determined by sucrose gradient fractionation. Depletion of PIP_2 from the DRM fraction with L10-Inp54p decreases the relative portion of Orai1 in the DRM fraction, whereas depletion of PIP_2 from the DSM fraction with S15-Inp54p increases the relative portion of Orai1 in the DRM fraction.

subregions depends on the concentration of PIP_2 in the respective pools.

4.5 Discussion

4.5.1 Thapsigargin mediated STIM1-Orai1 association is inhibited by PIP_2 in the disordered lipid subregions of the membrane and enhanced by PIP_2 in the ordered lipid subregions.

Our results support roles for cholesterol-dependent membrane heterogeneity and for segregated pools of phosphoinositides in the stimulated association of STIM1 with Orai1. Initial experiments revealed that depletion of cholesterol inhibits thapsigargin-stimulated association between donor-labeled Orai1 and acceptor-labeled STIM1 in parallel with the inhibition of SOCE (Figure 4.1A,B). Similarly, inhibition of PI4P synthesis by 10 μM wortmannin inhibits stimulated FRET between these labeled proteins (Figure 4.1C,D). These results, together with those from Vasudevan *et al*. (2009), led us to the hypothesis that PIP_2 synthesized by two different isoforms of PI5K is segregated in two different membrane domains. Although proteins are clearly involved, these domains arise in part by cholesterol-based ordering of lipids and are simply categorized as ordered lipid and disordered lipid subregions. To test this hypothesis, we evaluated the effects of PI5KIβ and Iγ overexpression on stimulated association between STIM1 and Orai1 as measured by FRET, and we compared these effects to alterations in PIP_2 levels in DRM (ordered lipids) and DSM (disordered lipids) fractions caused by these kinases. An increase in stimulated FRET due to overexpression of PI5KIβ correlated with an increase in PIP_2 in both DRM and DSM fractions, whereas a decrease in stimulated FRET caused by PI5KIγ correlated with a selective increase in PIP_2 in the DSM fraction (Figure 4.1). To directly reduce PIP_2

levels in either ordered lipid or disordered lipid subregions, we used respectively targeted inositol 5-phosphatases. We found that these resulted in changes in stimulated FRET that are consistent with consistent with PI5KIβ and Iγ overexpression, i.e. reduction in PIP_2 in ordered lipid pools inhibits stimulated FRET, whereas reduction in PIP_2 in disordered lipid pools enhances stimulated FRET.

Thus, a consistent result from our data is that the interaction between STIM1-mRFP and AcGFP-Orai1 is inhibited under conditions where there is a greater proportion of PIP_2 in disordered lipid subregions of the membrane than PIP_2 in ordered lipid subregions. This disproportionality can be generated by either hydrolysis of PIP_2 in ordered lipid subregions by targeted L10-Inp54p or when the pool of PIP_2 in disordered lipid subregions is enhanced by PI5KIγ. This consistent symmetry between the effects of PIP_2 distributed between ordered lipid and disordered lipid subregionsis is accompanied by an apparent insensitivity to the total amount of PIP_2 present in the membrane.. This pattern is consistent with previous reports that found little effect on Ca^{2+} mobilization or punctae formation without complete removal of PIP_2 from the plasma membrane (Korzeniowski 2009, Walsh 2010).These previous reports did not consider a differential effect of multiple pools of PIP_2, and did not use a direct measurement of the association between the two proteins.

4.5.2 The polybasic sequences on STIM1 and Orai1 confer the selectivity of DRM and DSM pools of PIP_2 to the STIM1-Orai1 interaction

When we removed either the C-terminal polylysine sequence from STIM1 or the N-terminal polyarginine sequence from Orai1,, the selectivity of the STIM1-Orai1 interaction for a particular pool of PIP_2 was largely lost, i.e. FRET between STIM1 and Orai1 constructs was similar for cells overexpresing L10-Inp54p and S15-Inp54p,

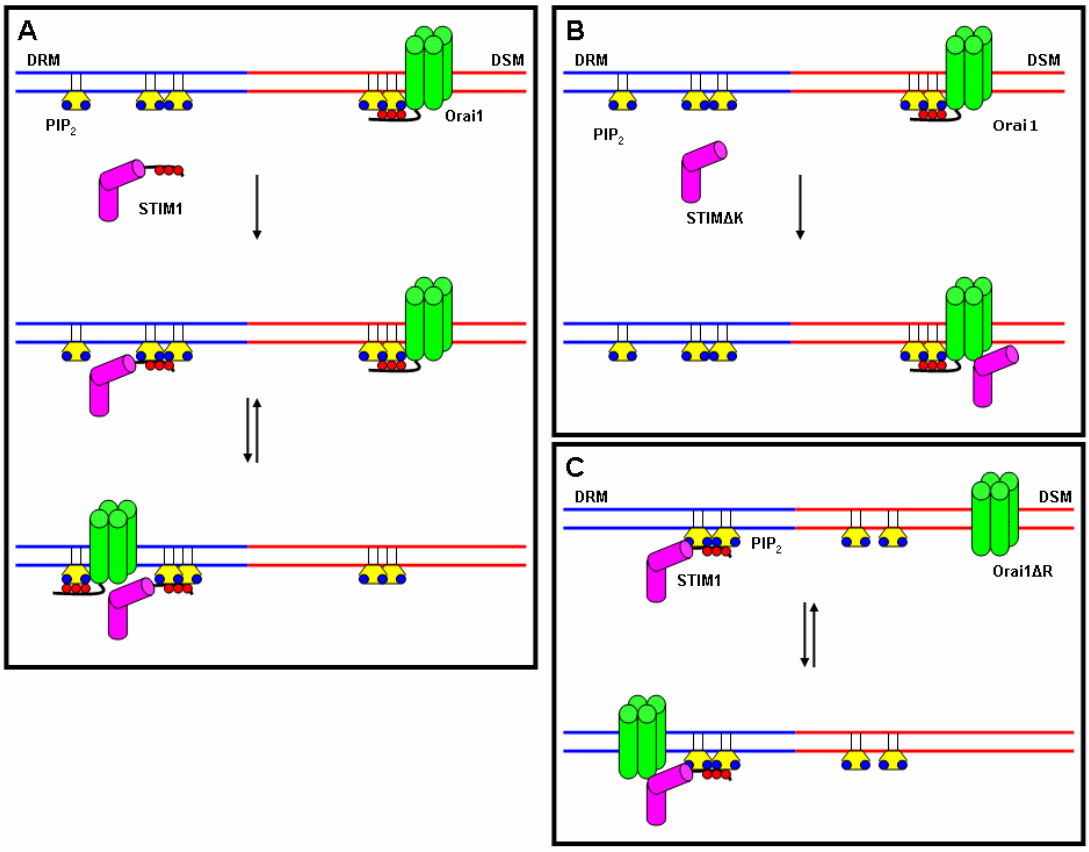

Figure 4.7: **Proposed scheme for the PIP_2 dependent association of STIM1 and Orai1.** A) In cells coexpressing the wild type proteins STIM1 and Orai1, SOCE is initiated by the translocation of STIM1 to DRM associated PIP_2 (ER membrane omitted for clarity). This is followed by the PIP_2 dependent equilibration of Orai1 between DRM and DSM fractions, to form the productive interaction with STIM1 in the DRM fraction. The equibration of Orai1 between membrane pools conferes the differential selectivity of the interaction to PIP_2 in the DRM and DSM pools. B) In cells expressing STIM1ΔK and wild type Orai1, STIM1 lacks the polylysine sequence directing it to interact with PIP_2, allowing STIM1 to engage Orai1 directly, without an intermediate PIP_2 binding step. PIP_2 pool selectivity is lost because productive interactions can be formed in both membrane fractions. C) In cells expressing wild type STIM1 and Orai1ΔR, Orai1 lacks the PIP_2 mediated redistribution between membrane pools. We predict that the productive interaction between STIM1 and Orai1ΔR most likely occurs in the DRM membrane fraction, but the redistribution of Orai1 into this fraction is no longer PIP_2 dependent.

or PI5KIβ and PI5KIγ. However, this selectivity was lost in very different ways for the two proteins. When the polylysine sequence from STIM1 was deleted, the FRET between STIM1ΔK-mRFP and AcGFP-Orai1 was as high or higher than the FRET between the wild-type proteins in every case (Figure 4.4). In contrast, the deletion of the N-terminal polyarginine sequence of Orai1, caused the FRET between STIM1-mRFP and AcGFP-Orai1ΔR to be as low or lower than every case involving the wild-type proteins (Figure 4.5). Nevertheless, in both cases, sensitivity to depletion or enhancement of a particular pool of PIP_2 was eliminated. These results are consistent with our model described below, in which wild-type proteins utilize both PIP_2-mediated translocation of Orai1 from disordered to ordered lipid pools and thapsigargin-stimulated association of STIM1 with PIP_2 in ordered lipid subregions.

The differences between removal of the polybasic sequences from STIM1 and Orai1may be accounted for by their competition with endogenous, wild-type counterparts. Removal of the polylysine sequence on STIM1 may allow its free engagement with Orai1 associated with either ordered or disordered lipid pools. This is consistent with previous results showing that, although the polylysine sequence on STIM1 is important for translocation to the plasma membrane in the absence of Orai1, interaction with Orai1 is sufficient to concentrate STIM1 into ER-plasma membrane punctae (Park 2009). The modest enhancement of the interaction between STIM1ΔK-mRFP and AcGFP-Orai1 seen at long time points, when the ordered lipid pool of PIP_2 is depleted by L10-Inp54p, may occur because inhibition of the interaction between endogenous, wild-type STIM1 and overexpressed AcGFP-Orai1 is reduced under these conditions, thereby freeing a larger pool of AcGFP-Orai1 to interact with the mutant STIM1ΔK-mRFP.

Conversely, removal of the polyarginine sequence of Orai1 appears to substantially limit its interaction with STIM1 following perturbation of the PIP_2

distribution. In particular, FRET between STIM1-mRFP and AcGFP-Orai1ΔR is the lowest when S15-Inp54p is expressed, despite being strong for the labeled wild-type proteins (Figure 4.5A). Similar to the situation in which STIM1ΔK-mRFP must compete with endogentous STIM1, AcGFP-Orai1ΔR may compete less efficiently with endogenous Orai1 for association with STIM1.

4.5.3 The thapsigargin mediated STIM1-Orai1 interaction requires the PIP_2 mediated translocation of Orai from disordered lipid subregions to ordered lipid subregions of the membrane

A simplistic model that accounts for all of our observations is summarized in Figure 4.7. It posits that the the STIM1 C-terminal polylysine sequence targets STIM1 to PIP_2 in ordered lipid subregions after stimulation by thapsigargin. The N-terminal polyarginine sequence of Orai1 contributes to its localization with disordered lipids in the resting state via its interaction with PIP_2 in those subregions. With stimulation, this model, Orai1 translocates to the ordered lipid subregions to engage STIM1.Thus the relative distribution of PIP_2 in the ordered lipid and disordered lipid subregions influences the propensity of Orai1 to redistribute into the ordered lipid subregions where it can engage STIM1. In a previous study, STIM1 from cell lysates was shown to fractionate with DRMs in sucrose gradients in a strongly thapsigargin dependent manner (Pani 2008). As shown in Figure 4.6, Orai1 fractionates largely with DSM in unstimulated cells, and this preference is reduced in S15-Inp54p-expressing cells. In cases were the proportion of PIP_2 in DSM is high (such as with coexpression of L10-Inp54p or PI5KIγ), Orai1 has a reduced propensity both to redistribute into the DRM pool and and to associate with STIM1 as measured by FRET. This model is consistent with our western blotting data showing that the distribution of Orai1 between DRM

and DSM fractions parallels the relative fraction of PIP_2 fractionating in these two pools (Figure 4.6). It is also consistent with our observations that removal of the polybasic targeting sequence ineither STIM1 or Orai1 interferes with the sensitivity of the STIM1/Orai1 to conditions of high PIP_2 levels in the ordered lipid pool, albeit by the different mechanisms described above.

Removal of polybasic sequences in the N-terminus of Orai1 or the C-terminus of STIM1 alters the mode of interaction between these two proteins. Removal of the polylysine sequence on STIM1 (Figure 4.7B) prevents the initial association of STIM1ΔK with the ordered lipid pool of PIP_2, but does not prevent the direct association of STIM1ΔK with Orai1 as measured by FRET (Figure 4.7B). This scheme is consistent with previous reports that characterized Orai1 dependent and independent modes of STIM1 association with the plasma membrane following thapsigargin mediated store depletion, and that identified the polylysine sequence on STIM1 as important for the Orai1-independent mode of association (Park 2009). The loss of PIP_2 selectivity in this case is due to the loss of stimulated association of STIM1ΔK with ordered lipid subregions in the membrane, thereby allowing STIM1ΔK to engage Orai1 in either the ordered or disordered lipid subregions. This mutation generally increases the association between STIM1ΔK and Orai1 and can be explained by the capacity of STIM1ΔK to engage Orai1 without restrictions imposed by PIP_2 in membrane subregions.

We also find that the removal of the polyarginine sequence on the N-terminus of Orai1 results in the loss of PIP_2 sensitivity, but this may not affect, the capacity of STIM1 to bind to PIP_2 in ordered lipid subregions or the capacity of Orai1 to diffuse into these subregions to engage STIM1. Removal of the polyarginine sequence causes Orai1 to fractionate with both DRM and DSM lipid pools in a PIP_2- independent fashion, corresponding to a loss of selectivity for PIP_2 in one subregion over the other.

In this case, the redistribution of Orai1 between lipid subregions may depend more on the intrinsic partitioning of Orai1 between ordered vs disordered lipid subregions, rather than on interactions with PIP_2 in these pools.

The present model cannot fully account for more subtle, quantitative relationships between PIP_2 localized to ordered lipid subregions or disordered lipid subregions of the membrane. For example, there is significant increase in the interaction between STIM1-mRFP and AcGFP-Orai1 following overexpression of PI5KIβ, which also causes an increase in PIP_2 that fractionate with both DRM and DSM. This result could be explained if enhancement of the STIM1-Orai1 interaction by PIP_2 in ordered lipid subregions is more potent than the inhibition by the PIP_2 in disordered subregions, but current data are insufficient to evaluate this posibility. In future experiments, the extent to which the regulation of PIP_2 levels in subregions of the membrane influences stimulated SOCE will need to be investigated systematically. Especially in the case of physiological stimulation by antigen, the balance between PIP_2 in distinctive subregions may be particularly important in regulating the functional outcome.

REFERENCES

Alicia, S., Angélica, Z., Carlos, S., Alfonso, S., and Vaca, L. (2008) STIM1 converts TRPC1 from a receptor-operated to a store-operated channel: moving TRPC1 in and out of lipid rafts. Cell Calcium. *44*, 479-91.

Bauer, M.C., O'Connell, D., Cahill, D.J., and Linse, S. (2008) Calmodulin binding to the polybasic C-termini of STIM proteins involved in store-operated calcium entry. Biochemistry. *47*, 6089-91.

Broad, L.M., Braun, F.J., Lievremont, J.P., Bird, G.S., Kurosaki, T., and Putney, J.W. (2001) Role of the Phospholipase C-Inositol 1,4,5-Trisphosphate Pathway in Calcium Release-activated Calcium Current and Capacitative Calcium Entry. J. Biol. Chem. *276*, 15945–52

Brown, D.A., and Rose, J.K. (1992) Sorting of GPI-anchored proteins to glycolipid-enriched membrane subdomains during transport to the apical cell surface. Cell. *68*, 533–44.

Calloway, N., Vig, M., Kinet, J.P., Holowka, D., and Baird, B. (2009) Molecular clustering of STIM1 with Orai1/CRACM1 at the plasma membrane depends dynamically on depletion of Ca^{2+} stores and on electrostatic interactions. Mol Biol Cell. *20*, 389-99.

Calloway, N., Holowka, D., and Baird, B. (2010) A basic sequence in STIM1 promotes Ca^{2+} influx by interacting with the C-terminal acidic coiled coil of Orai1. Biochemistry. *49*, 1067-71.

DeHaven, W.I., Jones, B.F., Petranka, J.G., Smyth, J.T., Tomita, T., Bird, G.S., and Putney, J.W. (2009) TRPC channels function independently of STIM1 and Orai1. J. Physiol. *587*, 2275-98.

Feske, S., Gwack, Y., Prakriya, M., Srikanth, S., Puppel, S. H., Tanasa, B., Hogan, P. G., Lewis, R. S., Daly, M. and Rao, A. (2006) A mutation in Orai1 causes immune deficiency by abrogating CRAC channel function. Nature *441*, 179–185.

Hoth, M., and Penner, R. (1993) Calcium release-activated calcium current in rat mast cells. J Physiol *465*: 359–86.

Huang, G.N., Zeng, W., Kim, J.Y., Yuan, J.P., Han, L., Muallem, S., and Worley, P.F. (2006) STIM1 carboxyl-terminus activates native SOC, I_{CRAC} and TRPC1 channels. Nat Cell Biol. *8*, 1003-10.

Hull, J.J., Lee, J.M., Kajigaya, R., and Matsumoto, S. (2009) Bombyx mori homologs of STIM1 and Orai1 are essential components of the signal transduction

cascade that regulates sex pheromone production. J Biol Chem. *284*, 31200-13.

Jardin, I., Salido, G.M., and Rosado, J.A. (2008) Role of lipid rafts in the interaction between hTRPC1, Orai1 and STIM1. Channels (Austin). *2*, 401-3.

Johnson, C.M., Chichili, G.R., and Rodgers, W. (2008) Compartmentalization of phosphatidylinositol 4,5-bisphosphate signaling evidenced using targeted phosphatases. J Biol Chem. *283*, 29920-8.

Korzeniowski, M.K., Popovic, M.A., Szentpetery, Z., Varnai, P., Stojilkovic, S.S., and Balla, T. (2009) Dependence of STIM1/Orai1-mediated calcium entry on plasma membrane phosphoinositides. J Biol Chem. *284*, 21027-35.

Liou, J., Kim, M. L., Heo, W. D., Jones, J. T., Myers, J. W., Ferrell, J. E., Jr. and Meyer, T. (2005) STIM is a Ca^{2+} sensor essential for Ca^{2+}-store-depletion-triggered Ca^{2+} influx. Curr. Biol. 15, 1235– 41

Liou, J., Fivaz, M., Inoue, T., and Meyer, T. (2007) Live-cell imaging reveals sequential oligomerization and local plasma membrane targeting of stromal interaction molecule 1 after Ca^{2+} store depletion. Proc Natl Acad Sci U S A. *104*, 9301-6.

Liu, Y., Casey, L., and Pike, L.J. (1998) Compartmentalization of phosphatidylinositol 4,5-bisphosphate in low-density membrane domains in the absence of caveolin. Biochem Biophys Res Commun. *245*, 684-90.

Pani, B., Ong, H.L., Liu, X., Rauser, K., Ambudkar, I.S., and Singh, B.B. (2008) Lipid rafts determine clustering of STIM1 in endoplasmic reticulum-plasma membrane junctions and regulation of store-operated Ca^{2+} entry (SOCE). J Biol Chem. *283*, 17333-40.

Park, C.Y., Hoover, P.J., Mullins, F.M., Bachhawat, P., Covington, E.D., Raunser, S., Walz, T., Garcia, K.C., Dolmetsch, R.E., and Lewis, R.S. (2009) STIM1 clusters and activates CRAC channels via direct binding of a cytosolic domain to Orai1. Cell. *136*, 876-90.

Sengupta, P., Holowka, D., and Baird, B. (2007) Fluorescence resonance energy transfer between lipid probes detects nanoscopic heterogeneity in the plasma membrane of live cells. Biophys J. *92*, 3564-74.

Sheets, E.D., Holowka, D., and Baird, B. (1999) Critical role for cholesterol in Lyn-mediated tyrosine phosphorylation of FcepsilonRI and their association with detergent-resistant membranes. J Cell Biol. *145*, 877-87.

Simons, K., and Toomre, D. (2000) Lipid rafts and signal transduction. Nat Rev Mol Cell Biol. *1*, 31-9.

Surviladze, Z., Dráberová, L., Kovárová, M., Boubelík, M., and Dráber, P. (2001) Differential sensitivity to acute cholesterol lowering of activation mediated via the high-affinity IgE receptor and Thy-1 glycoprotein. *31*, 1-10.

Vasudevan, L., Jeromin, A., Volpicelli-Daley, L., De Camilli, P., Holowka, D., and Baird, B. (2009) The β- and γ-isoforms of type I PIP5K regulate distinct stages of Ca^{2+} signaling in mast cells. J Cell Sci. *122*, 2567-74.

Vig, M., Peinelt, C., Beck, A., Koomoa, D. L., Rabah, D., Koblan-Huberson, M., Kraft, S., Turner, H., Fleig, A., Penner, R. and Kinet, J. P. (2006) CRACM1 is a plasma membrane protein essential for store-operated Ca^{2+} entry. Science *312*, 1220– 23

Walsh, C.M., Chvanov, M., Haynes, L.P., Petersen, O.H., Tepikin, A.V., and Burgoyne, R.D. (2010) Role of phosphoinositides in STIM1 dynamics and store-operated calcium entry. Biochem J. *425*, 159-68.

Yuan, J.P., Zeng, W., Dorwart, M.R., Choi, Y.J., Worley, P.F., and Muallem, S. (2009) SOAR and the polybasic STIM1 domains gate and regulate Orai channels. Nat Cell Biol. *11*, 337-43.

Zeng, W., Yuan, J.P., Kim, M.S., Choi, Y.J., Huang, G.N., Worley, P.F., and Muallem, S. (2008) STIM1 gates TRPC channels, but not Orai1, by electrostatic interaction. Mol Cell. *7*, 439-48.

Zhang, S. L., Yu, Y., Roos, J., Kozak, J. A., Deerinck, T. J., Ellisman, M. H., Stauderman, K. A. and Cahalan, M. D. (2005) STIM1 is a Ca^{2+} sensor that activates CRAC channels and migrates from the Ca^{2+} store to the plasma membrane. Nature *437*, 902– 5.

CHAPTER 5

FUTURE DIRECTIONS

5.1 Further investigations of the molecular basis of the STIM1-Orai1 interaction.

Using an electrostatic protein interaction model, we have identified four regions on STIM1 and Orai1 necessary for their interaction. On Orai1 we identified a C-terminal acidic coiled-coil important for clustering (chapter 2) and gating of Ca^{2+} influx (chapter 3). Additionally, in chapter 3 we identify the intermolecular binding partner for this region on STIM1, a short basic sequence in the CAD domain. Finally, in chapter 4 we identified polybasic sequences on both STIM1 and Orai1 important for their interaction with phosphoinositides at the plasma membrane. All of these sequences were identified using a simple structural model for protein surface charge density. In short, secondary structure is estimated using the periodicity of the sidechain hydrophobicity. Using this estimate, we identify structural elements of the protein with high positive or negative charge density. Once these regions are identified, any potential intramolecular charge-charge interactions are ruled out by examining the periodicity of the longitudinal charge density: Our assumption is that regions of alternating charge density are forming intramolecular interactions. Regions of higher charge density are assumed to have a longer periodicity if involved in long range intramolecular interactions. Any sequences that remain unpaired to intramolecular binding partners are considered important for intermolecular interactions. Using this technique, several other sequences in STIM1 and Orai1 were identified besides those that were investigated in this dissertation. Two regions of immediate interest on STIM1 are a stretch of glutamates in the CAD region (a.a. 318-

322), and a heptad of acid amino acids in the serine/praline rich domain (a.a. 475-483) (Figure 5.1). Also of interest is the juxtamembrane polybasic region immediately N-terminal to the first transmembrane region of Orai1 (a.a. 79-93). Although the function of these regions is unknown, the efficacy of this approach has been demonstrated for others in our previous studies.

5.2 The orchestrated movement of STIM1 and Orai1 at the plasma membrane.

In chapter 4, we outlined a scheme by which STIM1 translocates to pool of PIP_2 localized in ordered lipid subregions of ER-plasma membrane junctions, and Orai1 redistributes between the PIP_2 in disordered lipid ordered lipid subregions to engage STIM1. This scheme accounts for all the observations in chapter 4, but has not been directly tested. Therefore, we propose a study to quantify the distribution of STIM1 and Orai1 that fractionate with DRM (ordered lipids) and DSM (disordered lipids) following thapsigargin stimulation. Figure 4.6 shows some dependence of the distribution of Orai1 in DRM and DSM fractions on the concentration of PIP_2 in these fractions. To investigate further the movement of these proteins between lipid pools, we can similarly monitor the distribution of both STIM1 and Orai1 in DRM and DSM fractions following stimulation. To test the hypothesis that the polybasic sequences on STIM1 and Orai1 direct their movement between ordered and disordered lipid pools, these results can be compared to the distributions of STIM1 and Orai1 mutants lacking these sequences. Fusions of these polybasic sequences to fluorescent proteins could further help us evaluate whether these sequences alone are sufficient to direct this behavior, by allowing the direct observation of these membrane dynamics, either in model systems or in cells.

Orai1 Sequence

MHPEPAPPPSRSSPELPPSGGSTTSGSRRSRRRSGDGEPPGAPPPPPSAVTYPDWIG
QSYSEVMSLNEHSMQALSWRKLYLSRAKLKASSRTSALLSGFAMVAMVEVQLDADHD
YPPGLLIAFSACTTVLVAVHLFALMISTCILPNIEAVSNVHNLNSVKESPHERMHRH
IELAWAFST VIGTLLFLAEVVLLCWVKFLPLKKQPGQPRPTSKPPASGAAANVSTS
GITPGQAAAIASTTIMVPFGLIFIVFAVHFYRSLVSHKTDRQFQELNELAEFARLQD
QLDHRGDHPLTPGSHYA

STIM1 Sequence

MDVCVRLALWLLWGLLLHQGQSLSHSHSEKATGTSSGANSEESTAAEFCRIDKPLCH
SEDEKLSFEAVRNIHKLMDDDANGDVDVEESDEFLREDLNYHDPTVKHSTFHGEDKL
ISVEDLWKAWKSSEVYNWTVDEVVQWLITYVELPQYEETFRKLQLSGHAMPRLAVTN
TTMTGTVLKMTDRSHRQKLQLKALDTVLFGPPLLTRHNHLKDFMLVVSIVIGVGGCW
FAYIQNRYSKEHMKKMMKDLEGLHRAEQSLHDLQERLHKAQEEHRTVEVEKVHLEKK
LRDEINLAKQEAQRLKELREGTENERSRQKYAEEELEQVREALRKAEKELESHSSWY
APEALQKWLQLTHEVEVQYYNIKKQNAEKQLLVAKEGAEKIKKKRNTLFGTFHVAHS
SSLDDVDHKILTAKQALSEVTAALRERLHRWQQIEILCGFQIVNNPGIHSLVAALNI
DPSWMGSTRPNPAHFIMTDDVDDMDEEIVSPLSMQSPSLQSSVRQRLTEPQHGLGSQ
RDLTHSDSESSLHMSDRQRVAPKPPQMSRAADEALNAMTSNGSHRLIEGVHPGSLVE
KLPDSPALAKKALLALNHGLDKAHSLMELSPSAPPGGSPHLDSSRSHSPSSPDPDTP
SPVGDSRALQASRNTRIPHLAGKKAVAEEDNGSIGEETDSSPGRKKFPLKIFKKPLK
K

Figure 5.1: **Primary sequence analysis of Orai1 and STIM1.** Using the electrostratic protein interaction prediction technique described in section 5.1, we have identified the above highlighted sequences as of interest. The sequences highlighted in blue have already been investigated in the preceding chapters and have all been found to be important for the STIM1-Orai1 interaction. The sequences highlighted in red have not been investigated and are of unknown function.

5.3 The biophysical basis of PIP_2 phase selectivity.

As outlined in chapter 4, the phosphatidylinositol kinase PI5KIγ generates PIP_2 primarily associated with the disordered lipid pool, whereas PI5KIβ produces PIP_2 associated with both ordered and disordered lipid pools. Although we can reproducibly observe the effects of modulating these pools, the mechanism by which these pools are maintained is unclear. One explanation that can account for this selectivity is that the PIP_2 in the ordered lipid pool is chemically distinct from the PIP_2 in the disordered lipid pool. The acyl chain saturation of different PIP_2 species could direct their concentration into a particular lipid pool. Proteins could differentiate between PIP_2 pools either by the direct recognition of the acylation of a particular PIP_2 species or by recognizing the surrounding lipid domain. This explanation is attractive because it does not require inhibiting the diffusion of PIP_2 in a particular pool as long as the partition coefficients for different PIP_2 species are sufficiently different. Wenk, *et al.*, however, found that the vast majority of PIP_2 in the cell contains acyl chains with 38 carbons and 4 double bonds, total. This result would suggest that the majority of PIP_2 should reside in the disordered lipid subregions. However, in the results presented in chapter 4, we find that there is an approximately equal fractionation of PIP_2 with DRM and DSM. To understand the contribution of varying acylation on PIP_2 phase selectivity, we have begun a collaboration with Catherine Costello at Boston University School of Medicine to quantify the PIP_2 species extracted from DRM and DSM fractions under different perturbations and stimulatory conditions.

A separate mechanism that could contribute to the maintenance of PIP_2 pools is that the association with proteins or other molecules at the plasma membrane could maintating the concentration of PIP_2 into subregion. In chapter 1, we outlined an array of proteins that bind or crosslink PIP_2 at the plasma membrane. The lateral

organization of PIP_2 induced by association with polybasic peptides could drive its association with a particular subregion. We have found that overexpression of the MARCKS effector domain enhances the pool of PIP_2 associated with the DSM lipid fraction (data not shown), while others have demonstrated that GAP-43 drives association of PIP_2 with the DRM lipid fraction (Tong 2008). In chapter 4, we describe a model where the oligomerization of STIM1 drives the selective association of its C-terminal polylysine sequence with PIP_2 in the ordered lipid subregion. As described in chapter 2, we have found that small molecules such as spermine or D-sphingosine that change the electrostatics at the plasma membrane also inhibit the STIM1-Orai1 interaction, posing the possibility that this inhibition is due to modulating the concentration of PIP_2 in a particular pool. There are significant opportunities to expand our understanding of these processes, and understand how multiple pools of PIP_2 are formed and restricted to subregions the plasma membrane with functional consequences. For instance, *in vitro* studies of model membranes containing PIP_2 could elucidate whether the MARCKS effector domain simply recognizes the PIP_2 in disordered lipid subregions or whether it induces formation of these subregions. Similar studies could be performed on GAP-43, the STIM1 C-terminus, or peptide libraries to identify the precise molecular determinants of domain selectivity.

5.4 PIP_2 selectivity in the antigen mediated STIM1-Orai1 interaction

As outlined in chapter 4, we investigated the dependence of the thapsigargin stimulated STIM1-Orai1 interaction on DRM and DSM pools of PIP_2. Absent from this analysis was an investigation of the dependence of the antigen stimulated STIM1-Orai1 interaction on pools of PIP_2 or an analysis of the effect of the PIP_2 directing

sequences on STIM1 and Orai1 after antigen stimulation. There are two caveats associated with measuring the FRET between AcGFP-Orai1 and STIM1-mRFP following antigen stimulation: 1) Unlike with thapsigargin, antigen stimulation does not prevent store refilling, resulting in an attenuation of the STIM1-Orai1 interaction (chapter 2). 2) Antigen stimulation alters the PIP_2 pools by hydrolysis of PIP_2 to DAG and IP_3. Due to these complications, interpreting the antigen stimulated FRET after PIP_2 perturbation has been difficult. Moreover, the scheme presented in chapter 4 for the dependence of the interaction on PIP_2 in ordered vs disordered lipid subregions is insufficient to explain the results associated with antigen stimulation. A thorough accounting of the concentration of PIP2 fractionating with DRM and DSM pools of lipid is required to understand the precise conditions under which the antigen stimulated STIM1-Orai1 interaction occurs. Additionally, high speed Ca^{2+} imaging can be employed to investigate the role of the feedback between Ca^{2+} and PIP_2 in dictating the periodicity of Ca^{2+} oscillations in mast cells.

REFERENCES

Tong, J., Nguyen, L., Vidal, A., Simon, S.A., Skene, J.H., and McIntosh T.J. (2008) Role of GAP-43 in sequestering phosphatidylinositol 4,5-bisphosphate to Raft bilayers. Biophys J. *94*, 125-33.

Wenk, M.R., Lucast, L., Di Paolo, G., Romanelli, A.J., Suchy, S.F., Nussbaum, R.L., Cline, G.W., Shulman, G.I., McMurray, W., and De Camilli, P. (2003) Phosphoinositide profiling in complex lipid mixtures using electrospray ionization mass spectrometry. Nat Biotechnol. *21*, 813-7.

APPENDIX A

ANTIGEN-MEDIATED STIM1-ORAI1 ASSOCIATION

A.1 Enhancement of plasma membrane PIP_2 with PI5K increases the antigen mediated STIM1-Orai1 interaction

Similar to cells stimulated with thapsigargin (Figure 4.2), we stimulated cells expressing either PI5KIβ or PI5KIγ with antigen and measured the FRET between AdGFP-Orai1 and STIM1-mRFP. We found that although there is very little interaction between STIM1 and Orai1 in unperturbed cells following antigen stimulation (Figure A.1, black), there is significant interaction between STIM1 and Orai1 when they are overexpressed in the presence of either PI5K isoform (Figure A.1 cyan, red). The increase in FRET associated with stimulation is similar for both isoforms, although cells overexpressing PI5KIβ appear to have faster initial kinetics. The absolute degree of FRET after 10 minutes is similar to that seen when control cells are stimulated with thapsigargin (Figure 2.3). In contrast to thapsigargin stimulated cells, there appears to be no special selectivity for the degree of STIM1-Orai1 interaction in cells expressing the PI5KIβ verses the PI5KIγ isoform.

A.2 The antigen mediated STIM1-Orai1 interaction is sensitive to selective PIP_2 depletion with targeted phosphatases

In contrast to cells perturbed by PI5KI isoforms, the antigen mediated STIM1-Orai1 shows special selectivity for PIP_2 fractionating with DRM and DSM when these pools are selectively depleted using the PIP_2 phosphatases, L10-Inp54p and S15-Inp54p, that

target ordered lipid subregions and disordered lipd subregions of the membrane, respectively (described in chapter 4). Cells stimulated with antigen in the presence of overexpressed L10-Inp54p (Figure A.2, green) show a dramatic increase in the degree of FRET between AcGFP-Orai1 and STIM1-mRFP over unperturbed cells (Figure A.2, black), whereas there is only a very small enhancement of the interaction associated with overexpression of S15-Inp54p (Figure A.2, pink). This trend is the exact opposite than is seen for thapsigargin stimulated cells, where overexpression of L10-Inp54p is associated with inhibition of the interaction. This means that although the DRM pool of PIP_2 is associated with enhancement of the thapsigargin mediated interaction, this same pool inhibits the antigen mediated interaction.

A.3 Removal of the polybasic PIP_2 directing sequences on STIM1 or Orai1 removes the PIP_2 pool selectivity for the antigen mediated interaction

Similar to cells stimulated with thapsigargin, when either STIM1ΔK-mRFP or AcGFP-Orai1ΔR is paired with its wild type interaction partner, any major selectivity for PIP_2 in ordered vs disordered lipid subregions is lost (Figures A.3, A.4). Specifically, removal of either polybasic sequence removes the enhancement of the interaction associated with overexpression of L10-Inp54p (green). However, there is a small but significant enhancement of the interaction between STIM1ΔK and Orai1 associated with depletion of DSM PIP_2 with S15-Inp54p at long time points. Unlike thapsigargin-stimulated cells, both mutants are associated with a low level of STIM1-Orai1 association as measured by FRET, whereas cells expressing STIM1ΔK-mRFP typically showed enhanced responses to thapsigargin (Figure 4.3). One potential explanation for this result is that the enhancement of the interaction between STIM1ΔK and Orai1 following thapsigargin stimulation is contingent on the

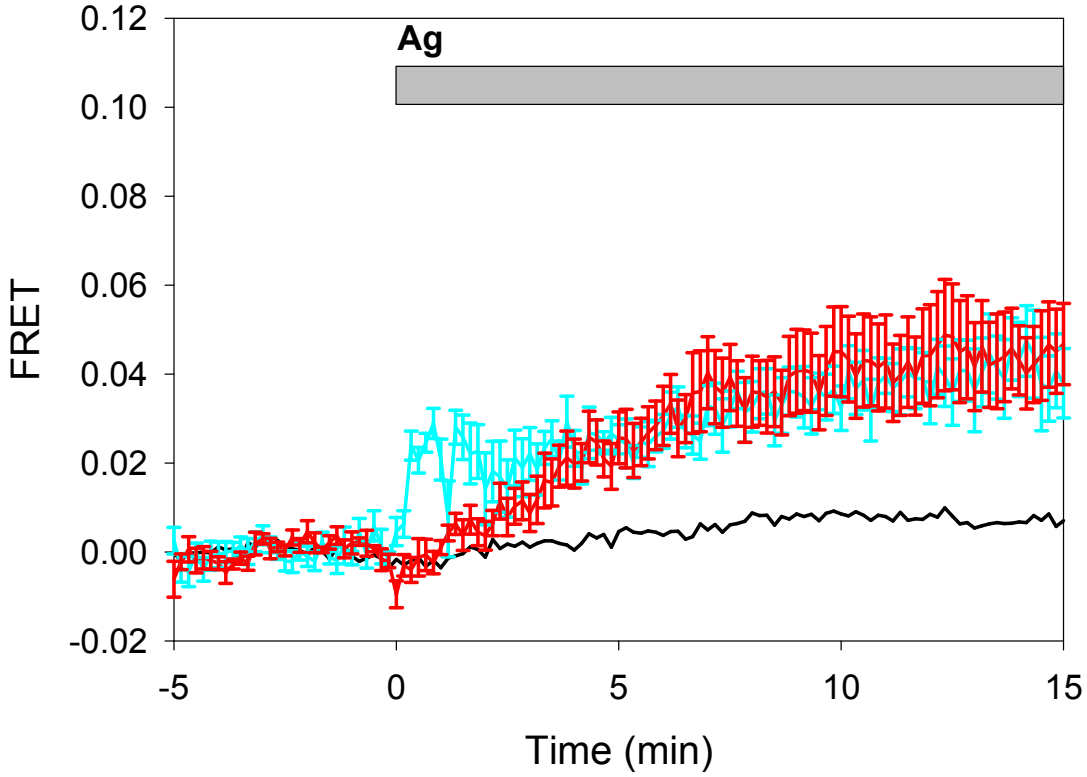

Figure A.1: **Antigen mediated FRET between AcGFP-Orai1 and STIM1-mRFP in the presence of PI5KI isoforms.** The antigen mediated interaction between STIM1 and Orai1 is enhanced when coexpressed with PI5KIβ (cyan) and PI5KIγ (red) when compared to unperturbed cells (black). Error bars show SEM.

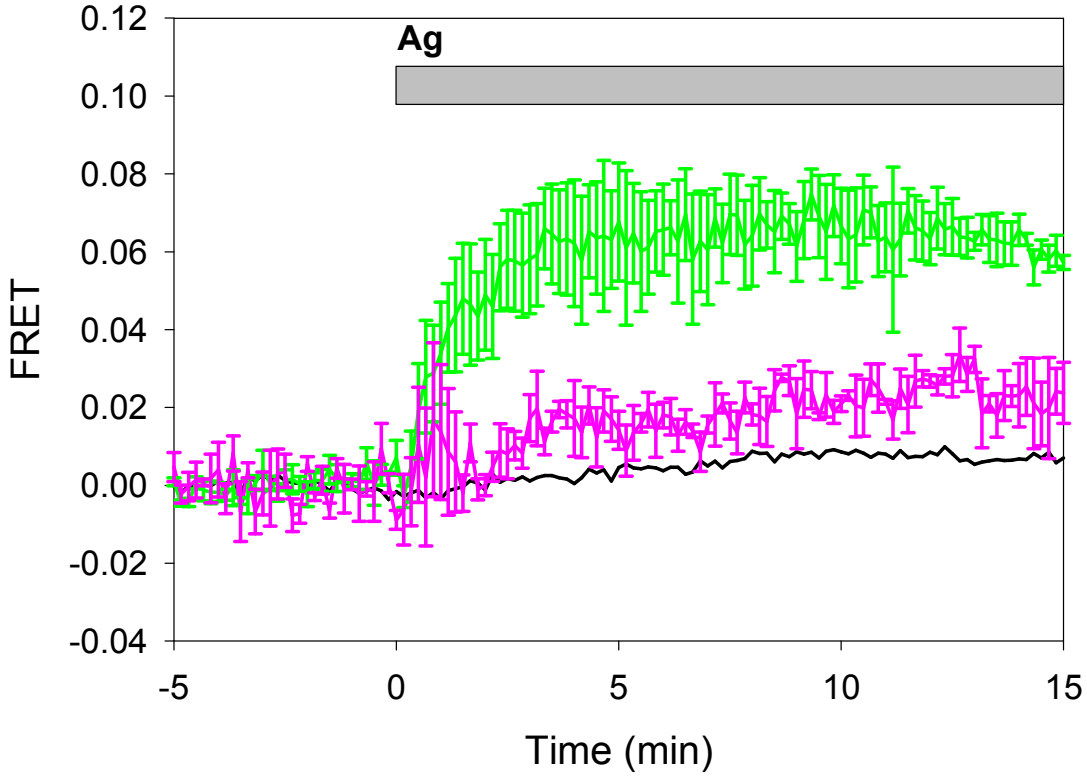

Figure A.2: **The antigen mediated STIM1-Orai1 interaction is selectively perturbed by targeted phosphatases.** The coexpression of the DRM targed PIP_2 phosphatase L10-Inp54p with AcGFP-Orai1 and STIM1-mRFP damatically enhances the interaction between the two proteins (green) in response to antigen, compared to unperturbed cells (black). There is also a small but significant increase the in the STIM1-Orai1 interaction associated with coexpression of the DSM targeted phosphatases S15-Inp54p (pink). The differential sensitivity to expression of L10-Inp54p and S15-Inp54p suggests that the antigen mediated STIM1-Orai1 interaction is selective for DRM and DSM pools of PIP_2. Error bars show SEM.

permanent depletion of Ca^{2+} stores. Based on these results using the polybasic deletion mutants, we can conclude that although the PIP_2 pool selection is different for antigen mediated cells than thapsigargin mediated cells, this selectivity is still mediated by the polylysine sequence on STIM1 and the polyarginine sequence on Orai1.

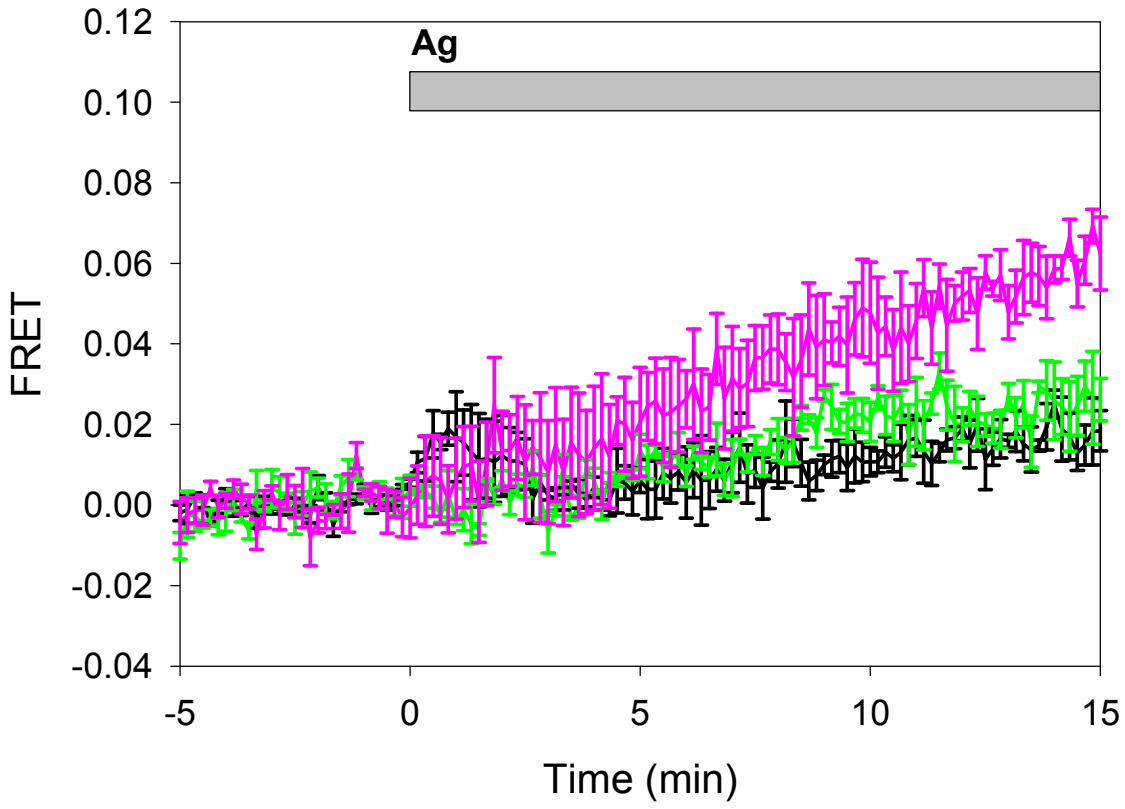

Figure A.3: **The antigen mediated interaction between STIM1ΔK and Orai1 shows altered PIP_2 selectivity.** Similar to the thapsigargin mediated interaction, (Figure 4.4A), removal of the STIM1 C-terminal polylysine sequence changes the selectivity of the STIM1-Orai1 interaction for DRM and DSM pools of PIP_2. When compared to the pairing of wild type proteins (Figure A.2), removal of the polylysine sequence removes the enhancement of the interaction associated with coexpression of L10-Inp54p (green). There is also an increase in the STIM1ΔK-Orai1 interaction associated with coexpression of S15-Inp54p at long time points (pink), and a transient increase in the STIM1ΔK-Orai1 interaction immediately after addition of antigen in the absence of perturbation (black). Error bars show SEM.

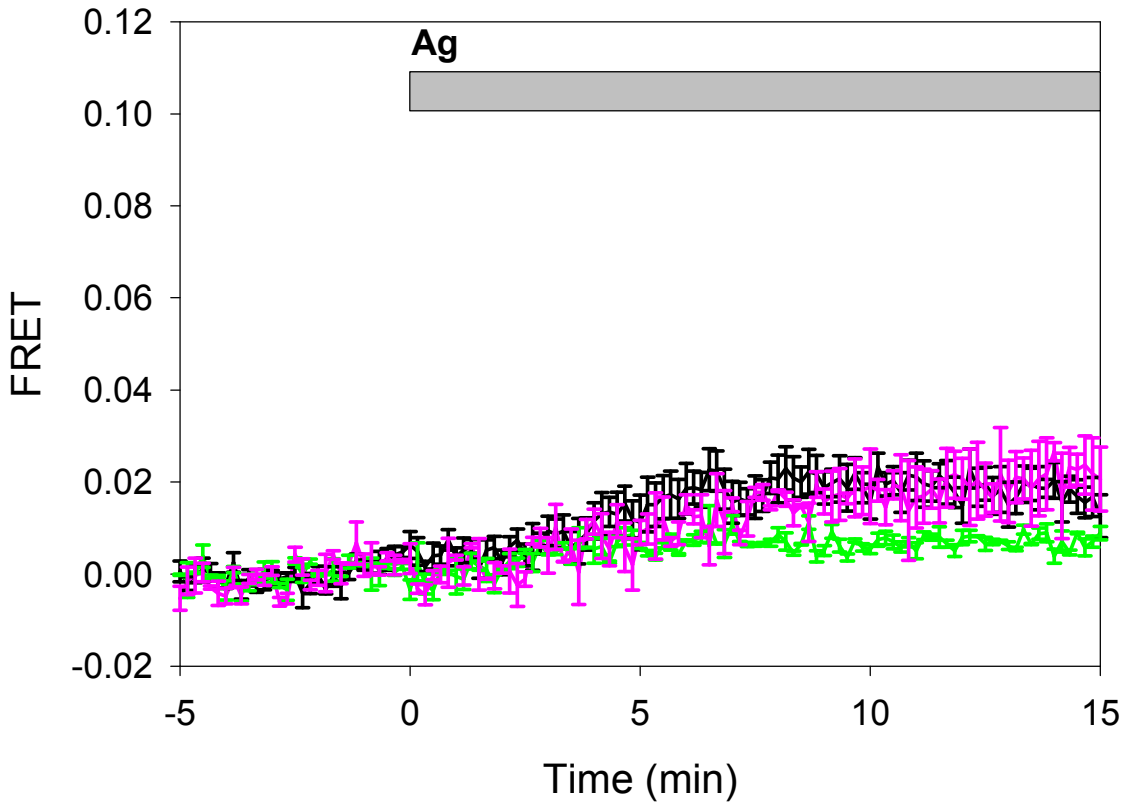

Figure A.4: **The antigen mediated interaction between STIM1 and Orai1ΔR shows altered PIP_2 selectivity.** The removal of the N-terminal polyarginine sequence of Orai1 results in low levels of FRET for all cases of perturbation. Although there is a small but significant enhancement of the interaction of STIM1 and Orai1ΔR when unperturbed (black) compared to the STIM1-Orai1 interaction (Figure A.2), the degree of interaction in the presence of the DSM targeted PIP_2 phosphatase S15-Inp54p (pink) was unchanged and the interaction in the presence of the DRM targeted phosphatase L10-Inp54p (green) was significantly attenuated. Error bars show SEM.

APPENDIX B

SUPPLEMENT FOR CHAPTER 2

B.1 Experimental

B.1.1 Primers used for cloning

STIM1-HA 5’ primer:

5’-GCATTGAAGCTTGCCACCATGGATGTATGCGTC-3’

STIM1-HA 3’ primer:

5’-

TGTCTGGCGGCCGCCTACGCATAATCCGGCACATCATACGGATACTTCTTA

AGAGGCTTC-3’

STIM1-mRFP 5’ primer:

5’-GCGATAGCGGCCGCATCAGGCATGGCCTCCTCCGAGGAC-3’

STIM1-mRFP 3’ primer:

5’-AAGTTCCTCGAGTTAGGCGCCGGTGGAGTG-3’

STIM1 5' Flanking (For eYFP-STIM1)

5’- GATTTCCAAGTCTCCACCCCATTGAC-3’

5' STIM1 signal sequence - eYFP

5’- CCTGCACCAGGGCCAGAGC ATGGTGAGCAAGGGCGAGGAGC-3’

3' STIM1 signal sequence - eYFP

5’- GCTCCTCGCCCTTGCTCACCATGCTCTGGCCCTGGTGCAGG-3’

5' eYFP - STIM1

5’- CTCGGCATGGACGAGCTGTACAAG GGCAGCGGCCTCAGCCA

TAGTCACAGTGAGAAGGC

3' eYFP - STIM1

5’-GCCTTCTCACTGTGACTATGGCTGAGGCCGCTGCCCTTGTAC

AGCTCGTCCATGCCGAG

3' STIM1 – STOP (For eYFP-STIM1)

5’- CCTCTCAAAATCTTTAAGAAGCCTCTTAAGAAGTAGGCGGCCG

CGTGACATGTCACGCGGCCGCCTACTTCTTAAGAGGCTTCTTAAAG

ATTTTGAGAGG-3’

3' STIM1 (for eYFP-STIM1-mRFP)

5’- CTTAAGAAGGCGGCCGCGTGACATGTCACGCGGCCGCCTTCTTA

AGAGGCTTCTTAAAGATTTTGAGAGG-3’

AcGFP1-Orai1/CRACM1 5’ primer:

5’-GCATTGAGATCTATGCATCCGGAGCCC-3’

AcGFP-Orai1/CRACM1 3’ primer:

5’-TGTCTGGGTACCCTAGGCATAGTGGCTGC-3’

AcGFP-Orai1/CRACM1 5’ Flanking Primer (For Oria1.CRACM1 mutants)

5’- GCCATCACCCACGGCATGGATGAGCTGTACAAGTCCGG-3’

AcGFP-Orai1/CRACM1 3’ Flanking Primer (For Oria1.CRACM1 mutants)

5’- CCCCTAGGGTGGGCGAAGAACTCCAGCATGAGATCCC-3’

AcGFP-Orai/CRACM1 ΔD 5’ mutagenesis primer

5’- CCCGCTTACAGAACCAGCTGAACCACAGAGGGAACCACCCCCTGAC-3’

AcGFP-Orai/CRACM1 ΔD 3’ mutagenesis primer

5’- GTCAGGGGGTGGTTCCCTCTGTGGTTCAGCTGGTTCTGTAAGCGGG-3’

AcGFP-Orai/CRACM1 ΔE 5’ mutagenesis primer

5’- GACAGTTCCAGCAGCTCAACCAGCTGGCGCAGTTTGCCCGC -3’

AcGFP-Orai/CRACM1 ΔE 3’ mutagenesis primer

5’- GCGGGCAAACTGCGCCAGCTGGTTGAGCTGCTGGAACTGTC-3’

B.1.2 Immunocytochemical staining of STIM1-HA, Tubulin-eGFP.

Cells were plated for immunocytochemical staining of STIM-HA as for live cell imaging, and STIM1-HA and Tubulin-eGFP were transfected into cells. Cells were fixed with 4% paraformaldehyde plus 0.1% glutaraldehyde solution for 20 min at room temperature. Cells were washed in PBS, pH 7.4, containing 10 mg/mL BSA and 0.01% NaN_3, and labeled by incubation in this buffer for 1 h with Alexa594-labeled anti-HA mAb (1:200 dilution; Covance Research Products, Inc).

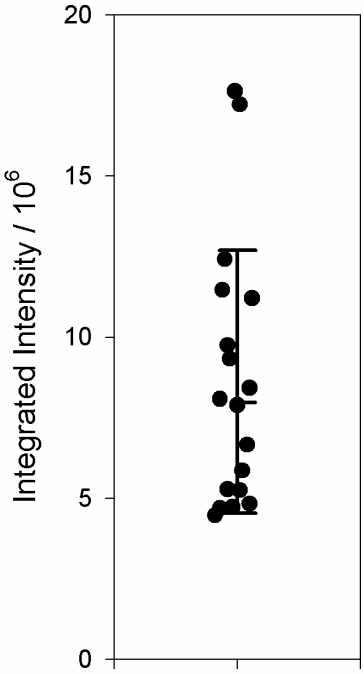

Figure B.1: **The integrated AcGFP fluorescence intensity for 18 cells used in Figure 2.6A to calculate FRET after thapsigargin stimulation**. These data are presented to demonstrate that the error in the FRET observed in Figure 2.6A is smaller than variations in protein expression levels.

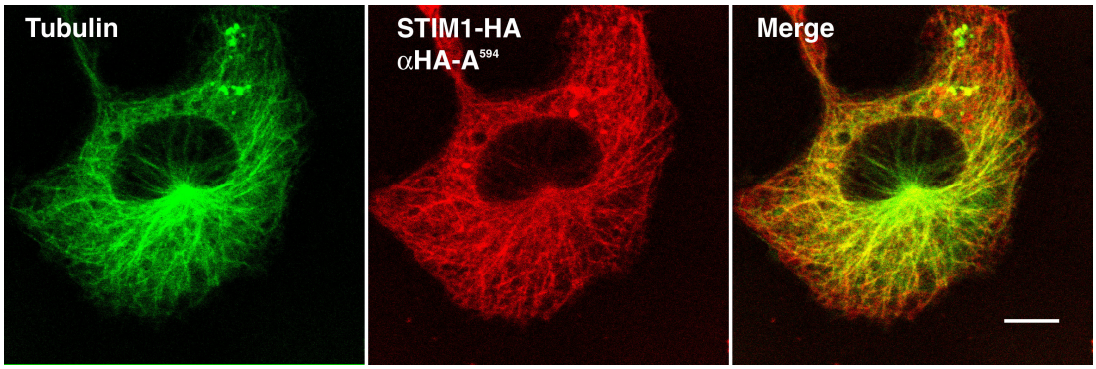

Figure B.2: **α-Tubulin-eGFP (green), STIM1-HA with Alexa594-anti-HA (red), and overlay, demonstrating localization of epitope-tagged STIM1 with microtubules in fixed RBL cells**. Experiment was performed as a control to evaluate the distribution of STIM1expressed without the fluorescent protein attached.

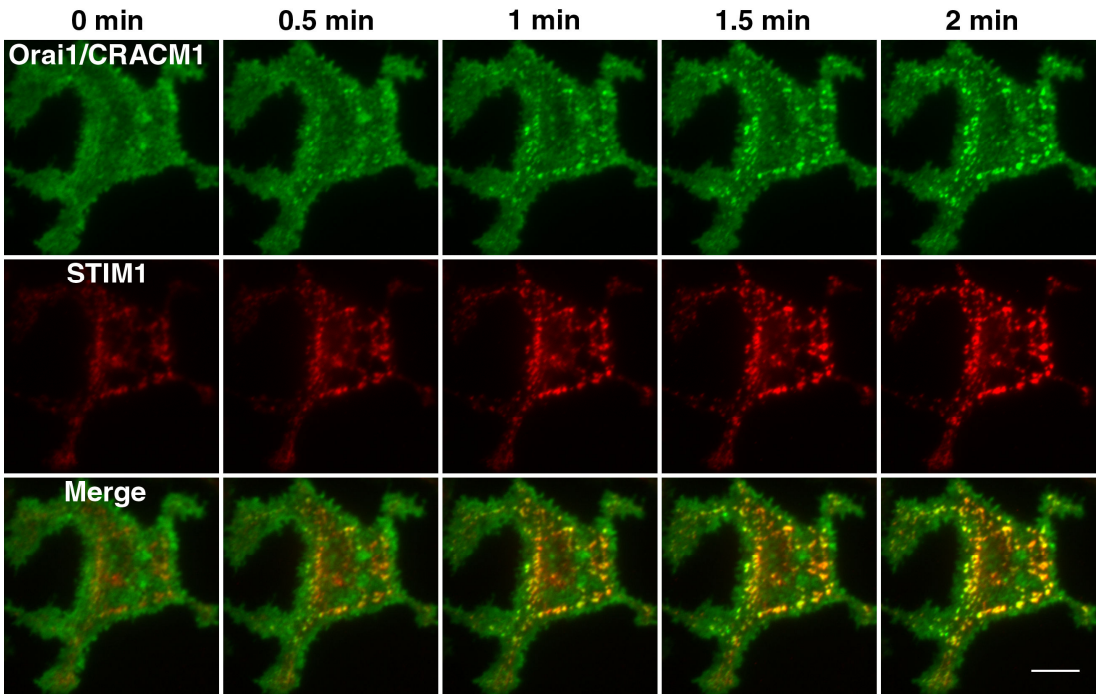

Figure B.3: **Timecourse thapsigargin-stimulated formation of AcGFP-Orai1/CRACM1 (green) and STIM1-mRFP (red) co-labeled plasma monitored by TIRF.** Cells were prepared for TIRF microscopy in the same manner as described for confocal imaging. Cells were imaged on a Nikon TiE perfect focus inverted microscope with a Nikon CFI Plan Apo. TIRF 100X N.A. 1.49 objective and stimulated under the same conditions as described for confocal imaging. Scale bar indicates 10 μm.

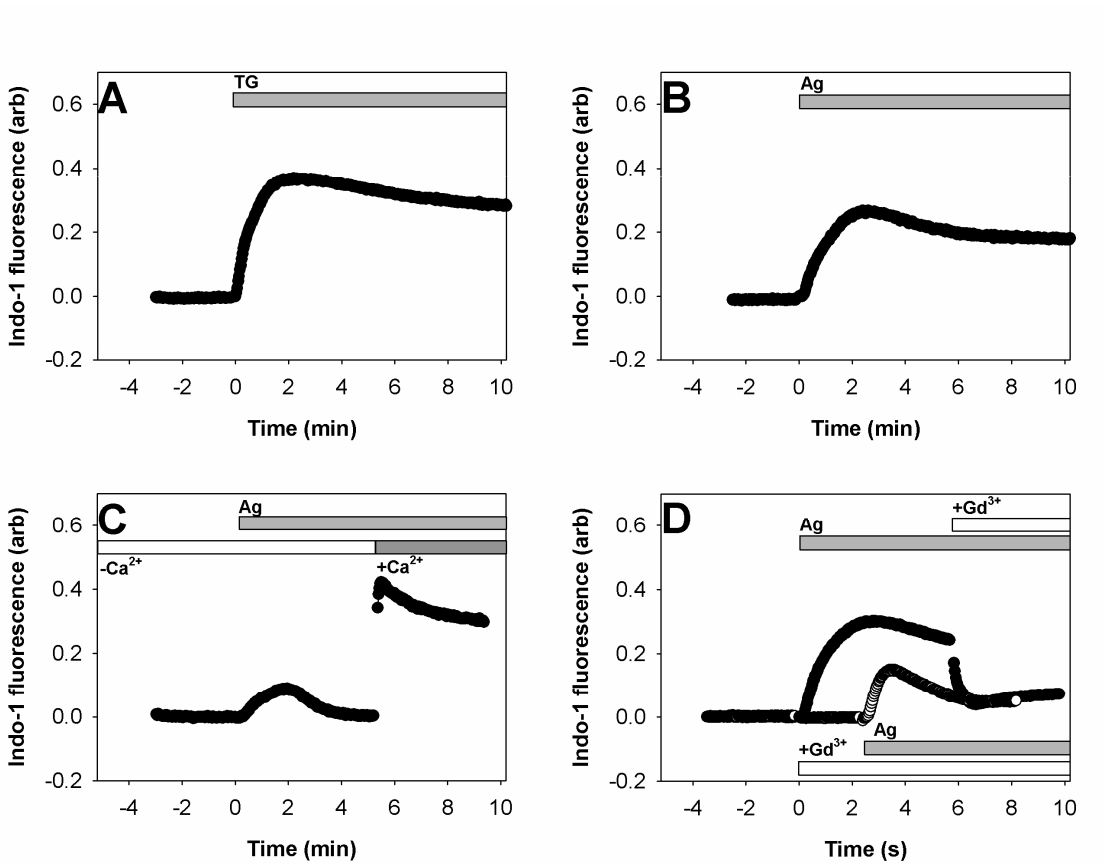

Figure B.4: **Intracellular calcium response monitored by indo-1 fluorescence from suspended RBL mast cells** A) Ca^{2+} response to 150 nM thapsigargin (indicated by bar) B) Ca^{2+} response to stimulation by 3 nM DNP-BSA in BSS. C) Ca^{2+} response to same antigen but in the absence of extracellular Ca^{2+}. $CaCl_2$ (1.8 mM) was restored as indicated by bar. D) Ca^{2+} response to antigen stimulation followed by addition of 6 μM $GdCl_3$ (upper trace) or to antigen stimulation after $GdCl_3$ addition (lower trace).

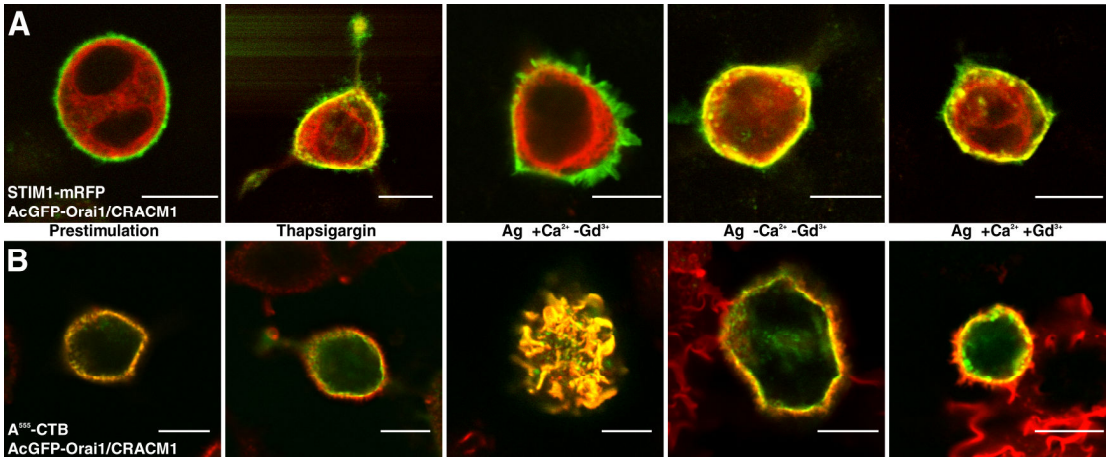

Figure B.5: **Equitorial Cross-sections** A) Equatorial cross-sections of RBL mast cells expressing AcGFP-Orai1/CRACM1 (green) and STIM1-mRFP (red) under specified conditions of stimulation. Note negligible co-pixelation between STIM1-mRFP and AcGFP-Orai1/CRACM1 in unstimulated and antigen-stimulated cells in BSS (with $CaCl_2$). This contrasts with thapsigargin-stimulated cells, antigen stimulated cells in the absence of extracellular Ca^{2+} (Ag, -Ca), and antigen stimulated cells in the presence of $GdCl_3$ (Ag, $+Gd^{3+}$), for which extensive co-pixelation at the plasma membrane is seen. B) Cross-sectional images of RBL mast cells expressing AcGFP-Orai1/CRACM1 that were stimulated or not as in A, then fixed and labeled with A555-CTB. Scale bars indicate 10 μm.

APPENDIX C

SUPPLEMENT FOR CHAPTER 3

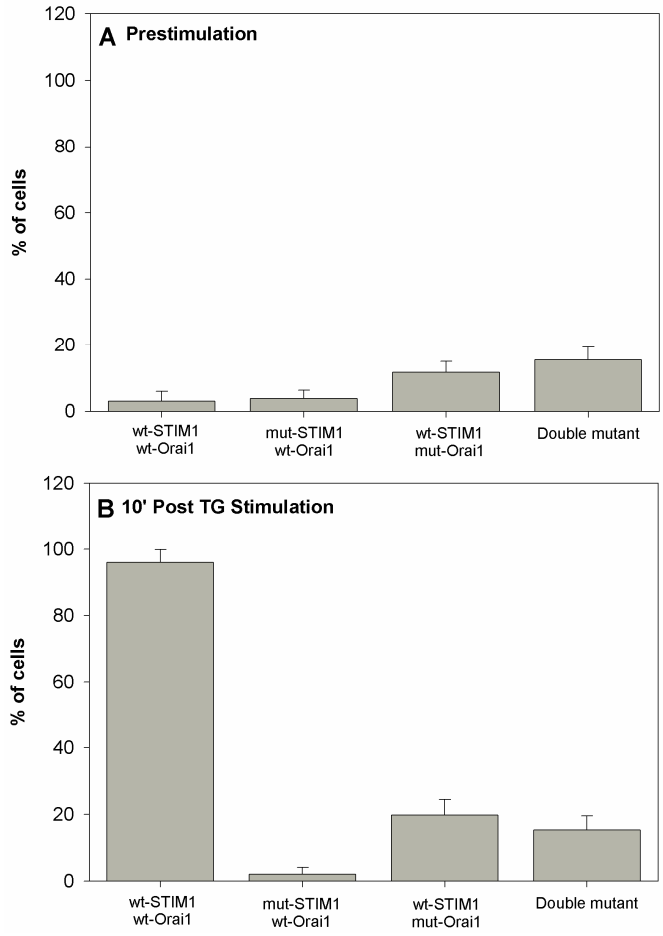

Figure C.1: **Population distributions of Ca^{2+} levels.** Bars show the percentage of cells showing greater than 3x the Ca^{2+} of untransfected, prestimulation cells. Ca^{2+} levels (Fluo-4 fluorescence) were normalized to the average prestimulation Ca^{2+} level in untransfected cells for each experiment as in Figure 3. Distributions of Ca^{2+} levels in A) unstimulated cells, and B) cells after 10 min. in the presence of 150 nM thapsigargin. Cells scored in each sample were transfected with a pair of wild type or mutant STIM1 and Orai1. Each STIM1/Orai1 pair represents 20-60 cells, and error bars show SE.

APPENDIX D

SUPPLEMENT FOR CHAPTER 4

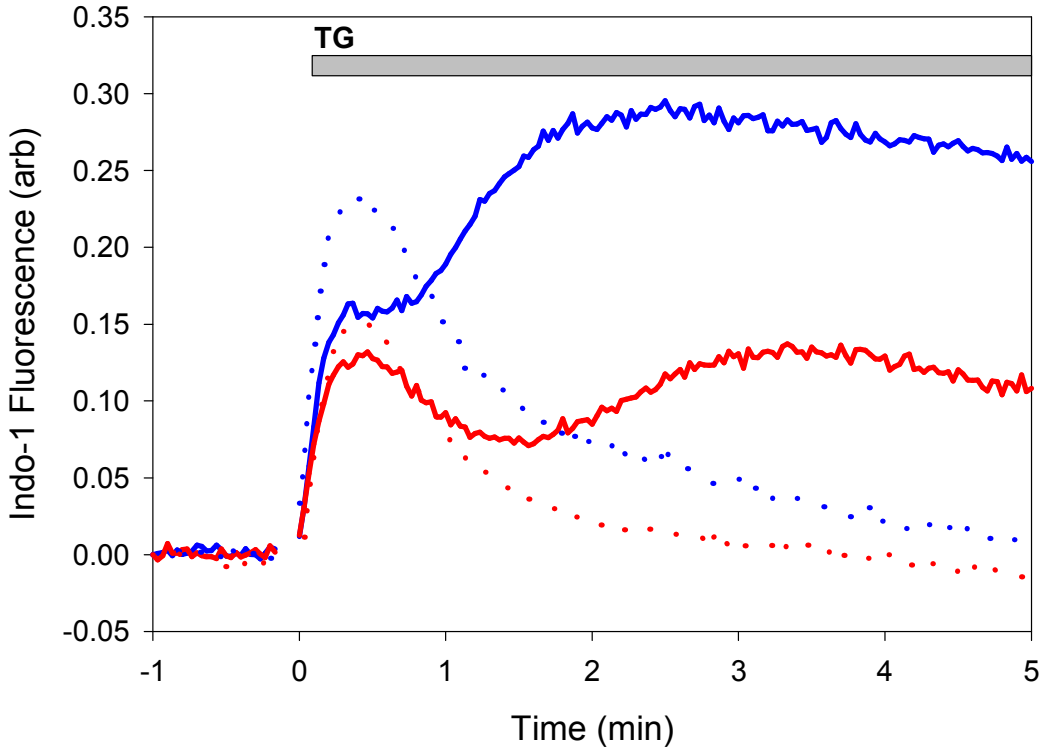

Figure D.1: **Inhibition of SOCE by cholesterol depletion and membrane depolarization.** The indo-1 detected Ca^{2+} response to thapsigargin in cells treated with either 5 mM MβCD for 10 minutes (red) or no MβCD (blue) both in the presence (dotted line) or absence (solid line) of depolarizing K^+ concentrations (140 mM). These results show that treatment of RBL-2H3 cells with MβCD does not desensitize their SOCE response to depolarization by high K^+.

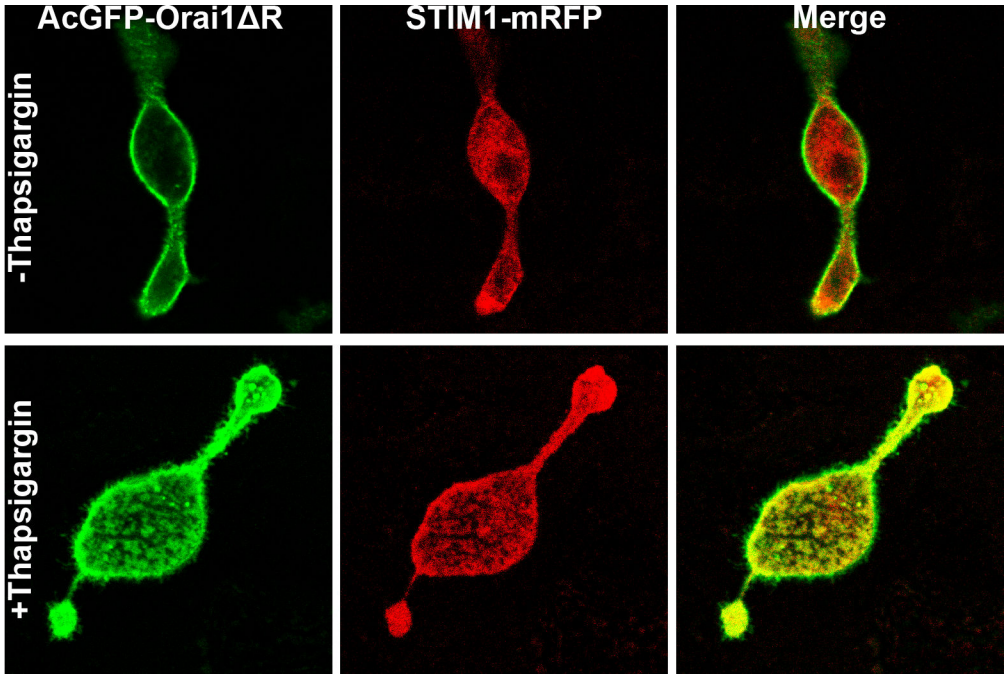

Figure D.2: **Distribution of AcGFP-Orai1ΔR before and after thapsigargin stimulation.** AcGFP-Orai1ΔR (green) and STIM1-mRFP (red) before (top panel) and after (bottom panel) stimulation by thapsigargin. These results show that AcGFP-Orai1ΔR is similarly distributed to wild-type AcGFP-Orai1 both before and after stimulation of SOCE.